2014

APPLICATIONS OF GAS CHROMATOGRAPHY/MASS SPECTROMETRY AND CAPILLARY ELECTROPHORESIS FOR THE ANALYSIS OF LIGNOCELLULOSIC BIOMASS PRETREATMENT

Dawn M. Kato
University of Kentucky, dawn.kato@uky.edu

STUDENT AGREEMENT:

I represent that my thesis or dissertation and abstract are my original work. Proper attribution has been given to all outside sources. I understand that I am solely responsible for obtaining any needed copyright permissions. I have obtained needed written permission statement(s) from the owner(s) of each third-party copyrighted matter to be included in my work, allowing electronic distribution (if such use is not permitted by the fair use doctrine) which will be submitted to UKnowledge as Additional File.

I hereby grant to The University of Kentucky and its agents the irrevocable, non-exclusive, and royalty-free license to archive and make accessible my work in whole or in part in all forms of media, now or hereafter known. I agree that the document mentioned above may be made available immediately for worldwide access unless an embargo applies.

I retain all other ownership rights to the copyright of my work. I also retain the right to use in future works (such as articles or books) all or part of my work. I understand that I am free to register the copyright to my work.

REVIEW, APPROVAL AND ACCEPTANCE

The document mentioned above has been reviewed and accepted by the student's advisor, on behalf of the advisory committee, and by the Director of Graduate Studies (DGS), on behalf of the program; we verify that this is the final, approved version of the student's thesis including all changes required by the advisory committee. The undersigned agree to abide by the statements above.

Dawn M. Kato, Student

Dr. Bert C. Lynn, Major Professor

Dr. Dong Sheng-Yang, Director of Graduate Studies

APPLICATIONS OF GAS CHROMATOGRAPHY/MASS SPECTROMETRY AND CAPILLARY ELECTROPHORESIS FOR THE ANALYSIS OF LIGNOCELLULOSIC BIOMASS PRETREATMENT

DISSERTATION

A dissertation submitted in partial fulfillment of the
requirements for the degree of Doctor of Philosophy in the
college of Arts and Sciences
at the University of Kentucky

By:

Dawn M. Kato

Lexington, KY

Director: Dr. Bert C. Lynn, Professor of Chemistry

Lexington, KY

ABSTRACT OF DISSERTATION

APPLICATIONS OF GAS CHROMATOGRAPHY/MASS SPECTROMETRY AND CAPILLARY ELECTROPHORESIS FOR THE ANALYSIS OF LIGNOCELLULOSIC BIOMASS PRETREATMENT

The focus of this dissertation centers on the development and applications of gas chromatography/mass spectrometry and capillary electrophoresis methodologies to quantify monomeric compositions of the β-O-4 linkages in lignin. Pretreatment is a required step in the utilization of lignocellulosic biomass for biofuels. Lignin is the target of pretreatment because it hinders the accessibility of enzymes and chemicals to cellulose. The effects of pretreatment are commonly assessed utilizing enzymatic saccharification and lignin assays. However, these techniques do not elucidate the effects of pretreatment on the monomeric make up of lignin.

The overarching hypothesis of this dissertation is that changes in individual monolignol content upon pretreatment can be observed from quantification. To test the hypothesis, a pretreatment, solution phase Fenton chemistry, was conducted on various lignocellulosic biomass feedstocks. Enzymatic saccharification studies showed a significant increase in glucose production upon Fenton pretreatment, however, lignin assays did not show a significant decrease in lignin content.

Project two of this dissertation aimed to synthesize analytical standards in order to develop a quantitative thioacidolysis technique. The successful synthesis of the three arylglycerols were conducted utilizing and epoxidation reaction scheme which was hypothesized to produce a single diastereomer, as supported by GC/MS and chiral CE analysis. Upon method development, a quantitative thioacidolysis GC/MS method was applied to untreated and Fenton treated biomass. Results from this project revealed there was no significant change in the three lignin monomers. To verify the method, quantitative thioacidolysis GC/MS method was applied to a pretreatment method known

to degrade lignin, alkaline peroxide pretreatment. The results of this project showed a significant change in monolignol concentrations upon alkaline peroxide pretreatment.

Analytical degradative techniques, such as thioacidolysis, has traditionally assessed lignin as monomeric ratios. However, as this dissertation showed, upon alkaline peroxide pretreatment, no significant change was seen in the monomeric ratios, but there was a significant difference in all three monolignol concentrations. These results support the overall hypothesis that changes in individual monolignol content upon pretreatment can be observed from quantification. The works of this dissertation provides an analytical method which contributes to the elucidation of lignin.

Dawn M. Kato

12/9/2014

APPLICATIONS OF GAS CHROMATOGRAPHY/MASS SPECTROMETRY AND CAPILLARY ELECTROPHORESIS FOR THE ANALYSIS OF LIGNOCELLULOSIC BIOMASS PRETREATMENT

By: Dawn M. Kato

Bert C. Lynn

(Director of Dissertation)

Dong Sheng-Yang

(Director of Graduate Studies)

12/9/2014

Dedicated to my friends and family whom supported me through this journey.

ACKNOWLEDGEMENTS

I would like thank God for all the blessings he has bestowed upon me and for seeing me through the storm. I would like to thank my family who pushed and supported me throughout my life, without their love and support I would not have persevered. My family is my heart and soul, they lift me up when I am weary and give me light in my darkness. My life has always been adventurous, "never a dull moment", as my mom always says, but they have been my rock through it all.

It goes without saying that my advisor, Dr. Bert C. Lynn, has been invaluable in my efforts towards this degree. Not only has he made me into the chemist I am today, but he never gave up on me despite our dark times. I will never be able to express the gratitude I have for all the knowledge and skills he has taught me. Despite any hard times we may have gone through, I could not have chosen a better advisor. He will miss me regardless of what he says. I'd also like to thank my committee members, Dr. Mark Lovell, Dr. Stephen Testa and Dr. Robert Lodder for their guidance and professional development throughout the years. I'd like to thank Dr. Michael Flythe for serving as my outside examiner, but also for collaborating with me/my research group the past several years, it has been a pleasure working with him.

I want to thank all past and present Lynn group members. I'd specifically like to thank Dr. Michael Timmons for taking me under his wing and teaching me the ropes of the Lynn lab. I'd like to thank Brent Casper and Fan Huang for keeping me sane and feeling my pain through the process. No one understands the journey like your group members. I would also like to send a big mahalo to Dr. Timothy Croley for believing in

me and saving my behind on numerous occasions. I hope to one day possess his swagger.

I would like to thank all my friends who stuck by me through this journey. My best friend, Celine Sumiye, has always been a sister to me, she is my true other half. Anne Oberlink started this journey with me and has been my numero uno through it all. Cecilia Lowe has been my roommate for the past couple years and I am so appreciative of her and her family for taking me in as one of their own and being there for whatever I needed through this process, I know it hasn't always been easy. Lastly, I would like to thank my main man who always lifts my heart and makes me smile. My son, Ray ray, has truly been the biggest blessing.

TABLE OF CONTENTS

LIST OF TABLES

LIST OF FIGURES

LIST OF ABBREVIATIONS AND SYMBOLS

AC	Analog current
AFEX	Ammonia Fiber Expansion
AISL	Acid insoluble lignin
ASL	Acid soluble lignin
BGE	Background electrolyte
BSTFA	N,O-Bis(trimethylsilyl)trifluoroacetamide
°C	Degrees Celsius
CAER	Center for Applied Energy Research
CD	Cyclodextrin
CE	Capillary electrophoresis
CE/MS	Capillary electrophoresis/mass spectrometry
CI	Chemical ionization
CS	Corn stover
CZE	Capillary zone electrophoresis
DC	Direct current
DFRC	Derivatization followed by reductive cleavage
EI	Electron ionization
EIC	Extracted ion chromatogram
EOF	Electroosmotic flow
eV	Electron volts
FPU	Filter paper units
GC	Gas chromatography
GC/MS	Gas chromatography/mass spectrometry
Gg	Guaiacyl glycerol
Gly	Glycine
Gt	Guaiacyl thioacidolysis monomer
H_2O_2	Hydrogen peroxide
Hg	*p*-hydroxyphenyl glycerol
HP-β-CD	2-hydroxypropyl-beta-cyclodextrin
HRAMMS	High resolution accurate mass mass spectrometry
HRMS	High resolution mass spectrometry
Ht	*p*-hydroxyphenyl thioacidolysis monomer
IS	Internal standard
$KMnO_4$	Potassium permanganate
kV	Kilovolts
MΩ	Mega ohms
mbar	millibar
min	Minute
mis	miscanthus
mM	millimolar
MS	Mass spectrometry

MW	Molecular weight
m/z	Mass/charge
$Na_2B_4O_7$	Sodium borate
NaOH	Sodium hydroxide
NMR	Nuclear magnetic resonance
NREL	National renewable energy laboratory
PDA	Photodiode array
PPP	*p*-phenylphenol
psi	Pounds per square inch
Rf	Radiofrequency
RSD	Relative standard deviation
Sg	Syringyl glycerol
SG	switch grass
St	Syringyl thioacidolysis monomer
Stdev	Standard deviation
TIC	Total ion chromatogram
TLC	Thin layer chromatography
TMS	Trimethylsilated
Trt	Treated
WS	wheat straw
Unt	Untreated

1. Chapter 1 : Background

1.1. Biofuels

Worldwide energy consumption continues to increase while petroleum based resources are quickly being consumed, thus a need for alternate energy sources. The need for other energy sources has regenerated an interest in renewable resources of energy to generate biofuels. Biofuels are fuels produced from biological sources or feedstocks such as biomass. Bioethanol and biodiesel are two common examples of first generation biofuels. Biodiesel is made by combining alcohol with vegetable oil, animal fats or recycled cooking grease. Bioethanol is typically made from corn, sugar cane or sugar beets.[1] Vehicles are currently fueled by a gasoline-ethanol mixture.

In 2011, roughly 78% of the energy consumed worldwide was from fossil fuels, 3% from nuclear energy and 19% from renewable energy sources, according to the renewable energy policy network (Figure 1.1).[2] There are various sources of renewable energy, biomass being the largest utilized source (Figure 1.2). Majority of commercially available biofuels are produced using sugars extracted from agriculture feedstocks or by conversion of starch into monomeric sugars, primarily from grains.[2]

Currently, 85 million barrels of crude oil are processed and used to meet the world's energy demands. This demand is projected to increase by 116 million barrels by 2030, this could deplete the worlds crude oil resources.[2] The US Department of Energy (DOE) and the US Department of Agriculture (USDA) mandated that 5% of heat and power energy, 20% of liquid transportation fuel

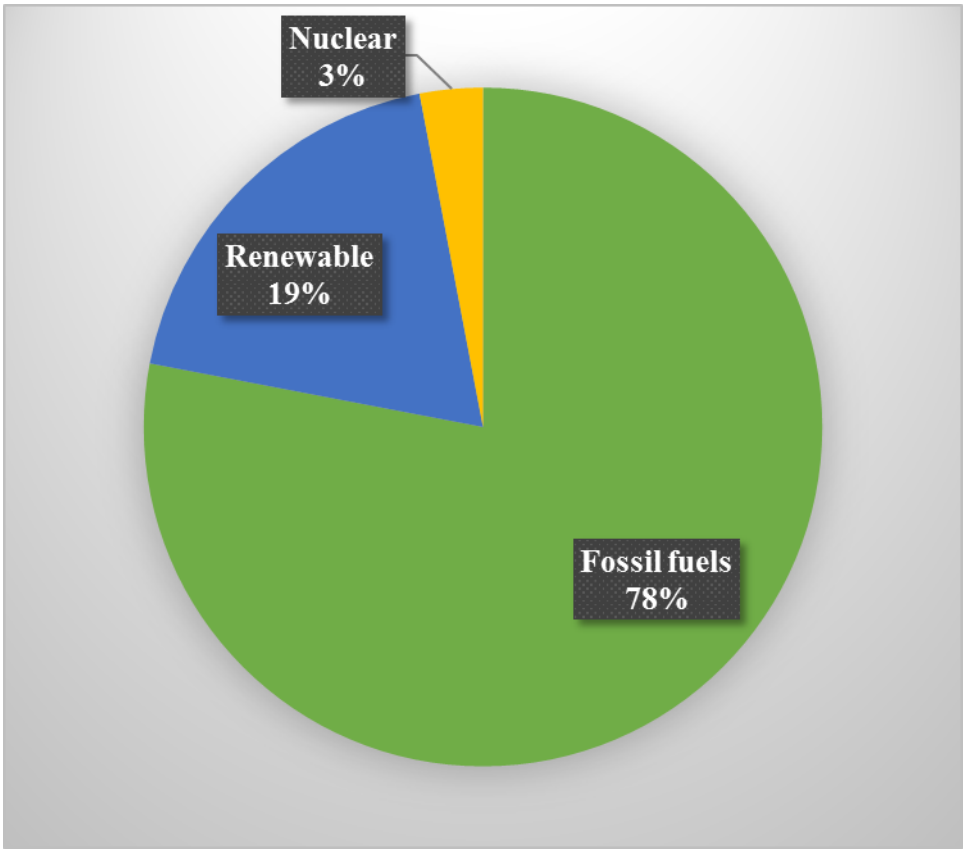

Figure 1.1 Worldwide energy consumption in 2011.[2]

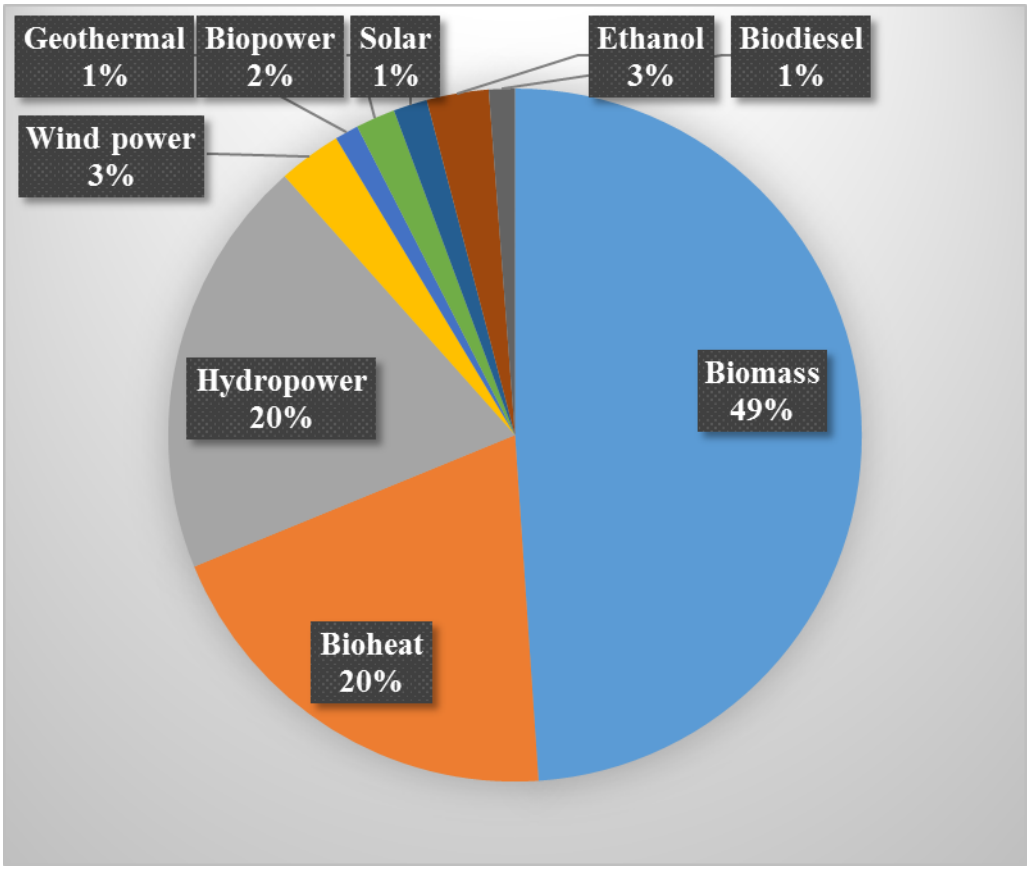

Figure 1.2 Worldwide renewable energy consumption in 2011.[2]

and 25% of chemicals and materials should originate from biomass by 2012.[2] In order to meet this mandate, about 36 billion gallons of liquid transportation fuels are needed. Of that 36 billion, approximately 15 billion are anticipated to come from sugar and starch based bioethanol, but the remaining 21 billion gallons will need to be meet using lignocellulosic biomass.[2] To accomplish these goals, biorefineries will need to fully utilize/convert all the biomass feedstock's potential energy sources for energy in order to be highly profitable.

First generation biomass utilizes feedstocks such as corn, wheat, cassava, barley, rye, soybean, sugarcane, sugar beet, and sweet sorghum. Biofuels, bioethanol, are extracted from sugarcane, sugar beet, and sweet sorghum, by squeezing the sugars from the stems or with water. Wheat, rye, corn and soybean require thermochemical processing such as jet cooking using steam followed by the hydrolysis of starch with amylase in order to utilize these feedstocks for fuels.[2] Currently, Brazil and the US are the largest biofuel consumers. BP has established bioethanol refineries in Brazil which has contributed 38% of biofuel production.[3] A major disadvantage of first generation bioethanol production lies in the food vs. fuel debate. The price of food sources, such as corn, increases as fuel production increases.[4] In addition, there is controversy that several million people are without sufficient food supply. Thus, government established a cap on the amount of ethanol produced from corn and other food resources.

Using nonedible feedstocks, such as lignocellulosic biomass, for biofuels provides several benefits: 1) a renewable and sustainable resource, 2) facilitation of local economic development and stimulation, 3) energy security for countries

depending on imported oil, such as the US, 4) biorefineries create job opportunities for both higher level STEM (Science, Technology, Engineering and Mathematics) fields and daily plant operation positions. A large disadvantage of utilizing nonedible feedstocks is the conversion costs Currently, the conversion costs of nonedible feedstocks is greater than that of crude oil. However, as technology matures, cost is expected to decrease.[2]

Second generation biofuels are produced from the cellulose present in non-food and waste crops often referred to as lignocellulosic biomass.[5] There are two routes for cellulose conversion: 1) thermochemical (biomass-to-liquid, BTL) conversion by pyrolysis or gasification to produce synthetic gas, syngas (a mix of carbon monoxide and hydrogen gas), the gases are then reformed into fuel, 2) biochemical route to transform cellulose and hemicellulose to simple sugars which are then fermented to produce fuels.[2] Second generation biofuel production thus far has faced the challenge of the development of an efficient conversion strategies which is also cost effective.

1.2. Lignocellulosic biomass

Bioenergy plants, such as lignocellulosic biomass, are split into two categories: 1) gymnosperms (softwoods, i.e. pine, spruce, fir, cedar) or 2) angiosperms (monocots: all perennial grasses, i.e. switchgrass, miscanthus, sorghum, sugarcane, and bamboo, and herbaceous species, i.e. corn, wheat and rice; dicots: flowering plants, i.e. alfalfa, soybean, hardwoods, i.e. poplar, willow and black locust).[2] Figure 1.3 shows the percentage of various feedstocks used in bioethanol production in 2011, corn being the largest utilized feedstock.[2]

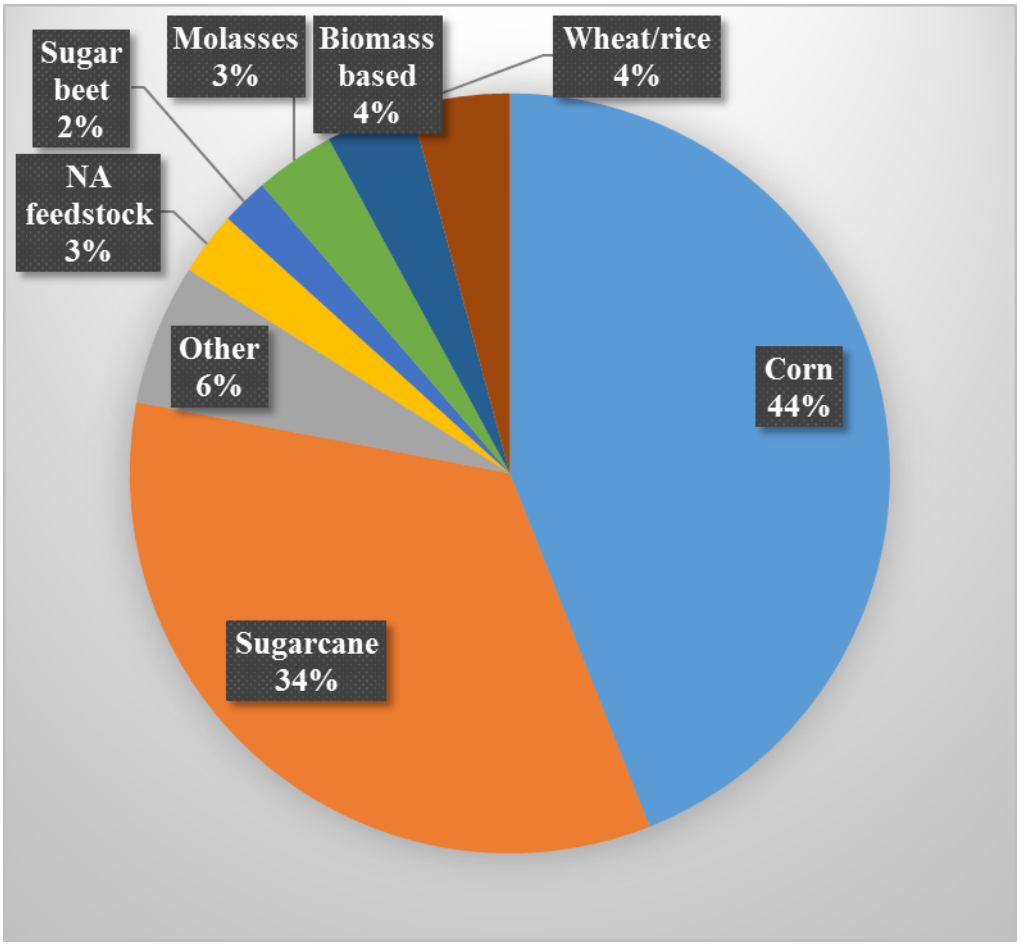

Figure 1.3 Feedstocks used for ethanol production worldwide in 2011.[2]

Lignocellulosic biomass is mainly composed of three polymers: lignin (15-20%), cellulose (30-50%) and hemicellulose (20-35%).[2] Protein, pectin, extractives (nitrogenous compounds, waxes and chlorophyll), and ash are also present, but only in minor amounts.[6] The compositions of these constituents can vary from one plant species to another.[6] Additionally, the same feedstock harvested from the same field during different times of the year can display changes in the ultrastructural composition due to the environmental conditions.[2]

Cellulose is a linear homopolymer consisting of D-glucose subunits linked by β-(1,4)-glycosidic bonds, as seen in Figure 1.4.[6-7] Cellulose aggregate by hydrogen bonding and Van der Waals interactions which cause cellulose polymers to form microfibrils.[6] Biomass cellulose consist of both crystalline and amorphous cellulose. Amorphous cellulose is more susceptible to degradation, but is only present in minor amounts.[6]

Hemicellulose is a heteropolymer composed of various sugars such as pentoses, hexoses and uronic acids. Hemicellulose have shorter branches than cellulose and are linked by β-(1,4)-glycosidic bonds and the occasional β-(1,3)-glycosidic bonds.[6] Hemicellulose and lignin can cross link to cover the microfibrils formed by cellulose, providing structural rigidity.[6]

Lignin is a complex amorphous polymer resulting from the oxidative combinatorial radical coupling of phenylpropanoid units.[6, 8] Lignin is deposited mainly in cell walls and provide plant structural rigidity. Lignin also contributes to plant recalcitrance characteristics and plant resistance to chemicals and enzymes, thus protecting cellulose.[8a] As mentioned previously, cross linking of

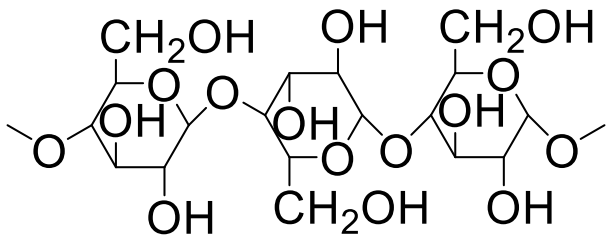

Figure 1.4 Cellulose (D-glucose units linked by β-(1,4)-glycosidic bonds.

lignin with carbohydrates increases strength and rigidity.[9] *Para*-coumaryl (H), coniferyl (G) and sinapyl (S) alcohols are the three main hydroxycinnamyl alcohols, also known as monolignols, which compose the building blocks of lignin as seen in Figure 1.5.[8a] When these monolignols are incorporated into the lignin polymer, they are referred to as *p*-hydroxyphenyl (H), guaiacyl (G) and syringyl (S) subunits.[10]

Plant composition can vary between and within plant species. Gymnosperm lignin is composed of mainly coniferyl alcohol or G subunits, whereas, angiosperm lignins are composed of both coniferyl (G) and sinapyl (S) alcohols.[8a] Grass lignin is composed of all three monolignols, H, G and S. Monolignols polymerize through the following linkages : phenylpropane-β-aryl ether (β-O-4), biphenyl and dibenzodioxocin (5-5), phenylcoumaran (β-5), 1,2-diaryl propane (β-1), phenylpropane-α-aryl ether (α-O-4), diaryl ether (4-O-5), and resinol or β-β linked structures (β-β), as depicted in Figure 1.6.[8a]

1.3. Biomass to biofuel processing

As briefly discussed previously, second generation biofuel production is focused on the conversion of lignocellulosic biomass to biofuels such as acetone, butanol and ethanol (ABE). The aim is to ferment the simple sugar subunits, glucose, that compose cellulose, into these biofuels. However, lignocellulosic biomass is resistant to enzymes or chemicals due to its recalcitrant nature or structural rigidity provided mainly by lignin. In order to get to cellulose, pretreatment is a necessary step in biomass to biofuel processing.[6] The goal of pretreatment is to alter the structure of lignin such that cellulose become more

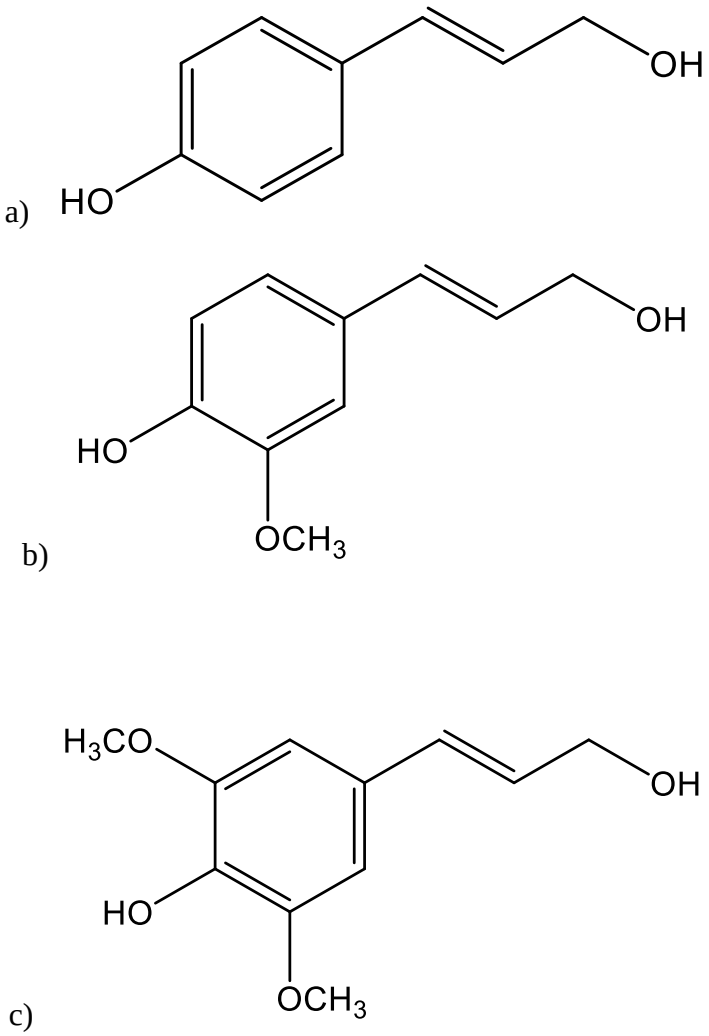

Figure 1.5 Monolignol structures a) *p*-coumaryl alcohol (H) b) coniferyl alcohol (G) c) sinapyl alcohol (S).

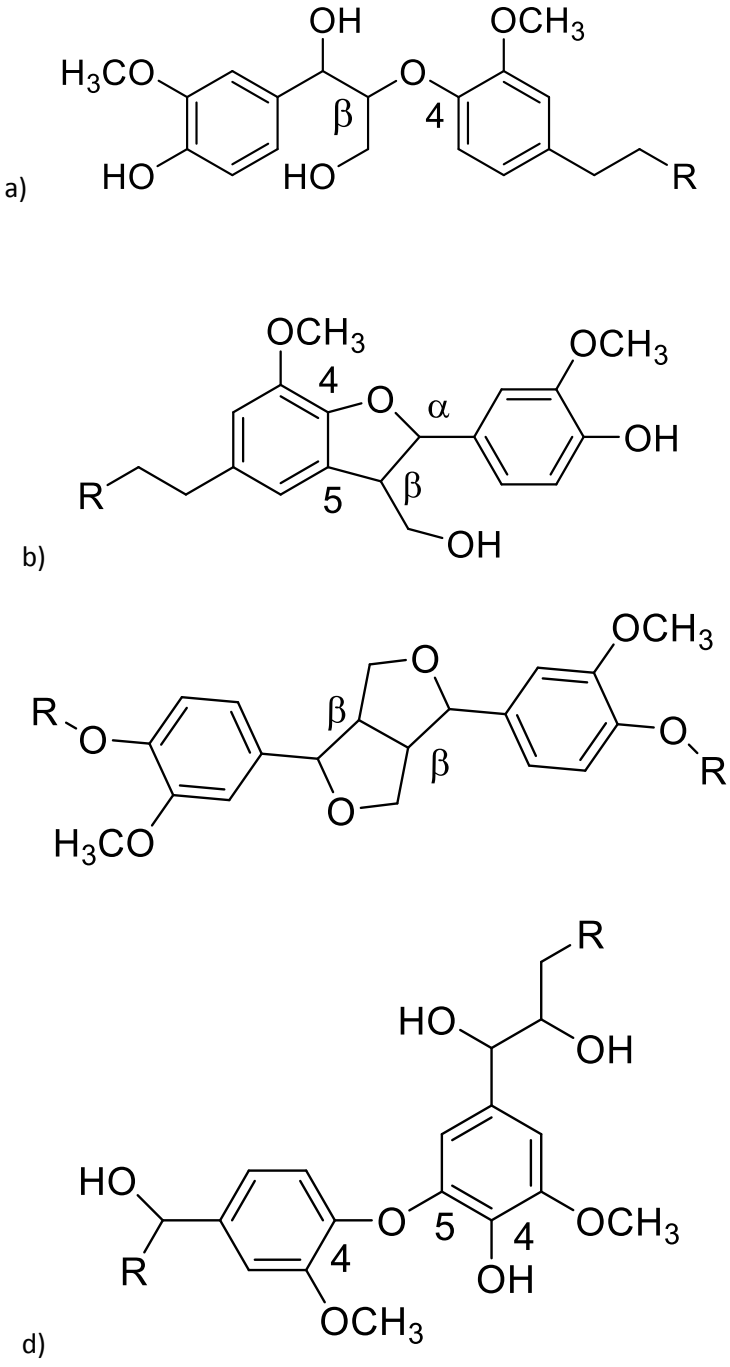

Figure 1.6 Common lignin linkages : a) β-O-4 (β-aryl ether) b) β-5/α-O-4 (phenylcoumaran) c) β-β (resinol) d) 4-O-5 (biphenyl ether).

bioavailable to chemicals or enzymes. Compositional changes in plant cell wall and differences in ultrastructure greatly influence the pretreatment strategy and the conversion efficiencies.[2] Pretreatment has the potential to drastically change the properties of biomass (specific surface area, cellulose crystallinity index, degree of polymerization, lignin content, etc.).[2]

Biomass to biofuel processing occurs through the scheme seen in Figure 1.7.[6] Harvested biomass is pretreated making cellulose more bioavailable, cellulose is then hydrolyzed into simple sugars. Sugars are then fermented, via microbial species, into a crude mixture which is separated/purified producing biofuels.[6]

Biomass pretreatment strategies are broken into three categories: physical, chemical or biochemical pretreatment.[7, 8b] Physical pretreatment strategies include reduction in biomass particle size utilizing a mechanical approach or thermal strategies such as steam explosion and hydrothermolysis.[8b] Chemical pretreatment strategies consist of biomass exposure to acid, base, alkaline hydroxide, ammonia fiber expansion (AFEX) or a combination of these techniques.[8b] An example of a biochemical pretreatment would be exposure to lignocellulolytic *Basidiomycetes* such as white-rot or brown-rot fungi which have enzymes that degrade the polymeric components of biomass.[11]

When evaluating pretreatment strategies, it is common practice to not only evaluate the bioavailability of cellulose, but to analyze changes in lignin upon pretreatment or lack thereof. This is typically done according to national renewable laboratory (NREL) protocols that describe lignin content, acid soluble

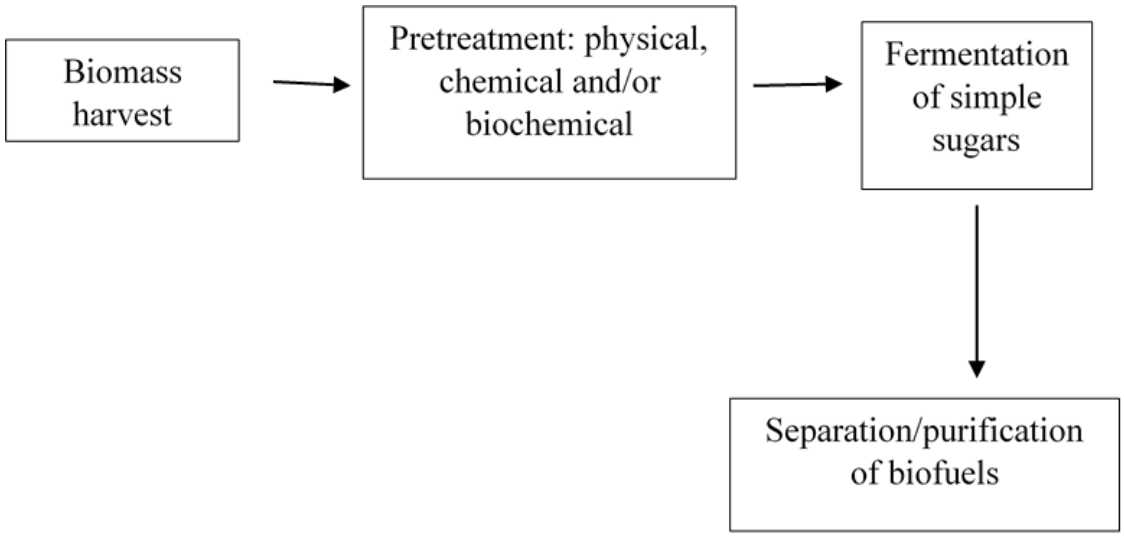

Figure 1.7 General biomass to biofuel processing scheme.

and acid insoluble. However, this does not provide insight to the monomeric composition of lignin. Analytical lignin degradation techniques have been developed in order to degrade polymeric lignin into its monomeric form which will provide polymeric compositional information. Gas chromatography (GC) is commonly used to analyze the products of analytical lignin degradation techniques.

1.4. Gas chromatography/mass spectrometry

Gas chromatography (GC) is an analytical technique used to analyze complex mixtures of volatile compounds in the gas phase. The main components of a gas chromatograph are an injector, a capillary column housed in an oven (Figure 1.8) and a detector. A sample is injected, volatilized and carried through the column by a carrier gas, typically helium or nitrogen, where the mixture is separated by a substituted polysiloxane stationary phase based on volatility and structure. In a typical GC experiment, temperature is increased at a certain rate to elute analytes. The temperature ramp determines analyte retention times and separation efficiency.[12] The detector used throughout this dissertation was a mass spectrometer.

Mass spectrometry (MS) coupled to a gas chromatograph not only provides sensitivity, but it allows for structural elucidation. A mass spectrometer analyzes ions based on size and charge. Mass spectrometers are comprised of three main components: an ionization source, mass analyzer and a detector. Gas chromatography/mass spectrometry (GC/MS) techniques have two common ionization techniques, electron ionization (EI) and chemical ionization (CI). All

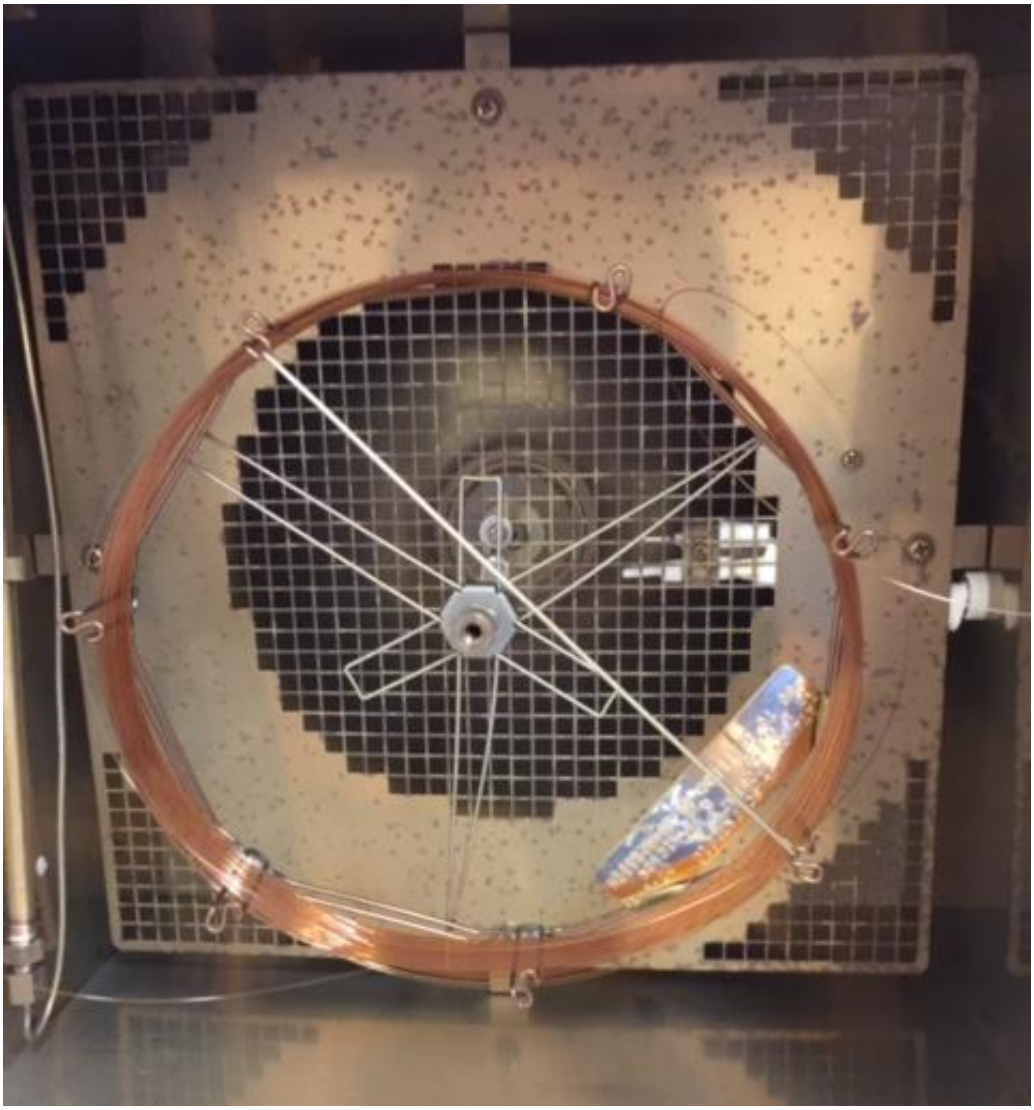

Figure 1.8 Gas chromatograph oven housing the separation column.

GC/MS analyses conducted throughout this dissertation utilize EI. Electron ionization occurs according to the mechanism, as seen in Figure 1.9, where the molecular species resonates with an electron of 70 eV, causing the ejection of an electron from the molecular species generating a radical cation.

All GC/MS studies were conducted on a quadrupole mass filter. A quadrupole mass filter is comprised of two pairs of rods oriented parallel to each other (Figure 1.10) that are 180° out of phase. At a given radio frequency (Rf) and direct current (DC) voltage, only ions of a certain mass to charge (*m/z*) are allowed to pass through and reach the detector.[13] The filtering characteristic of the quadrupole mass filter occurs with the combination of DC (time dependent) and AC/Rf (time independent) potentials applied to the rods.[13] Considering the effects of the applied AC potential on a beam of ions traveling in the X-Z plane, the X electrodes spend a half cycle in positive potential and half in negative potential.[13] During the positive cycle, positively charged ions will be focused to the center axis. During the negative cycles, positively charged ions will be defocused from the center. The Y electrodes will operate with potential equal, but opposite to potentials of the X electrode.[13] Ions are filtered based on *m/z.* Considering both the DC and Rf potentials being applied to the pairs of electrodes, heavier ions are affected more by the DC potential with negligible influence from the Rf, thus, lighter ions are governed further by the Rf potential[13] In order for an ion to pass through to the detector, it must remain stable in both the X-Z (high pass filter) and Y-Z (low pass filter) planes.[13]

$$M + e^{-} (70\ eV) \rightarrow M^{*+\cdot} + 2e^{-}$$

Figure 1.9 Electron ionization mechanism.

Figure 1.10 Quadrupole mass filter.

1.5. Capillary electrophoresis

Capillary electrophoresis (CE) has become a well-established separation technique utilized in pharmaceutical research and clinical applications due to the high resolving power, rapid analysis time, and small sample volume and reagents required.[14] A CE system consists of a fused-silica capillary, typically 10-100 µm inner diameter that is 40-100 cm long, extended between two buffer reservoirs that hold electrodes, a high voltage source, and a detector, Figure 1.11.[15]

The unprecedented resolution of CE is a ramification of the techniques unparalleled separation efficiency. We can describe CE using the Van Deemter equation, as we do with other chromatographic separation techniques:

$$H = A + \frac{B}{v_x} + C v_x$$

$$where\ A, B\ and\ C\ are\ constants$$

As plate height, H, decreases, the number of theoretical plates, N, increases.[16] The terms A and Cv_x are eliminated due to the separation occurring in a single phase of uniformly flowing mobile phase, thus, removing eddy diffusion and the resistance to mass transfer. The sole source of band broadening is longitudinal diffusion, $\frac{B}{v_x}$. Capillary electrophoresis, typically, has 50,000 to 500,000 theoretical plates which contributes to the high separation efficiency of the technique.[16] Advantages of CE are its quick analysis times, minimal sample and reagent volumetric requirements and it is a more affordable instrumental system. Electrophoresis is the migration of ions under the influence of an applied electric

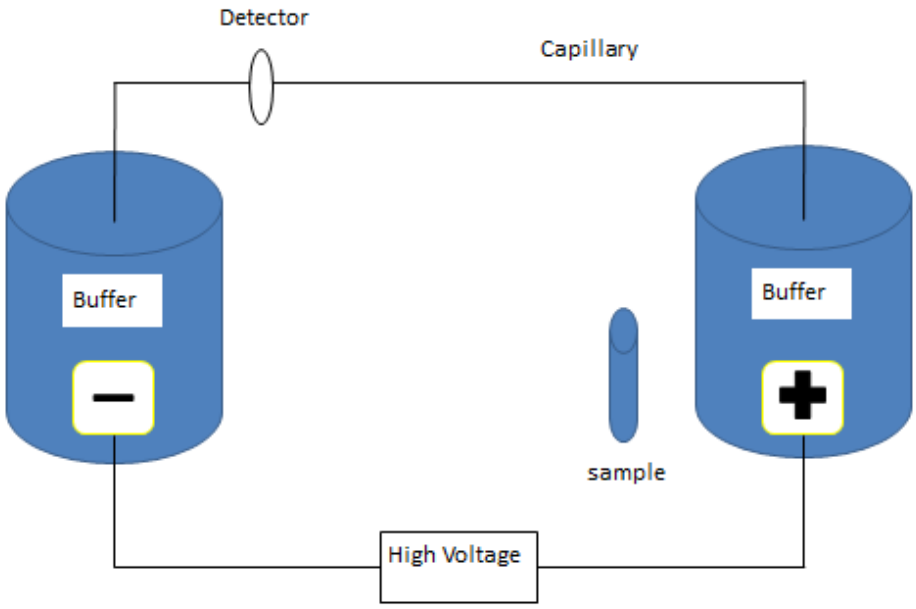

Figure 1.11 Capillary electrophoresis system schematic.

potential. The force, F_E, imparted by the electric field is directly proportional to its effective charge, q, and the electric field strength, E, according to the following equation[16]:

$$F_E = qE$$

The movement of an ion in this electric field is opposed by a retarding frictional force, E_f, which is proportional to the velocity of the ion, v_e, and the friction coefficient, f, according the following equation[16]:

$$F_f = fv_e$$

This ion almost instantaneously reaches a steady state velocity where the acceleration force equals the frictional force according to the following equations[16]:

$$qE = fv_e$$

$$v_e = \frac{q}{f}E = \mu_e E$$

where μ_e is the electrophoretic mobility of the ion

When a voltage is applied across the capillary, containing a buffer solution, an electrical double layer develops at the silica/solution interface, this is also known as the Stern layer. At pH values greater than 3, the surface silanol groups are negatively charged. Buffer cations congregate along the negative surface as a double layer, one immobilized and one a diffuse outer layer, a doubly diffused layer known as the Stern layer, as mentioned previously.

Electroosmosis refers to the movement of the buffer in the capillary under the influence of an applied electric potential. The positive ions in the diffuse part of the Stern layer migrate towards the negatively charged cathode, in doing so, they entrain the waters of hydration, resulting in the electroosomtic flow (EOF). The EOF velocity, v_{eo}, is defined by the following equations[16]:

$$v_{eo} = \mu_{eo} E$$

$$where\ \mu_{eo}\ is\ the\ electroosmotic\ mobility$$

$$\mu_{eo} = \frac{\varepsilon \xi}{4\pi\eta}$$

$$where\ \varepsilon\ is\ the\ dielectric\ constant\ of\ the\ buffer$$

$$\xi\ is\ the\ zeta\ potential$$

$$\eta\ is\ the\ buffer\ viscocity$$

Zeta potential is the potential developed at the capillary wall-buffer interface and is largely dependent on the electrostatic nature of the capillary surface and to a smaller extent, the ionic strength of the buffer.[16] In a fused silica capillary, the EOF is diminished at low pH due to the protonation of the silanol surface, causing a decrease in zeta potential. Another consideration, high ionic strength buffer systems, decrease the EOF due to the collapse of the double layer.[16]

The EOF is greater than the electrophoretic migration velocities (the velocity of the ion as it moves towards the electrode of interest) of the individual ions, producing bulk flow. When sample analytes are introduced into the CE

system, they migrate based on their electrophoretic mobility, essentially size and charge. Cations move towards the cathode (negatively charged) and anions move towards the anode (positively charged). Small ions move faster than larger ones, and multiply charged ions move faster than singly charged ions.[15] Neutral species move with the same velocity as the bulk flow, hence, it is a measure of the system EOF (Figure 1.12).[17]

The apparent mobility, μ_{app}, of an analyte is a vector summation of the electrophoretic mobility, μ_e, of the analyte and the electrophoretic mobility of the buffer solution, μ_{eo}, according to the following equation[16]:

$$\mu_{app} = \mu_e + \mu_{eo}$$

The apparent velocity, v_{app}, of an analyte is directly proportional to its apparent mobility and the electric field strength across the capillary according to the following equation[16]:

$$v_{app} = \mu_{app} E$$

Another advantage of CE is the minimal sample volume used. Injection volumes are in the picoliter to nanoliter range. Sample injection can be done two ways, hydrodynamically or electrokinetically. The amount of sample injected, hydrodynamically, is described by Poiseuille's equation[16]:

$$V_c = \frac{\Delta P \pi d^4 t}{128 \eta L_{eff}}$$

$$where\ V_c\ is\ the\ calculated\ injection\ volume$$

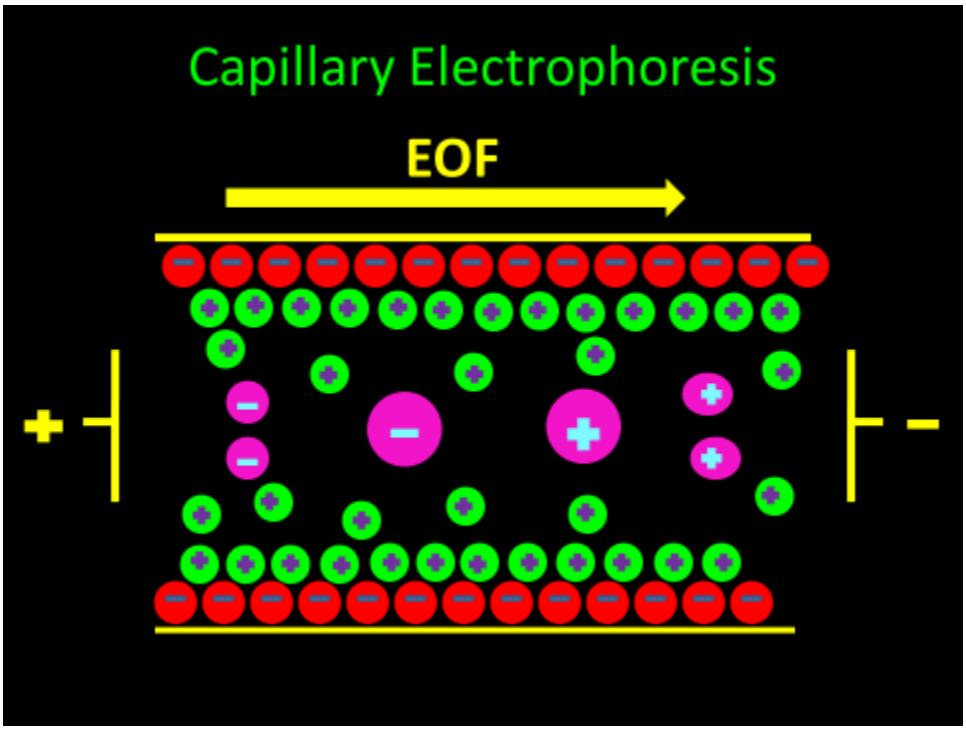

Figure 1.12 Capillary electrophoresis separation mechanism.

$$\Delta P \text{ is the pressure difference between the ends of the capillary or pressure applied}$$

$$d \text{ is the inner diameter of the capillary}$$

$$t \text{ is the injection time}$$

$$\eta \text{ is the sample viscocity}$$

$$L_{eff} \text{ is capillary length to the dector}$$

Electrokinetic injection is expressed by the following equation[16]:

$$Q_i = v_{app}\left(\frac{k_b}{k_s}\right) t\pi r^2 C_i$$

$$\text{where } Q_i \text{ is the inner diameter of the capillary}$$

$$t \text{ is the injection time}$$

$$\frac{k_b}{k_s} \text{ is the ratio of conductivities of the separation buffer and sample}$$

$$r \text{ is the capillary radius}$$

$$C_i \text{ is the molar concentration of the } i^{th} \text{ analyte}$$

Electrokinetic injections are not suitable for quantitative experiments because the injections are biased as a result of each analyte having a different mobility.

Joule heating is a consequence of the resistance of the solution to the flow of current. The heat produced, H, is directly proportional to the applied voltage

between the electrodes, V, the electric current, I, and time, t, according to the following equation[16]:

$$H = VIt$$

2. Chapter 2 : Pretreatment of Lignocellulosic Biomass Using Fenton Chemistry

Parts of this dissertation chapter are taken from Kato, D. M., Elia, N., Flythe, M., Lynn, B. C., "Pretreatment of lignocellulosic biomass using Fenton chemistry." *Bioresource Technology*. 162 (2014), 273-278.

2.1. Introduction

The need for alternate energy sources has led to renewed interest in sustainable sources of energy such as lignocellulosic plant materials or biomass. Biomass feedstocks like miscanthus (*Miscanthus giganteus*), switchgrass (*Pancium virgatum*), wheat (*Triticum aestivum*) straw, and corn (*Zea mays*) stover are dedicated energy crops or agricultural waste products, both of which are renewable and can be utilized for biofuel production.[18] Biomass to biofuel conversion into two and four carbon alcohols occurs via microbial fermentation. However, the fermentation process is hindered by the recalcitrant nature of lignocellulosic biomass to chemicals and enzymes.[19]

As previously discussed in Chapter 1, cellulose is highly sought after because it can be microbially converted to biofuels such as acetone, butanol and ethanol, and is also highly utilized in the paper industry. However, lignin negatively affects cellulose availability and must be removed or modified by pretreatment.

There are various types of pretreatment strategies utilized such as physical, thermochemical and biochemical methods or a combination of the three strategies. An example of a physical pretreatment is ball milling or disk milling. This involves the grinding of material to finely ground particle sizes, approximately 0.2-2 μm. This approach has lower cellulose conversion

efficiency relative to other pretreatment strategies.[2] Thermochemical pretreatment strategies commonly used are, pyrolysis or gasification of biomass to produce synthetic gas or syngas. The gas is then reformed into fuel using either a catalytic process or by biological conversions.[2] Other chemical pretreatments such as alkaline peroxide, lime, etc. degrade lignin providing increased access to cellulose. Acid pretreatments have the potential to provide enriched cellulosic materials, but can also hydrolyze cellulose into glucose units, eliminating the need to hydrolyze the polysaccharide.[2] Table 2.1 reviews the reaction conditions, advantages and disadvantages of the various pretreatment strategies.[2] An ideal pretreatment protocol removes the need to reduce biomass particle size, prevents cellulose degradation, and limits formation of microbial inhibitory compounds.[8b, 11]

Lignocellulolytic *Basidiomycetes* have the ability to degrade the polymeric components of biomass and are split into two categories: white-rot fungi and brown-rot fungi.[11] Exposure to white-rot fungi, like *Phanerochaete chrysosporium*, or brown-rot fungi, like *Gloeophyllum trabeum*, are examples of an *in vivo* biochemical pretreatment using Fenton (iron/peroxide) chemistry.[20] These fungi have enzymes, such as peroxidases, some of which have iron at the catalytic center, which slowly degrade lignin via the catalytic decomposition of hydrogen peroxide by the ferrous ion, generating hydroxyl radicals, also known as Fenton chemistry.[21]

In order to conduct solution phase Fenton chemistry, a metal, typically iron, will serve as an electron donor to hydrogen peroxide which then

disproportionates. This is also known as the catalytic decomposition of hydrogen peroxide shown in the basic reaction scheme by Haber and Weiss.[22]

Table 2.1 Lignocellulosic pretreatment strategies.[2]

Pretreat-ment	Chemicals Used	Composition of Solid Post Pretreatment	Composition of Liquid Post Pretreatment	Process Conditions	Advantages	Disadvantages
Disk milling	N/A	Whole Biomass	N/A	Milling (10-30 mm) & grinding, particle size (0.2-2 μm)	no chemicals used, scalable	poor sugar conversion, high energy intensive process
Dilute acid	Dilute sulfuric acid	Enriched cellulose and some hemicellulose	Soluble xylose	140-190 °C, 0.1-2% H_2SO_4, 1-40 min	applicable to large range of materials, produce hydrolyzed xylose during pretreatment	need expensive waste alloy reactor, difficult to control reaction conditions, expensive to remove acid and recycle water
Concentrated acid	H_2SO_3, HF, HCl, H_3PO_4, HNO_3	Condensed lignin	Soluble glucose & xylose, or soluble cellulose which is a precipitate	Shorter reaction time	do not need enzymes to hydrolyze cellulose, effective on softwoods	corrosion, energy intensive acid recovery step
Organosolv	Methanol, ethanol, acetone, ethylene glycol & tetrahydrofurfuryl alcohol	Enriched cellulose & most of hemicellulose	Lignin and some of hemicellulose	acetone-water pretreatment (acetone:water 1:1 molar	separates pure lignin, lignin removal, increased	high risk of high pressure operation, flammability,

				ratio) @ 195 °C	cellulose digestibility	volatility of solvents
Ammonia Fiber Expansion (AFEX)	Liquid or gaseous anhydrous ammonia	Whole Biomass	N/A	100-140 °C, 1:1-2:1 ammonia to biomass loading, 30-60 min	Volatile ammonia can be recovered and released, dry to dry method, lower reaction by-products	Safety precautions for handling ammonia, ammonia recovery step adds cost, not efficient for hardwood
NaOH	NaOH	Amorphous cellulose & some hemicellulose	Soluble lignin, some hemicellulose	NaOH	conversion of highly reactive cellulose, soluble lignin	longer reaction times, larger water usage, scale-up issues, expensive recovery costs
Alkaline peroxide	NaOH, H_2O_2	Enriched cellulose & some hemicellulose	Soluble degraded lignin & some hemicellulose	0.5-2% NaOH, 0.125 g H_2O_2/g biomass, 22 °C, 48 h	milder conditions, scalable, used by paper industry	larger water usage, energy content of lignin is lost due to oxidation
Lime	CaO with & without oxygen	Whole Biomass	N/A	25-160 °C, 120 min-wks, 0.07-5g CaO/g biomass	can be done using inexpensive reactor systems, dry to dry process, less reaction by-products	larger water usage, long reaction time, expensive to recovery process
Steam	Steam & SO_2	Enriched	Soluble	180-210 °C, 1-	works well for	expensive

explosion		cellulose	hemicellulose	120 min	both hardwood and herbaceous biomass	reactor system and requires high pressure
Ionic liquids	1-allyl-3-methylimidazoliumchloride ([AMIM]Cl), 1-ethyl-3-methylimidazoliumacetate ([EMIM]Ac)	Enriched lignin & some of hemicellulose	Lignin and some of hemicellulose	100-150 °C, few min to hours	Carbohydrate loss is low	high solvent cost, high solvent loading, high cost of solvent regeneration
Biological	Microbes like fungi and bacteria	Whole Biomass (with reduced cellulose and hemicellulose content)	N/A	25-30 °C, solid state fermentation, 10-15 days	Mild conditions, low energy consumption, no chemicals used	slow process and slow throughput, needs to be continuously monitored, large space requirements

$$Fe^{2+} + H_2O_2 \rightarrow Fe^{3+} + OH^{\cdot} + OH^{-}$$

The hydroxyl radicals will then conduct a radical chain reaction on any organic compound in close proximity.

Biochemical pretreatment can be a time/energy intensive procedure with low throughput and requires continuous monitoring. In attempt to mimic white-rot and brown-rot fungi enzymes, solution phase Fenton chemistry provides a non-selective oxidation of organic compounds.[20c, 23] Solution phase Fenton chemistry holds the potential to provide a quick, higher throughput, straight forward and efficient pretreatment for biofuel production.[24] The hypothesis and goal of this study is that solution based Fenton chemistry will enhance cellulose bioavailability.

This study will show the effectiveness of solution phase Fenton chemistry as a pretreatment on various biomass feedstocks. Utilization of lignin and enzymatic saccharification assays will evaluate the ability of solution phase Fenton pretreatment to make cellulose more bioavailable for microbial fermentation leading to biofuel production from various biomass feedstocks.

2.2. Methods

All chemicals of reagent grade were obtained and used without further purification. Ferrous chloride tetrahydrate ($FeCl_2 \cdot 4H_2O$), potassium iodide, ammonium molybdate, ammonium hydroxide, sulfuric acid, starch, sodium thiosulfate and hydrogen peroxide (H_2O_2, 50%) were purchased from Thermo Fisher Scientific (Waltham, MA, USA). *Trichoderma reesei* cellulase enzyme

was obtained from Alltech (Nicholasville, KY, USA). Distilled water (18 MΩ) was used to make appropriate solutions/dilutions. Miscanthus, switchgrass, corn stover and wheat straw samples (all ~ 2 mm particle size) were obtained from collaborators in the Michael Montross Laboratory, University of Kentucky, Lexington, KY, USA.

Solution phase Fenton pretreatment

In a typical Fenton pretreatment experiment, 10 grams of dry biomass (~ 2 mm) was further ground using a commercial coffee grinder (Hamilton Beach Fresh-Grind coffee grinder model #80335 to ≤ 2 mm particle size). The biomass was added to an Erlenmeyer flask (1000 mL) followed by addition of 100 mL of an aqueous Fe^{2+}, as the $FeCl_2 \cdot 4H_2O$ salt, solution and 100 mL of the specified hydrogen peroxide solution. This stirred mixture was allowed to react for a specified amount of time according to individual experiments. Upon filtration, the solid was dried (105 °C) overnight and the filtrate was kept for future experimentation.[24-25] Control experiments were conducted by adding ground, dry biomass (10 g) to an erlenmeyer flask (1000 mL) with distilled water (18 MΩ, 200 mL). The suspension was left to react for a specified amount of time according to individual experiments. Upon filtration, the solid was dried (105 °C) overnight and the filtrate was kept for future experimentation.

Hydrogen peroxide consumption

Hydrogen peroxide consumption assays were conducted using an iodometric titration according to the published procedure from US peroxide.[26]

At various time points, an aliquot of supernatant (1 mL) was taken from the suspension and weighed. Distilled water (50 mL), 4% sulfuric acid solution (10 mL), 1% (w/v) KI solution (10 mL), and ammonium molybdate solution (0.4 M, 2 drops) were added to the procured aliquot followed by a titration with sodium thiosulfate (0.1 N) to a faint yellow color. Upon the addition of a 1% (w/v) starch solution (2 mL), titration proceeded until completion, indicated by a flash of blue color.[26]

Enzymatic Saccharification

Enzymatic saccharification assays were conducted according to the published National Renewable Energy Laboratory (NREL) protocols with slight modifications.[27] Biomass feedstocks were added to a glass test tube with cellulase provided by Alltech, Lexington, KY, USA, (150 mg, activity: 56 FPU/mL), distilled water (5 mL) and 0.1 M sodium citrate buffer pH 4.8 (5 mL). The reaction tubes were heated in a sand bath (50 °C) and rocked overnight. Glucose was measured using an over the counter Abbott Precision Xtra glucometer and Abbott Precision Xtra blood glucose test-strips purchased from Thermo Fisher Scientific (Waltham, MA, USA) in order to conduct a relative quantification of glucose.

Lignin determination

Acid-soluble (ASL) and acid-insoluble (AISL) lignin assays were conducted according to the National Renewable Energy Laboratory (NREL) procedures.[28] Briefly, biomass (300 mg) was weighed out into a glass culture

tube and dried (105 °C) overnight to determine the total solids. A 72% sulfuric acid solution (2 mL) was added, mixed and incubated in a water bath (30 °C, 1 hour, stirring every 10 min). The suspension was diluted to a 4% sulfuric acid solution with distilled water (18 MΩ), transferred to an autoclavable bottle, and autoclaved on a 40 min, 121 °C, liquid cycle. It was then vacuum filtered using ashless quantitative filter paper in order to prevent material loss during transfer. The filtrate was analyzed with a single beam UV-VIS spectrophotometer (Cary 50 scan, Varian) at 205 nm to determine ASL, and the solid remained on the ashless filter paper and was transferred to a constant weight crucible to dry overnight (105 °C). The sample was reduced to ash in a muffle furnace for 4 hours (575 °C) to determine AISL.[28]

Total organic carbon (TOC) analysis

Total organic carbon (TOC) analyses were conducted using a Shimadzu TOC 5000A. Control and Fenton pretreated filtrates were diluted 1:3 with distilled water (18 MΩ). Total organic carbon was determined based on external calibration curves conducted using the instrument software by subtracting the inorganic carbon from the total carbon.

2.3. Results and Discussion

Solution based Fenton chemistry pretreatment

Due to the recalcitrant nature of biomass, pretreatment is required to increase cellulose conversion efficiency for biofuel production. A variety of fungal and chemical pretreatment methods have been studied.[7, 24-25, 29] White-rot fungal pretreatment utilizes enzymes that generate hydroxyl radicals through *in*

vivo Fenton chemistry. These hydroxyl radicals have been shown to degrade lignin.[20b, 20c, 23b, 23c, 30] In attempt to mimic the ability of white-rot fungi enzymes to degrade lignin, solution based Fenton chemistry was used for hydroxyl radical generation with the goal of making cellulose more bioavailable for microbial fermentation.[23b, 25a, 31] However, treatment with high concentrations of iron and hydrogen peroxide can lead to cellulose degradation and radical scavenging, preventing the reduction of the ferric ion and further hydroxyl radical formation.[22, 24, 25b, 32] Additionally, studies have shown one set of reagent parameters are not optimal across all biomass feedstocks.[24] Therefore, experiments were conducted in order to determine the appropriate hydrogen peroxide percentage, iron concentration and mass to volume ratio for each biomass feedstock. The experimental parameters were assessed using enzymatic saccharification and hydrogen peroxide consumption assays.

Hydrogen peroxide consumption assays provide an insight to the rate of H_2O_2 consumption (weight percent) when the biomass is treated with various amounts of reagent. The Fenton reaction is an oxidation in which an electron donor, iron, donates an electron to hydrogen peroxide generating a hydroxyl radical, thus the decomposition of H_2O_2.[22, 24, 25b, 32] A constant, shallow slope of H_2O_2 consumption is thought to provide optimal reaction parameters to conduct solution phase Fenton chemistry. Using a 10 gram sample and a starting concentration of approximately 5% H_2O_2, various amounts of Fe^{2+} (aq) were added and the peroxide consumption of biomass, according to the experiment, was determined as a function of time (Figure 2.1). As predicted, low amounts of

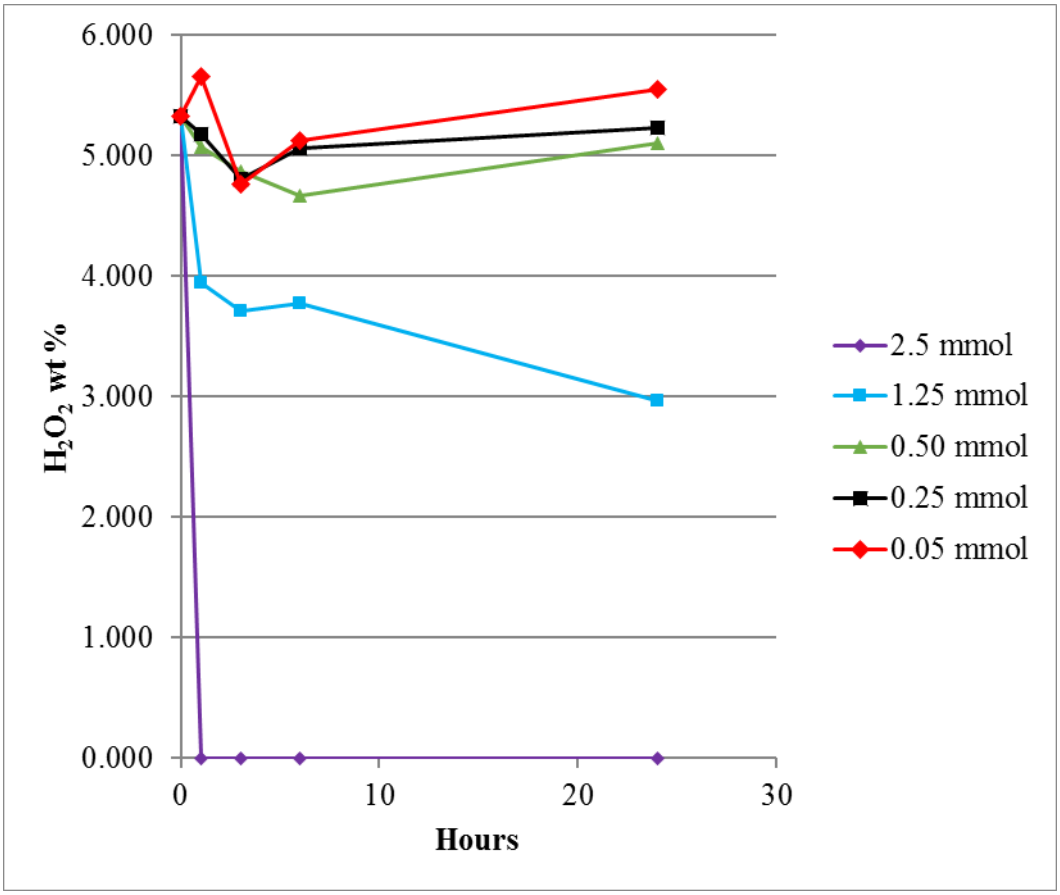

Figure 2.1 Hydrogen peroxide consumption of various concentrations of ferrous chloride tetrahydrate.

iron (10, 50 and 100 mg $FeCl_2 \cdot 4H_2O$; 2.8, 14, and 28 mg Fe^{2+} respectively) did not show H_2O_2 consumption in a 24 hour period. Without peroxide consumption, it can be inferred that hydroxyl radicals are not generated. At 250 mg $FeCl_2 \cdot 4H_2O$ (aq) (100 mL, 70 mg Fe^{2+}) per 10 grams of miscanthus, ~5% H_2O_2 initial concentration, a gradual decrease of peroxide consumption was seen over 24 hours. Higher amounts of iron, 500 mg $FeCl_2 \cdot 4H_2O$ (aq) (100 mL, 140 mg Fe^{2+}) per 10 grams of miscanthus, for example, showed a high rate of hydrogen peroxide consumption, depleting the H_2O_2 concentration within an hour, inferring the prevention of further hydroxyl radical generation and completion of the reaction. Michalska *et al.* (2012) showed an increase in reactants does not provide a more effective reaction, but can lead to secondary reactions and radical scavenger generation, decreasing reaction efficiency. Radical scavenging was also seen in studies done by Kang *et al.* (2005) and Zazo *et al.* (2002).[24, 25b, 32] In attempts to prevent radical scavenging, 250 mg $FeCl_2 \cdot 4H_2O$ (aq) (100 mL, 70 mg Fe^{2+}) per 10 grams of biomass was chosen to be the optimal amount of iron to substrate ratio.

A series of control experiments were conducted to determine that the effects seen from solution phase Fenton chemistry were indeed from the Fenton chemistry and not any single reagent or parameter the biomass was exposed to. Miscanthus was exposed to: 1) water without Fenton reagents, 2) an aqueous metal solution (same mass/volume ratio), no H_2O_2, and 3) various percentage H_2O_2 solutions, no metal. Experimental controls 1 and 2 did not show a significant difference ($P < 0.05$) in enzymatic saccharification assays (data not

shown), and did not show consumption of H_2O_2, which was no surprise due to the absence of H_2O_2 (data not shown). The H_2O_2 consumption assay for experimental control three, where 10 grams of miscanthus were treated with various percentages of H_2O_2 (5.42%, 3.17%, and 1.10%) solutions without metal showed minimal H_2O_2 ($\leq$ 0.21%, 0.14%, and 0.03% respectively) was consumed within a 24 hour period (Figure 2.2). With the absence of the electron donor, iron, Fenton chemistry cannot be conducted.

Reagent ratio (iron : peroxide) experimentation showed 250 mg $FeCl_2 \cdot 4H_2O$ (aq) (100 mL, 70 mg Fe^{2+}), 3% H_2O_2 per 10 grams of biomass provided a steady rate of H_2O_2 consumption and the largest increase in glucose production via enzymatic saccharification (discussed in the following section). Using 250 mg $FeCl_2$ $4H_2O$ (aq) (100 mL, 70 mg Fe^{2+}; per 10 grams of biomass) versus 500 mg $FeCl_2$ $4H_2O$ (aq) (100 mL, 140 mg Fe^{2+}; per 10 grams of biomass) produces a gradual consumption of H_2O_2 over an extended time versus a short, large burst, in addition to a lower probability of radical scavenging.

Enzymatic Saccharification

After reagent concentrations were established, it was necessary to evaluate the effects on cellulose bioavailability of the Fenton pretreatment for various time periods (0-120 hours). Utilizing an enzymatic saccharification of cellulose from untreated and pretreated lignocellulosic biomass to glucose describes the maximum extent of digestibility possible. Enzymatic saccharification assays showed an increase in glucose production relative to untreated control with increasing time of exposure to Fenton pretreatment: 0 hours, being control, 0%, 1

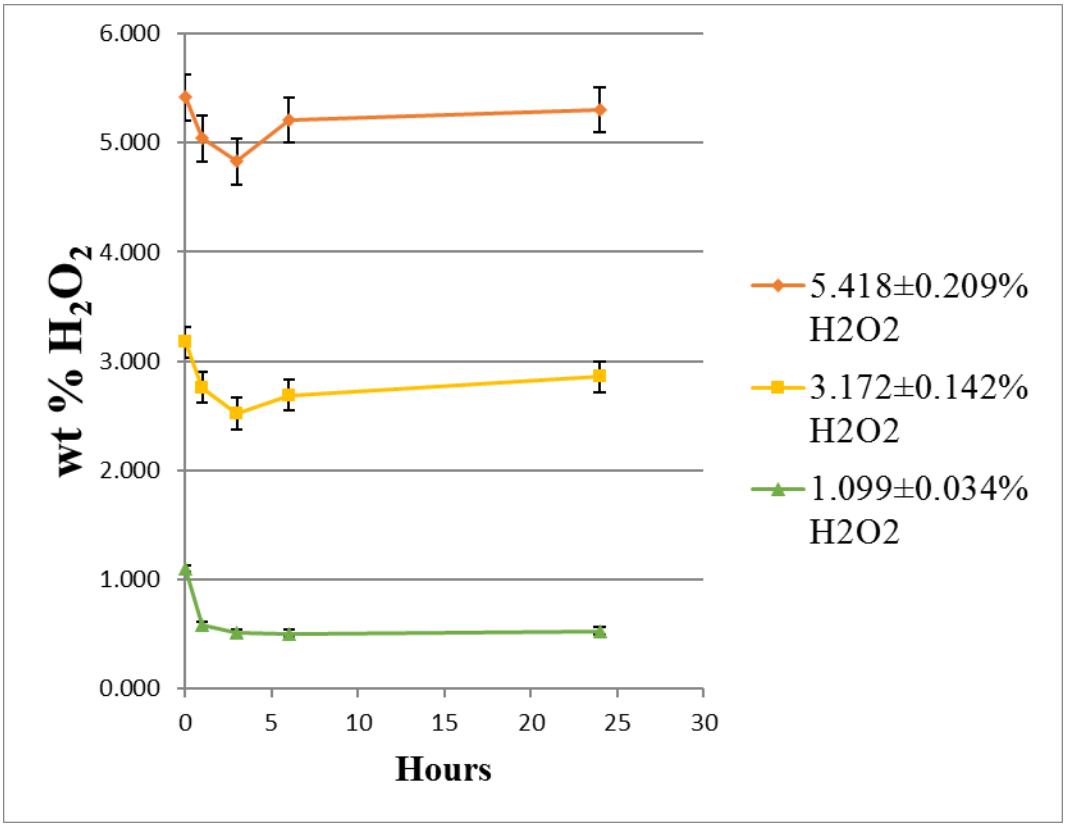

Figure 2.2 Hydrogen peroxide consumption of biomass without metal.

hour – 22% (1.22-fold), 3 hours – 128% (2.28-fold), 24 hours – 92% (1.92-fold), 72 hours – 215% (3.15-fold), and 120 hours – 414% (5.14-fold) increase (Figure 2.3). Pretreatment for 120 hours showed the largest increase in glucose production, thus, suggesting cellulose to be more bioavailable upon 120 hours of Fenton pretreatment. Miscanthus, switchgrass, corn stover and wheat straw were treated with solution phase Fenton chemistry (Figure 2.4), according to the established Fenton protocol discussed in the previous section (10 g – ground, 100 mL 6% H_2O_2, 100 mL 250 mg $FeCl_2$ $4H_2O$ (aq, 70 mg Fe^{2+}) for 120 hours. Enzymatic saccharification showed a significant ($P < 0.05$) increase in glucose production relative to the untreated material upon solution based Fenton pretreatment. An average 212% increase upon Fenton pretreatment relative to the untreated material across the four different biomass feedstocks: miscanthus - 219% (3.19-fold), switchgrass - 414% (5.14-fold), corn stover - 80% (1.80-fold), wheat straw - 133% (2.33-fold), as seen in Figure 2.5.

Upon application of a Student's t-test, a significant increase ($P < 0.05$) in enzymatic saccharification suggests Fenton chemistry altered the properties of the four biomass feedstocks to different extents. However, one experimental condition was not optimal across all feedstocks because each lignocellulosic biomass feedstock has a unique composition. It can be suggested that this is demonstrated with the larger increase in enzymatic saccharification for dedicated energy crops, miscanthus and switchgrass. However, upon Fenton pretreatment, all four biomass feedstocks provided a large increase in cellulose bioavailability to *in vitro* cellulase exposure suggesting a reduction in the

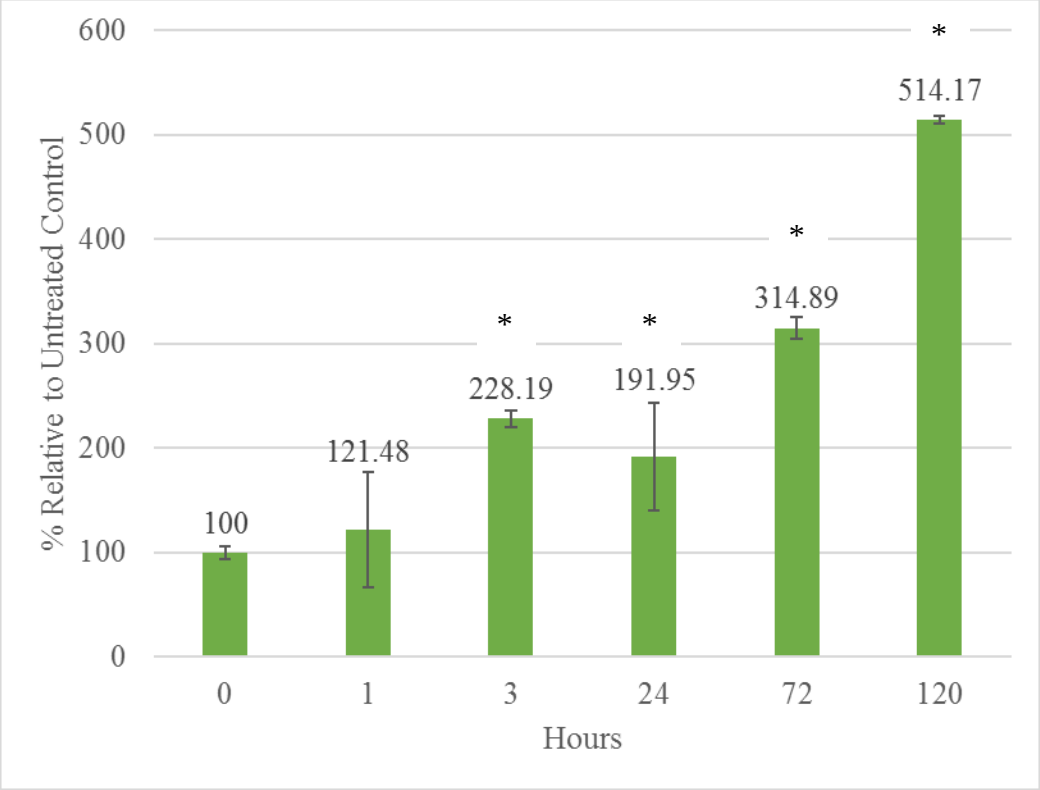

Figure 2.3 Enzymatic saccharification of various times of Fenton pretreatment on switch grass.

(10 g – ground, 100 mL 6% H_2O_2, 100 mL 250 mg $FeCl_2$ $4H_2O$ (aq, 70 mg Fe^{2+}))

Data is shown with error bars indicating ± one standard deviation. [*: statistically significant ($P < 0.05$)].

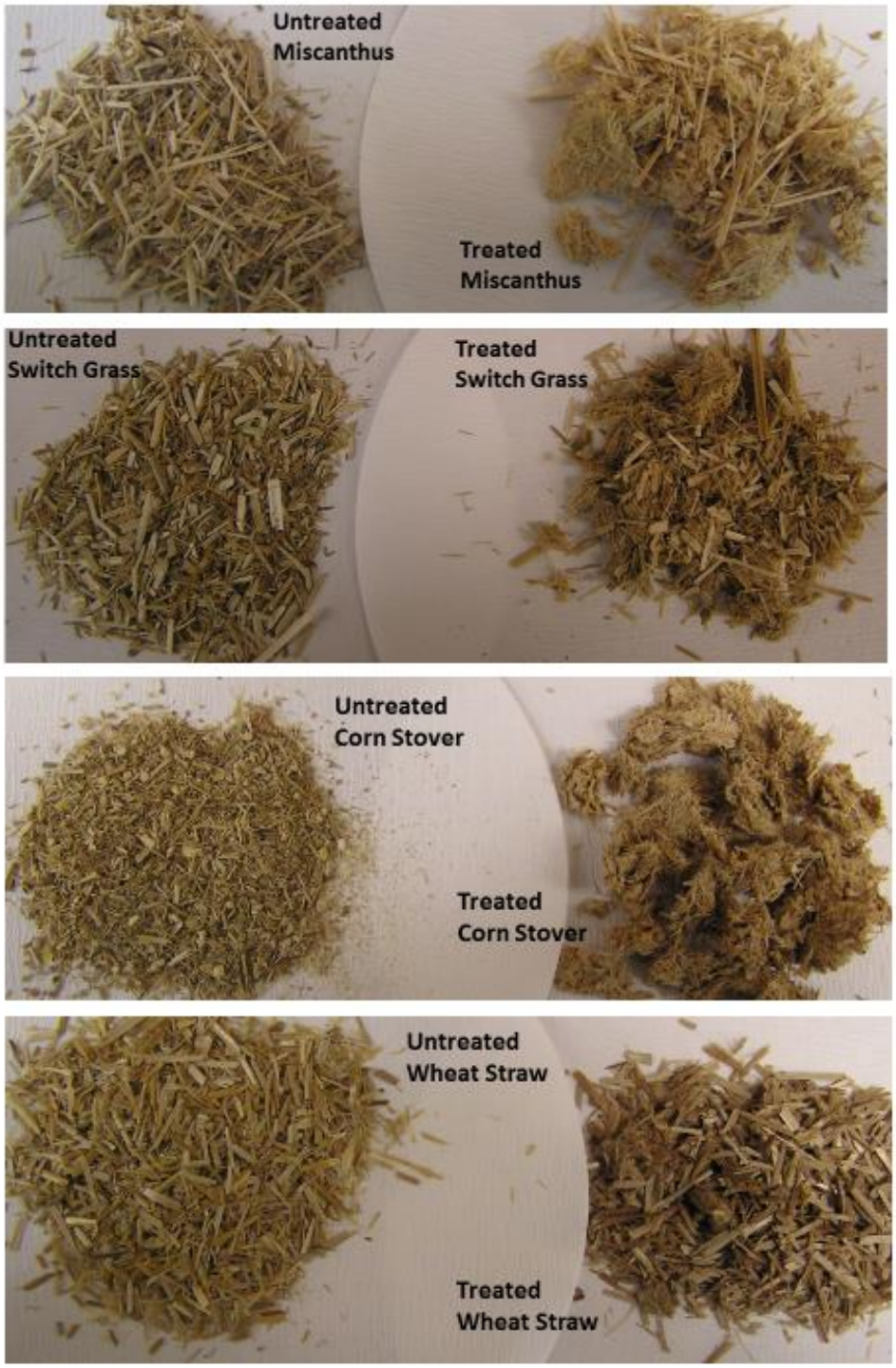

Figure 2.4 Untreated and Fenton pretreated lignocellulosic biomass.

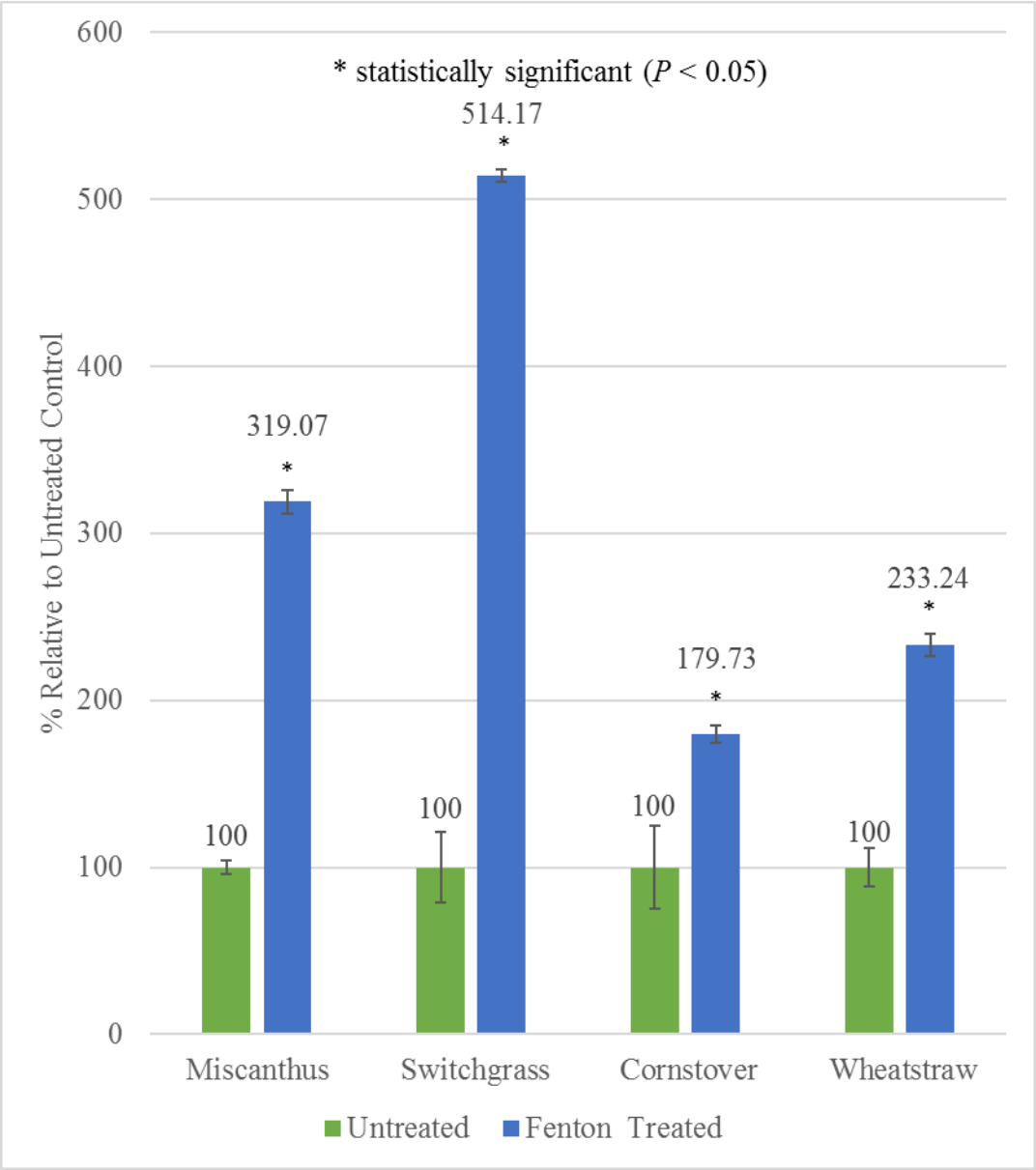

Figure 2.5 Enzymatic saccharification data showing the effects of Fenton pretreatment (10 g – ground, 100 mL 6% H_2O_2, 100 mL 250 mg $FeCl_2$ $4H_2O$ (aq, 70 mg Fe^{2+}) relative to the untreated control on various biomass feedstocks.

Data is shown with error bars indicating ± one standard deviation. [*: statistically significant (P < 0.05)].

recalcitrant nature inherent to lignocellulosic materials. Lignin assays must be conducted to show if solution phase Fenton chemistry is mimicking the ability of fungal *in vivo* Fenton chemistry to degrade lignin.

Lignin assays

Since Fenton pretreated biomass produced an average glucose increase of 212% relative to untreated biomass, questions about the mechanism arise. Was the increase in glucose due to an increase in cellulose bioavailability due to the "delignification" of biomass via solution based Fenton chemistry? To address this question, acid-soluble and acid-insoluble lignin assays were conducted. Figure 2.6, shows the acid-insoluble lignin (AISL) assays for miscanthus, switchgrass, corn stover and wheat straw, untreated and Fenton treated (120 hours) relative to control. An average 8.27% decrease in acid-insoluble lignin present, relative to the untreated biomass, was seen across the four feedstocks. A significant decrease in acid-insoluble lignin content was seen for miscanthus (6.63%), corn stover (14.1%) and wheat straw (8.76%), but switchgrass (3.59%) did not produce a significant ($P < 0.05$) decrease in AISL content. Figure 3 shows the acid-soluble lignin (ASL) content assays for miscanthus, switchgrass, corn stover and wheat straw, untreated and Fenton treated (120 hours) relative to control. An average 33.5% decrease in acid-soluble lignin content was seen across the four feedstocks. Switchgrass (22.6%) and wheat straw (16.8%) showed a significant ($P < 0.05$) decrease in ASL, but miscanthus (4.61%) and corn stover (0%) did not show a significant decrease in ASL relative to the untreated biomass.

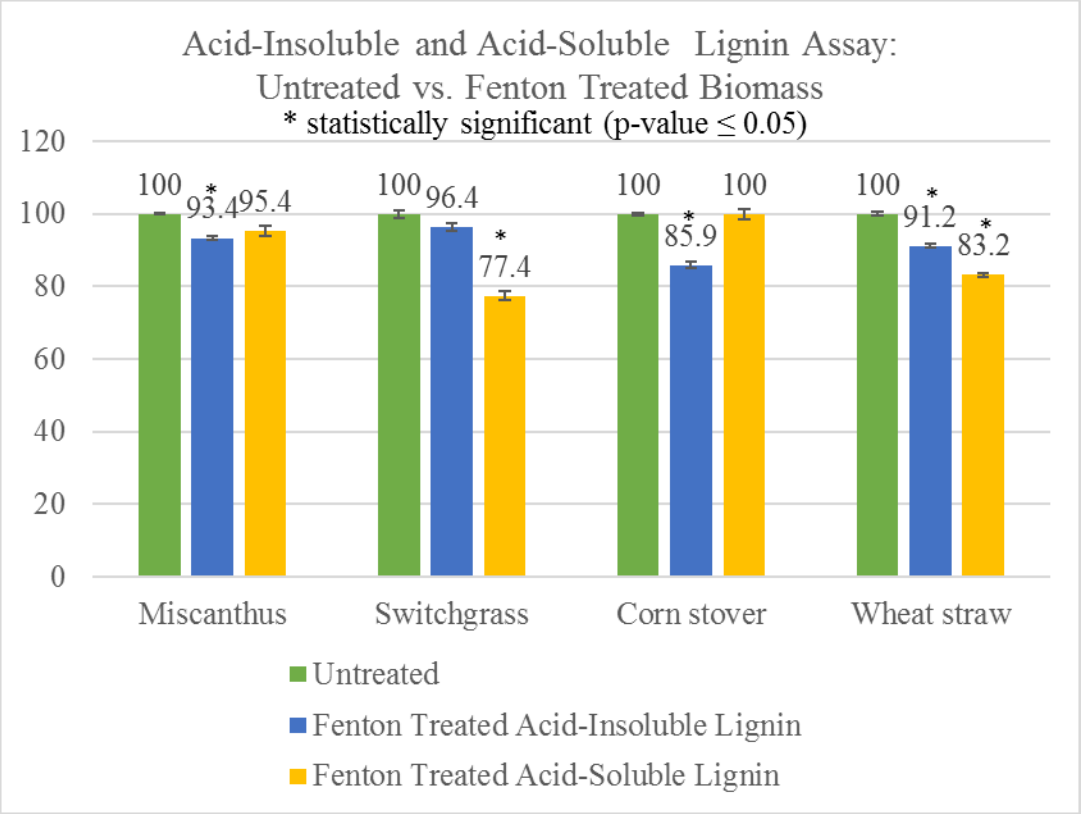

Figure 2.6 Acid-insoluble and acid-soluble lignin assay: Fenton pretreatment (10 g – ground, 100 mL 6% H_2O_2, 100 mL 250 mg $FeCl_2$ $4H_2O$ (aq, 70 mg Fe^{2+}) relative change to untreated control across the various feedstocks.

Data is shown with error bars indicating ± one standard deviation. [*: statistically significant ($P < 0.05$)].

Acid-insoluble and acid-soluble assays showed a slight decrease in lignin content after Fenton pretreatment across the four different biomass feedstocks. However, this slight decrease does not support "delignification", thus, these results do not support the hypothesis that increased cellulose availability is due to extensive lignin degradation. Other mechanisms must be explored to answer the question of bioavailability.

Total organic carbon (TOC)

Enzymatic saccharification showed a significantly large increase in glucose production upon Fenton pretreatment across all four feedstocks. Lignin assays, AISL and ASL, show a minimal decrease in various lignin content across the feedstocks. Total organic carbon (TOC) assays were conducted (Table 2.2) on the filtrates of untreated control, and Fenton treated (120 hour treated samples) miscanthus and switchgrass because those feedstocks showed the largest increase from *in vitro* fermentation. An average 1416 mg/L increase of total organic carbon was detected in the filtrate of Fenton treated biomass. These results were consistent with the small decrease of lignin content upon treatment. From AISL and ASL lignin assays, a large decrease in lignin content was not seen, and TOC analyses of the filtrates, did not suggest large amounts of total organic carbon present after pretreatment which would suggest delignification.

Based on the enzymatic saccharification, AISL, ASL and TOC assays, the hypothesis that solution phase Fenton pretreatment degrades lignin is not supported. Solution phase Fenton pretreatment may not be degrading lignin as seen in *in vivo* Fenton chemistry of white-rot fungi, but it is altering the biomass

Table 2.2. Total organic carbon (TOC) analyses of untreated and Fenton pretreated miscanthus and switchgrass.

TOC	Average (mg/L)	Stdev	RSD	p-value
10g Miscanthus, 200 mL dI H_2O, FP	117.27	0.87	0.74	
10g Switchgrass, 200 mL dI H_2O, FP	131.38	0.93	0.71	
10g ground Miscanthus, 100 mL 6% H_2O_2, 100 mL 250 mg $FeCl_2$ $4H_2O$ (aq) - 120 hrs	1922.87	43.22	2.25	<0.05
10g ground Switchgrass, 100 mL 6% H_2O_2, 100 mL 250 mg $FeCl_2$ $4H_2O$ (aq) - 120 hrs	1158.44	20.02	1.73	<0.05

in a way that makes cellulose more bioavailable as seen in the significantly large increase in enzymatic saccharification.

An alternative pretreatment strategy, ammonia fiber expansion (AFEX), adds liquid ammonia to biomass under moderate pressure (100-400 psi) and temperature (70-200 °C) before rapidly releasing the pressure. It has been shown that this pretreatment strategy disrupts the crystalline nature of cellulose and hydrolyzes hemicellulose. In addition, AFEX has been shown to increase the size of the micropores on the cell wall. Therefore, all the aforementioned ramifications of the AFEX pretreatment significantly increases the cellulose conversion efficiencies. Thus, we postulate that Fenton pretreatment may possibly clip or alter the macrostructure of lignin, similar to the ammonia fiber expansion (AFEX) pretreatment, in a way that allows cellulase enzymes to better access cellulose.[6]

2.4. Conclusion

In an attempt to mimic white-rot fungi lignin degradation via *in vivo* Fenton chemistry, solution phase Fenton chemistry (10 g biomass, 176 mmol hydrogen peroxide and 1.25 mmol Fe^{2+} in 200 mL of water) was applied to four different biomass feedstocks. An enzymatic saccharification of Fenton pretreated biomass showed an average 212% increase relative to untreated control across all four feedstocks ($P < 0.05$, statistically significant). Microbial fermentation, of the same Fenton pretreated biomass showed a three-fold increase in gas production upon a sequential co-culture with C. *thermocellum* and C. *beijerinckii*, conducted by our collaborators in the Dr. Michael Flythe

laboratory. Based on the enzymatic saccharification and microbial fermentation experiments, it can be suggested that enzymes and microbes were better able to access the cellulosic component in biomass relative to the untreated biomass. These results demonstrate the use of solution phase Fenton chemistry as a viable pretreatment method to make cellulose more bioavailable for microbial biofuel conversion. Therefore, further evaluation of lignocellulosic biomass exposed to solution based Fenton pretreatment could shed light to the mechanistic questions generated during this study.

3. Chapter 3 : A One-step Synthesis of Arylglycerols

3.1. Introduction

Lignin is a complex heteropolymer composed of three phenylpropanoid units: *p*-coumaryl (H), coniferyl (G), and sinapyl (S) alcohols, or monolignols (Figure 3.1), as previously discussed .[33] Academic and industrial interest in lignin chemistry has significantly increased due to the role lignin plays in hindering hydrolysis of cellulose used for pulping or biofuel processing. Lignins from different plant sources contain different monolignol compositions. Additionally, the same feedstock harvested from the same field during different times of the year can display changes in the ultrastructural composition due to the environmental conditions.[2] Genetically modified lignin is being studied in attempts to enhance lignin extraction efficiency, increasing ease of cellulosic hydrolysis.[34] Compositional changes in plant cell wall and differences in ultrastructure greatly influence the pretreatment strategy and the conversion efficiencies.[2] Pretreatment has the potential to drastically change the properties of biomass (specific surface area, cellulose crystallinity index, degree of polymerization, lignin content, etc.).[2] As discussed previously, solution based Fenton pretreatment made cellulose more bioavailable to both enzymes and microbes, however, it is unknown how this occured. In order to study Fenton pretreatment on biomass, there is a need for better methods to obtain compositional and structural information of lignin.[35]

It has been long recognized that lignin is a material of significant non-uniformity and variability, thus, there are large challenges in the elucidation of

a)

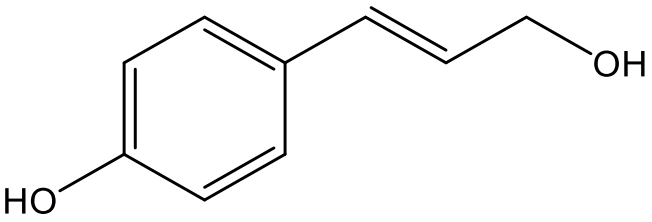

b)

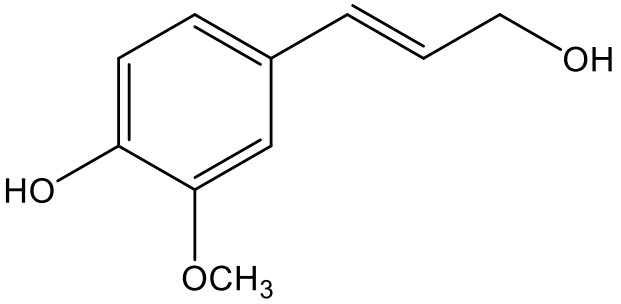

c)

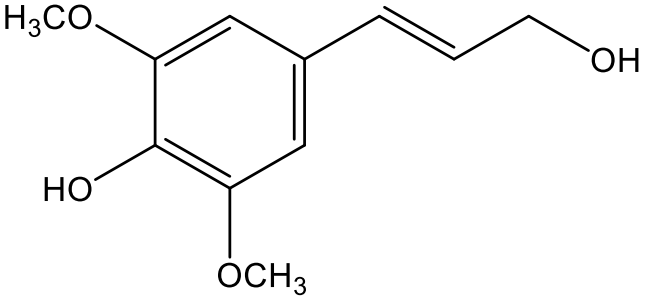

Figure 3.1 Monolignol structures a) *p*-coumaryl alcohol (H) b) coniferyl alcohol (G) c) sinapyl alcohol (S).

structural units.[36] As a large heteropolymer, lignin has been studied in its monomeric subunits via analytical lignin degradation techniques. These analytical degradation techniques hydrolyze various linkages of the lignin polymer in order to assess monomeric ratios. Proper elucidation of the lignin structure is highly dependent on the selectivity and reliability of these analytical degradation methods used.[37] Thioacidolysis is a commonly used analytical degradative method which has been used to study an array of lignocellulosic plant materials. There are a variety of analytical lignin degradation strategies that help to fill in the "picture puzzle" of lignin.

Permanganate oxidations degrade the propyl side chains attached to the aromatic ring to carboxylic acids (Figure 3.2).[36, 38] Permanganate oxidations reveal the pattern of substitution on the aromatic ring.[38] Nitrobenzene and cupric oxide oxidations can characterize lignins of different botanical origins, and it can differentiate between morphological regions of the plant by providing proportions or ratios of one phenyl propane unit to another, i.e. S/G (Figure 3.3).[36, 38] Ozonolysis is the antithesis of permanganate oxidations. This degradation method destroys the doubled bonds and aromatic rings, leaving the side chains in tact as carboxylic acids (Figure 3.4).[38] The degradation products also retain stereochemistry, thus, providing isomeric information.[38] The next several degradation techniques aim to cleave the main linkage of lignin, the arylglycerol-β-aryl ether, or β-O-4 linkage. Acidolysis is conducted in a 9:1 dioxane:water mixture in acidic solution (0.2 M HCl) at 100 °C. An acidolysis produces a complex mixture of ketone products, Figure 3.5 shows some of the ketones

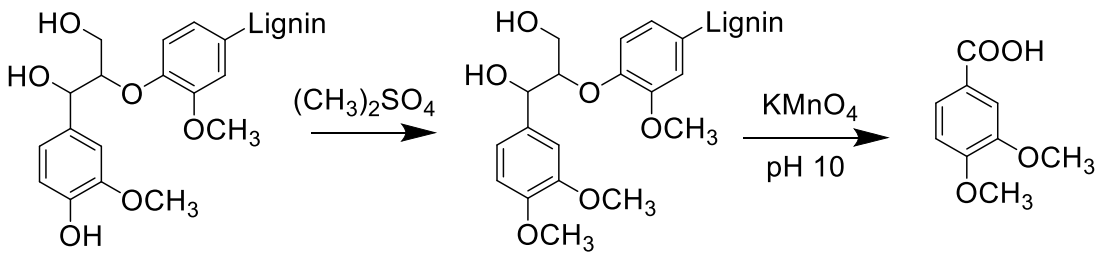

Figure 3.2 Permanganate oxidation of lignin (G-subunits).

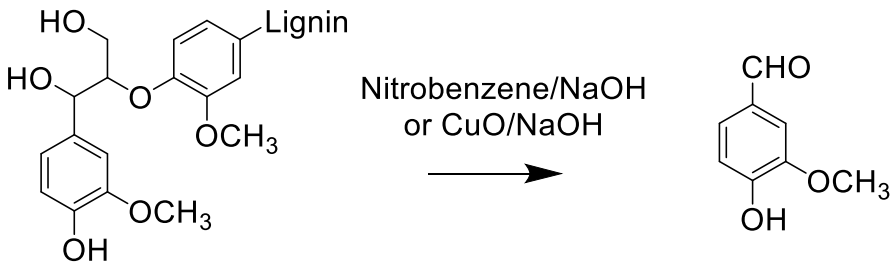

Figure 3.3 Nitrobenzene and cupric oxide oxidation of lignin (G subunits).

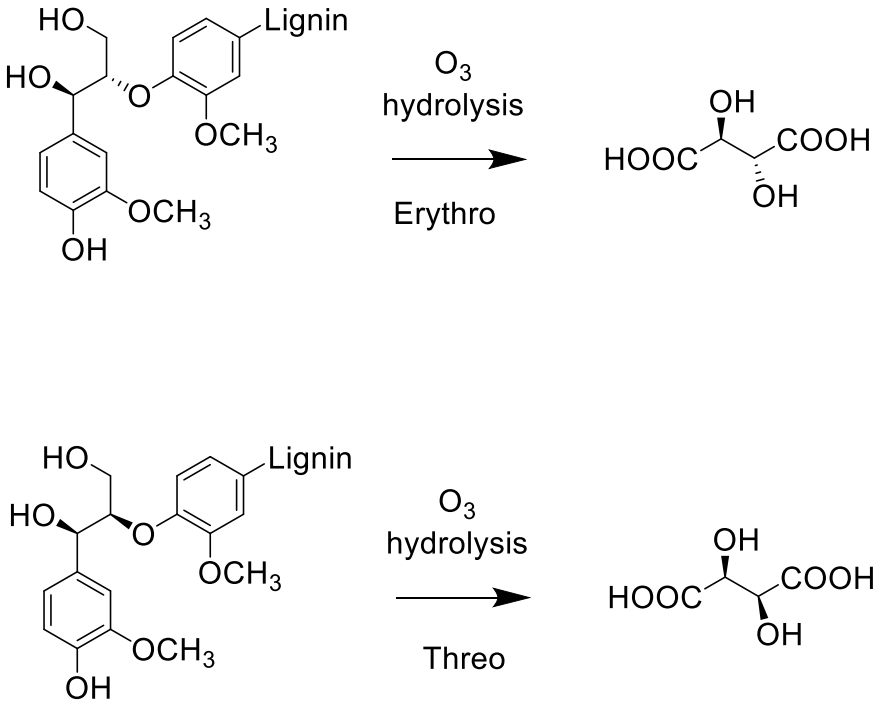

Figure 3.4 Ozonolysis oxidation of lignin (G subunits).

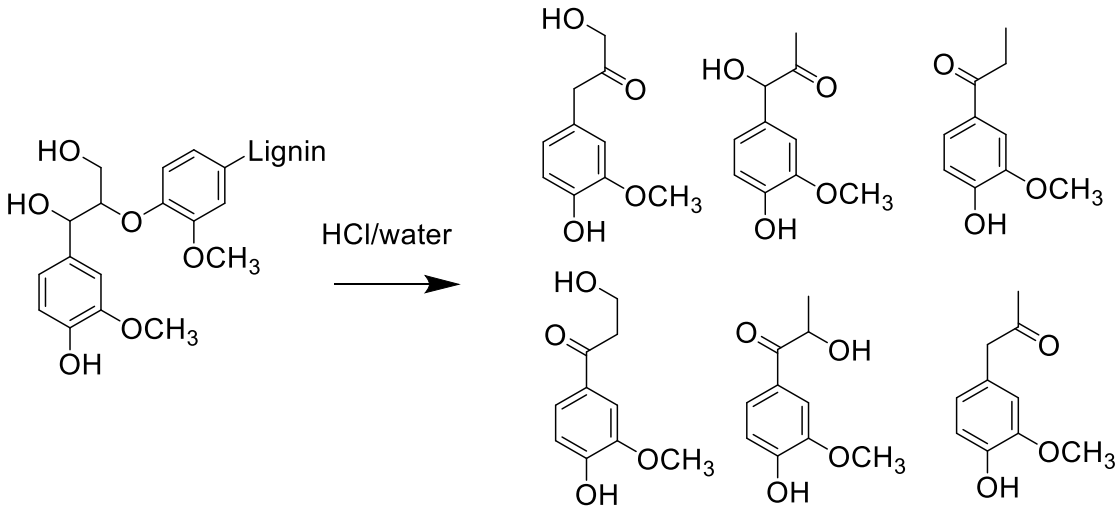

Figure 3.5 Acidolysis of lignin (G subunits).

identified as products of this reaction.[36, 38-39] Thioacidolysis cleaves the same β-O-4 linkage as seen in acidolysis, however, this reaction occurs in anhydrous conditions with ethanethiol and boron trifluoride etherate in dioxane (Figure 3.6).[36, 39-40] Derivatization followed by reductive cleavage (DFRC) also elucidates the β-O-4 linkages, but under milder conditions using no malodorous chemicals. This occurs via a three step process: 1) bromination of the benzylic position and concomitant acetylation of free hydroxyl groups by acetyl bromide 2) the β-O-4 linkages are then cleaved via zinc metal coordination followed by subsequent acetylation of the newly generated phenolic hydroxyl group, as seen in Figure 3.7.[41] Thioacidolysis, which utilizes malodorous chemicals, produces a significantly less complex product stream than acidolysis, and has been shown to provide higher monomeric yields than acidolysis and DFRC. Thus, a more accurate depiction of the lignin polymer.[39, 41]

To review, thioacidolysis is a Lewis acid-catalyzed reaction that depolymerizes lignin by cleaving arylglycerols at the aryl ether bonds (β-O-4 linkages) as seen in the mechanism shown in Figure 3.8.[40] Thioacidolysis monomers are not commercially available, however, the arylglycerol monomers can be synthesized. Subsequently, the hydroxyl units of these arylglycerols can be substituted with thioethyl groups to generate lignin-derived thioacidolysis monomers, as seen in Figure 3.9.[42] The motivation to synthesize these compounds lie in the ability to elucidate quantitative compositional information on various biomass materials. As discussed previously, the composition of lignin is a multivariable dependent polymer. A large challenge of analytical

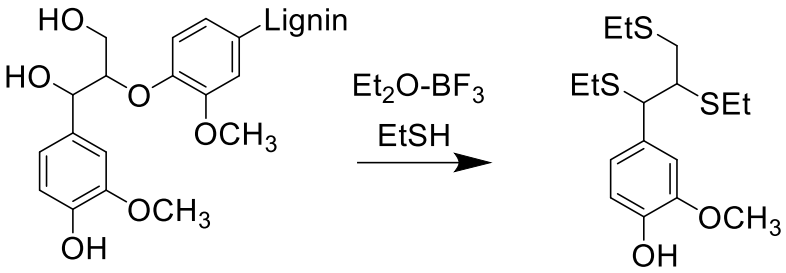

Figure 3.6 Thioacidolysis of lignin (G subunits).

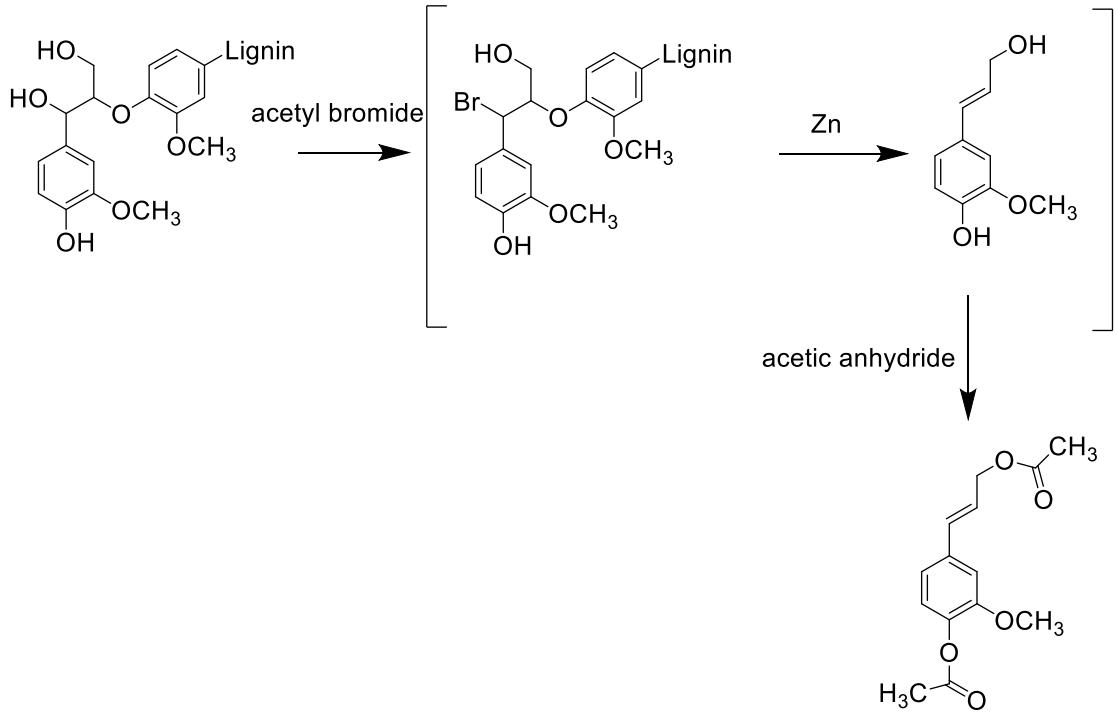

Figure 3.7 Derivatization followed by reductive cleavage (DFRC) of lignin (G subunits).

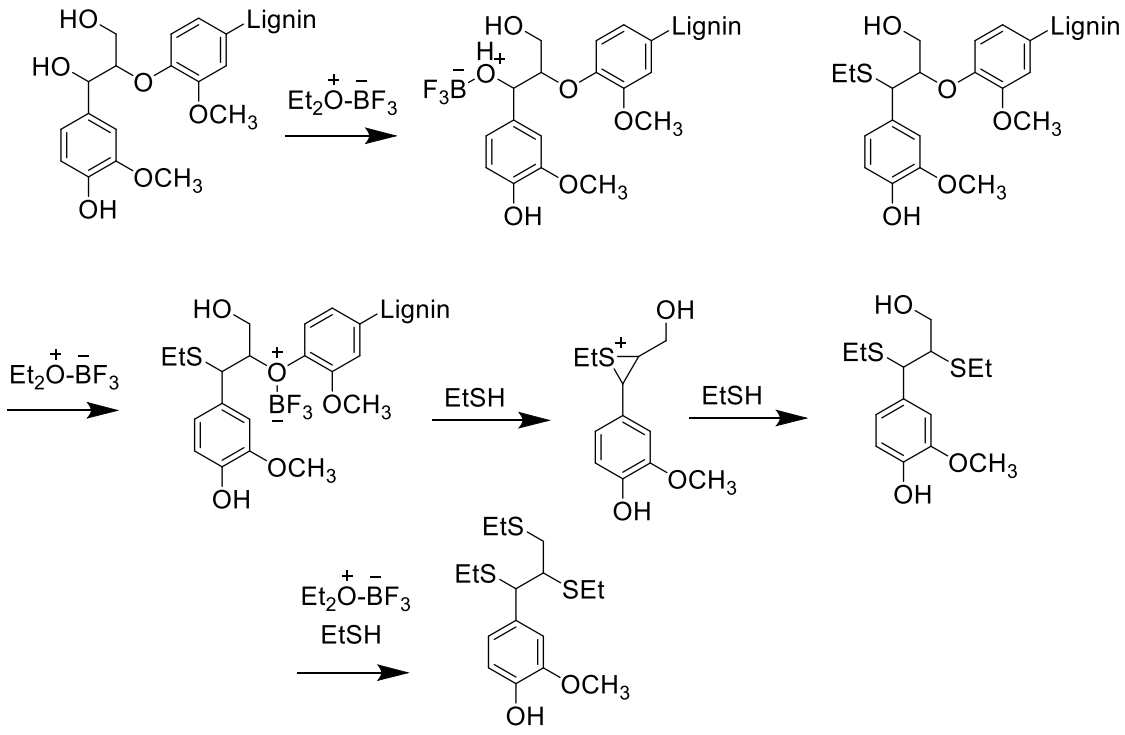

Figure 3.8 Thioacidolysis mechanism of lignin (G subunits).

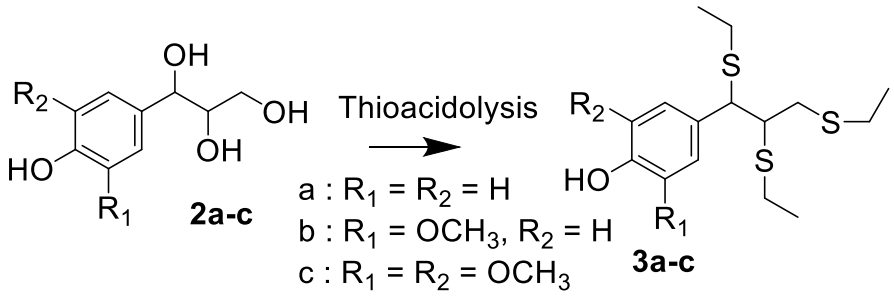

Figure 3.9 Lignin-derived thioacidolysis monomers (compounds 1a-c) synthesized from (compounds 3a-c) from synthesized arylglycerol monomers (compounds 2a-c).

a) H b) G c) S

thioacidolysis to elucidate the lignin structure exists in the inability, thus far, to provide quantitative information on each of the three monomeric subunits that make up lignin. Thioacidolysis provides monomeric information as phenylpropane unit proportions or ratios. However, this type of information does not describe if there is an increase in the numerator or a decrease in the denominator, i.e. an increase in S/G does not describe if S subunits increased or if G subunits decreased. In addition to the already complex problem, interpretation adds another layer of complexity to the already fuzzy "puzzle picture".

Traditional thioacidolysis can be conducted on synthesized arylglycerol compounds in order to obtain analytical standards. These arylglycerol monomers (Figure 3.10, compounds 2a-c) have been previously synthesized and/or isolated from various plant material. However, these synthetic routes/isolations involve labor/time intensive, multi-step, multi-reagent protocols.[42-43]

Epoxides are versatile intermediates commonly utilized in organic synthesis due to the high reactivity of the oxirane ring.[44] Organic peroxy acids (peracids) are oxidizing agents that can be utilized to convert alkenes to oxirane rings which spontaneously open or di-hydroxylate in acidic conditions (Figure 3.11).[45] A one-step synthesis of H, G and S glycerols via epoxidation from the corresponding alcohols has been proposed. These arylglycerols can then undergo classical thioacidolysis to provide the lignin-derived thioacidolysis monomers. This would provide a shorter/less complex route to analytical standards for quantitative thioacidolysis elucidation of lignin.

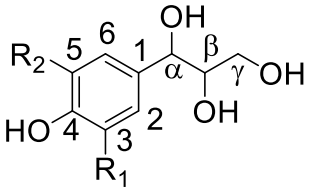

a : $R_1 = R_2 = H$
b : $R_1 = OCH_3$, $R_2 = H$
c : $R_1 = R_2 = OCH_3$

Figure 3.10 Arylglycerol monomers.

a) *p*-hydroxyphenyl glycerol b) guaiacyl glycerol c) syringyl glycerol.

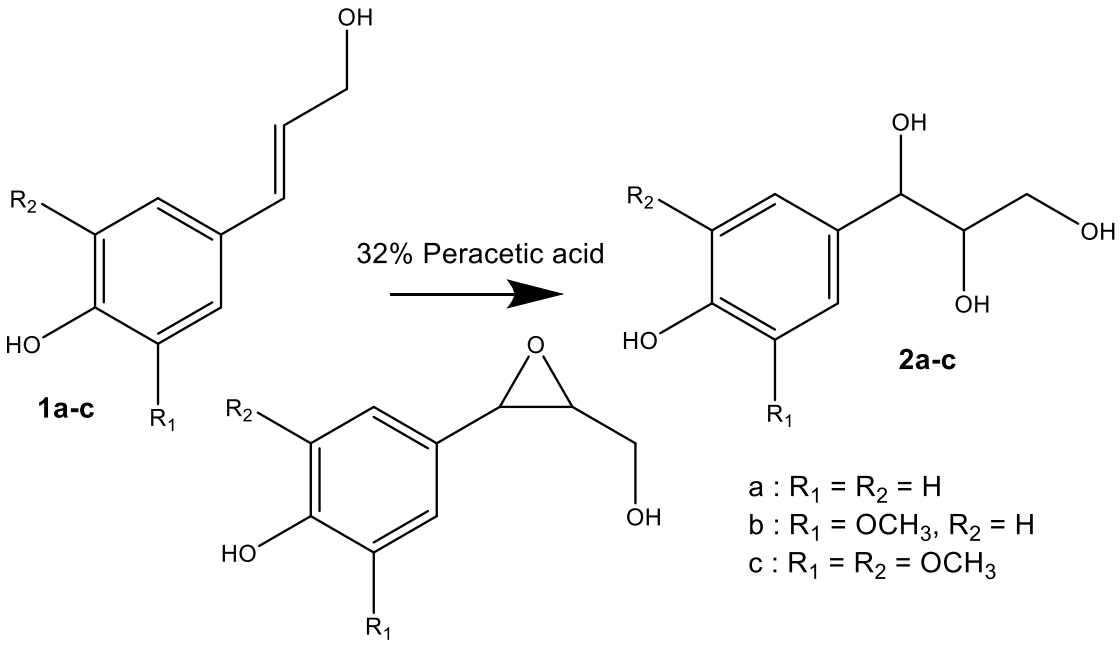

Figure 3.11 Synthetic strategy to arylglycerol monomers (compounds 2a-c) through an alkene epoxidation from the starting monolignols (compounds 1a-c).

a) H b) G c) S

3.2. Materials and methods

Materials.

Ethyl acetate, anhydrous sodium sulfate, acetone, hydrochloric acid and methylene chloride were purchased from Thermo Fisher Scientific (Waltham, MA, USA). Hydroxycinnamic acids, peracetic acid, sodium bisulfite, BSTFA and pyridine were purchased from Sigma Aldrich (Milwaukee, WI, USA). All solvents were of reagent grade and used without further purifications.

Product purification and characterization.

Purification was performed using column chromatography with silica gel purchased from Sigma Aldrich (Milwaukee, WI, USA). Synthesized compounds were characterized by proton and ^{13}C nuclear magnetic resonance (NMR), gas chromatography-mass spectrometry (GC/MS), thin layer chromatography (TLC) and high resolution accurate mass mass spectrometry (HRAM MS). Nuclear magnetic resonance (NMR) spectra were acquired on a Varian Model NOVA400 (400 MHz) spectrometer. Proton and ^{13}C NMR were used to confirm and assign structural positions of synthesized compounds. All NMR samples were analyzed at a concentration of 10-100 mg samples in 0.6 mL of acetone-d_6 with solvent peaks used as internal reference peaks, δ_H/δ_C 2.05 (5)/29.62 (7), 206.68 (1). Gas chromatography/mass spectrometry (GC/MS) spectra were acquired on a Shimadzu QP500 with a DB5-MS capillary column. Helium was used as the carrier gas. GC thermal gradient was as follows: initial temperature, 100 °C, held for 5 min, ramped from 100 °C to 280 °C at 12 °C/min for 15 min, and held at

280 °C for 10 min. Aliquots (10 µL) were sampled from the reaction mixture, dried under nitrogen gas, and derivatized (10 µL pyridine, 10 µL BSTFA) prior to analysis (1 µL) by GC/MS. High resolution mass spectra were acquired by electrospray on a QExactive Orbitrap mass spectrometer (Thermo Scientific, San Jose, CA, USA). X-ray crystal structures were obtained with either a Nonius kappaCCD (Mo*Ka*) or a Bruker-Nonius X8 Proteum (Mo*Ka*) diffractometer, each equipped with LT-2 low-temperature devices from CryoIndustries of America (Manchester, NH). Crystal indexing and data processing were performed either with DENZO-SMN (KappaCCD)[46] or with Bruker APEX2 (X8 Proteum)[47]. The structures were solved by Shelxt, refined with Shelxl-2014[48], and checked with Platon[49] and an R-tensor[50].

Syntheses of Arylglycerols

Monolignols 1a-c were made, in house, from the corresponding hydroxycinnamic acids according to the previously published procedure.[51] The NMR spectra for compounds 1a-c were consistent with published spectra. [51 51 51 51 51 21]

In situ peracid experiments were conducted using a 50% hydrogen peroxide solution and glacial acetic acid purchased from Thermo Fisher Scientific (Waltham, MA, USA). Coniferyl alcohol, purchased from Sigma Aldrich (Milwaukee, WI, USA), was weighed into a vial (100 mg), acetic acid was added followed by the addition of 30% hydrogen peroxide solution, dropwise, and allowed to stir for the allotted time period. Aliquots were sampled from the

reaction mixture, evaporated under nitrogen gas, redissolved in methylene chloride and derivatized (1:1 BSTFA/pyridine, 20 µL).

Peracetic acid was used to convert compounds 1a-c to the corresponding arylglycerols, 2a-c. For example, coniferyl alcohol (300 mg) was suspended in 3 mL of water to which 3.5 mmol of peracetic acid (32% in acetic acid, 2.1 moles of peracetic acid to 1 mole of C=C) was added dropwise and allowed to stir for 1.5 hours at 0 °C. The reaction mixture was quenched with 7 mL of sodium bisulfite solution (10% w/v).[44] The mixture was transferred to a separatory funnel and extracted with ethyl acetate (25 mL). The water phase was re-extracted with ethyl acetate (4x25 mL) and organic fractions were combined, dried over anhydrous Na_2SO_4, and evaporated to dryness. The crude product was purified using a silica gel column and eluted with ethyl acetate.

Products 2b and 2c were recrystallized from acetone while product 2a remained an oil. Thin layer chromatography (TLC) showed a single spot suggesting a pure isolated product (2a-c). Subsequent GC/MS analyses of the trimethylsilyl derivatives were consistent with the TLC data, and showed compounds 2a-c were obtained in 86.8, 94.2, and 87.4% yields, respectively. The NMR spectra for compounds 2a-c are consistent with those previously published.[43b-d, 52] Compound 2a, NMR (acetone-d_6) δ_H: 3.37 (1H, dd, J = 6.0, 11.2 Hz, γ), 3.48 (1H, dd, J = 3.9, 11.2 Hz, γ), 3.64 (1H, m, β), 4.57 (1H, d, J = 6.4 Hz, α), 6.78 (2H, m, 3/5), 7.21 (2H, m, 2/6). NMR (acetone-d_6) δ_C: 63.91 (α), 74.67 (γ), 77.34 (β), 115.65 (C2/6), 128.86 (C4), 134.16 (C1), 157.55 (C3/5). HRMS: M + Na^+ *m/z* calculate 207.0628, found 207.0628. Compound 2b, NMR (acetone-

d$_6$) δ_H: 3.39 (1H, dd, J = 5.8, 11.0 Hz, γ), 3.49 (1H, dd, J = 3.9, dd, J = 3.9, 11.0 Hz, γ), 3.63 (1H, m, β), 3.82 (3H, s, 3-OMe), 4.56 (1H, d, J = 5.9 Hz, α), 6.76 (1H, dd, J = 3.3, 8.0 Hz, 6), 6.83 (1H, m, 5), 7.01 (1H, d, J = 1.8 Hz, 2). NMR (acetone-*d*$_6$) δ_C: 55.98 (3-OMe), 63.72 (γ), 74.59 (α), 77.08 (β), 110.95 (C2), 115.03 (C5), 120.11 (C6), 134.68 (C1), 146.47 (C4), 147. (C3). HRMS: M + Na^+ *m/z* calculate 237.0733, found 237.0734. Compound 2c, NMR (acetone-*d*$_6$) δ_H: 3.41 (1 H, br-dd, J = 5.5, 10.3 Hz), 3.51 (1 H, br-d, J = 10.3 Hz, γ), 3.64 (1 H, br-m, β), 3.80 (6H, s, 3/5-OMe), 4.56 (1H, d, J = 6.9 Hz, α), 6.70 (1H, s, 2/6). NMR (acetone-*d*$_6$) δ_C: 57.00 (3/5-OMe), 64.40 (γ), 75.44 (α), 77.70 (β), 105.55 (C2/6), 134.34 (C4), 136.43 (C1), 148.82 (C3/5). HRMS: M + Na^+ *m/z* calculate 267.0839, found 267.0840. Refer to Figure 3.10 for numerical assignments.

Thioacidolysis.

Thioacidolysis of the synthesized arylglycerol compounds were performed according to a previously published procedure.[40] The thioacidolysis reagent (3 mL) was freshly prepared, added to a glass culture tube containing the previously weighed out arylglycerol (5 mg) and stirred at 100 °C for four hours. The tube was cooled on ice for 10 min, the mixture was quenched with 0.4 M $NaHCO_3$ (7 mL), neutralized with 1 M HCl (2 mL) and extracted with CH_2Cl_2 (10 mL x 4). The organic phases were combined, dried over anhydrous Na_2SO_4 and evaporated under vacuum. The residue was dissolved in acetone (200 µL), derivatized (5 µL pyridine, 5 µL BSTFA), and analyzed by GC/MS.

3.3. Results and discussion

It has been previously shown that lignin-derived thioacidolysis monomers (compounds 3a-c) can be obtained through a traditional thioacidolysis reaction of the corresponding arylglycerol (compounds 2a-c**)**.[42] Previous synthetic models utilize a multi-step synthesis which have shown to provide ~90% yields per step and good selectivity. However, a multi-step synthesis utilizes many solvents and reagents and can be labor and time intensive. An alternate synthetic strategy has been proposed that utilizes a one-step epoxidation to the arylglycerol.

Epoxides are very versatile intermediates commonly used in organic synthesis due to the high reactivity of the oxirane ring.[44] Peracids can be utilized pre-formed or generated *in situ* to conduct an epoxidation, which is typically done in organic solvents.[44-45] However, organic solvents often decrease reaction rates, but confer selectivity with the goal of preventing di-hydroxylation. Since our goal is to synthesize the di-hydroxylated product, we can utilize this to our advantage. Thus, conducting the reaction in an aqueous environment provides higher reaction rates/lower reaction times ($\leq$ 2 hours), and increases di-hydroxylation. It has also been shown that increased peracid molar ratios, greater than 1.5 moles of peracid to 1 mole of C=C, increases di-hydroxylation.[44] Therefore, conducting an alkene epoxidation in aqueous/acidic media, due to the peracetic acid being in acetic acid and utilizing a slightly higher molar ratio at 2.1 moles of peracid to 1 mole of alkene, enhances the probability of di-hydroxylation of the oxirane (epoxide) according to the reaction scheme seen in Figure 3.11.

Preliminary experiments were conducted utilizing an *in situ* peracid approach where a solution of hydrogen peroxide and acetic acid were used to generate peracetic acid. Products were analyzed by GC/MS in order to characterize the intended arylglycerol product. Figure 3.12a,b shows the chromatogram of the reaction mixture and the hypothesized mass spectrum for the desired arylglycerol product. Without a spectrum match existing in the NIST (National Institute of Standard Technology) GC/MS library, we needed to identify the characteristic EI spectrum in order to optimize the reaction parameters. It was hypothesized the spectrum seen in Figure 3.12 was the desired arylglycerol product EI spectrum due to the major fragmentation seen. The analogous thioacidolysis monomer spectrum has been well established. The major fragmentation for that compound is seen at the α-β carbon-carbon bond on the alkyl side chain. This same fragmentation was proposed to occur for the arylglycerol monomer.

To test this hypothesis, an epoxidation reaction was conducted on the analogous ethyl esters of all three monomers. If the hypothesis that the major fragmentation will occur at the α-β carbon-carbon bond on the alkyl side chain is true, we should see the same major fragmentation for the ethyl esters as we did in the coniferyl alcohol epoxidation (reaction scheme seen in Figure 3.13). In addition, we should see a decrease in 30 mass units for H and an increase in 30 mass units for S due to the difference in a methoxy group between the said compounds. Indeed, we see the major fragmentation of G ethyl ester is *m/z* 297, S ethyl ester is *m/z* 327 and H ethyl ester is *m/z* 267 (Figure 3.14a-c). The ethyl

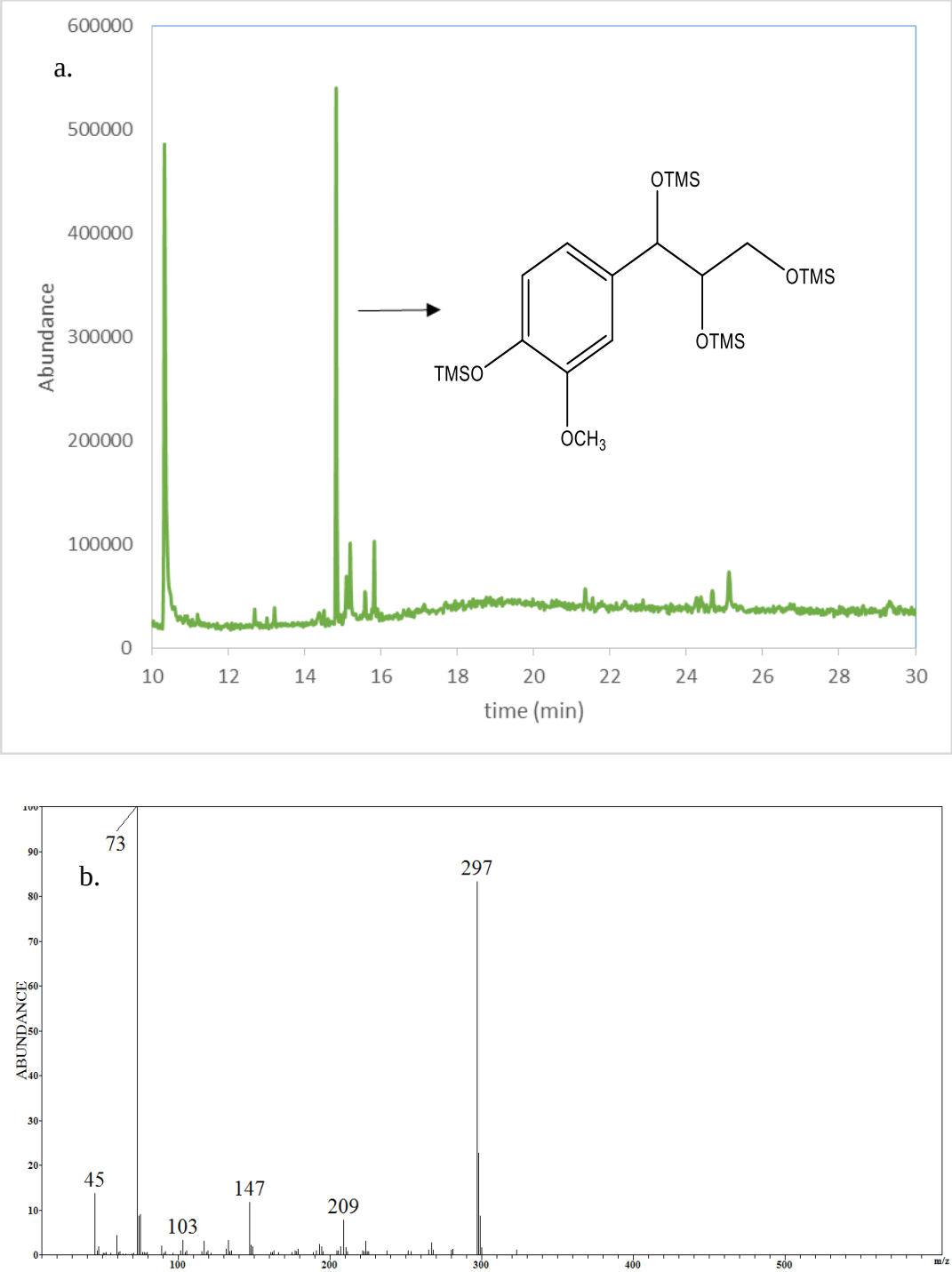

Figure 3.12 : TMS derivatives of coniferyl alcohol epoxidation reaction mixture (3 hr, RT, 1/20/5, C=C/glacial acetic acid/30% H_2O_2).

a) chromatogram b) mass spectrum of arylglycerol product.

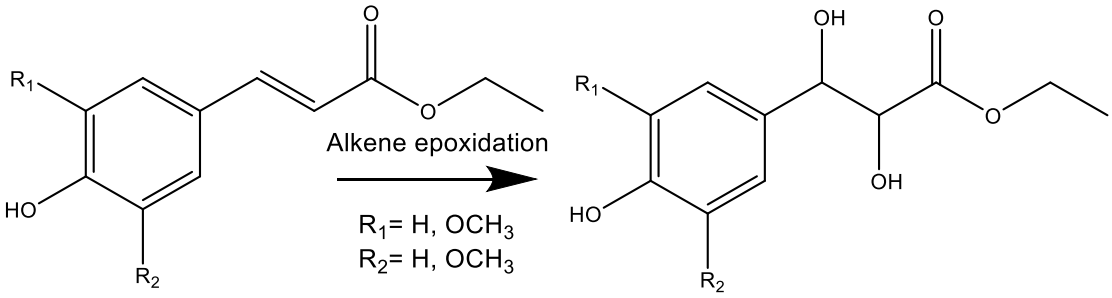

Figure 3.13 Ethyl ester epoxidation reaction scheme.

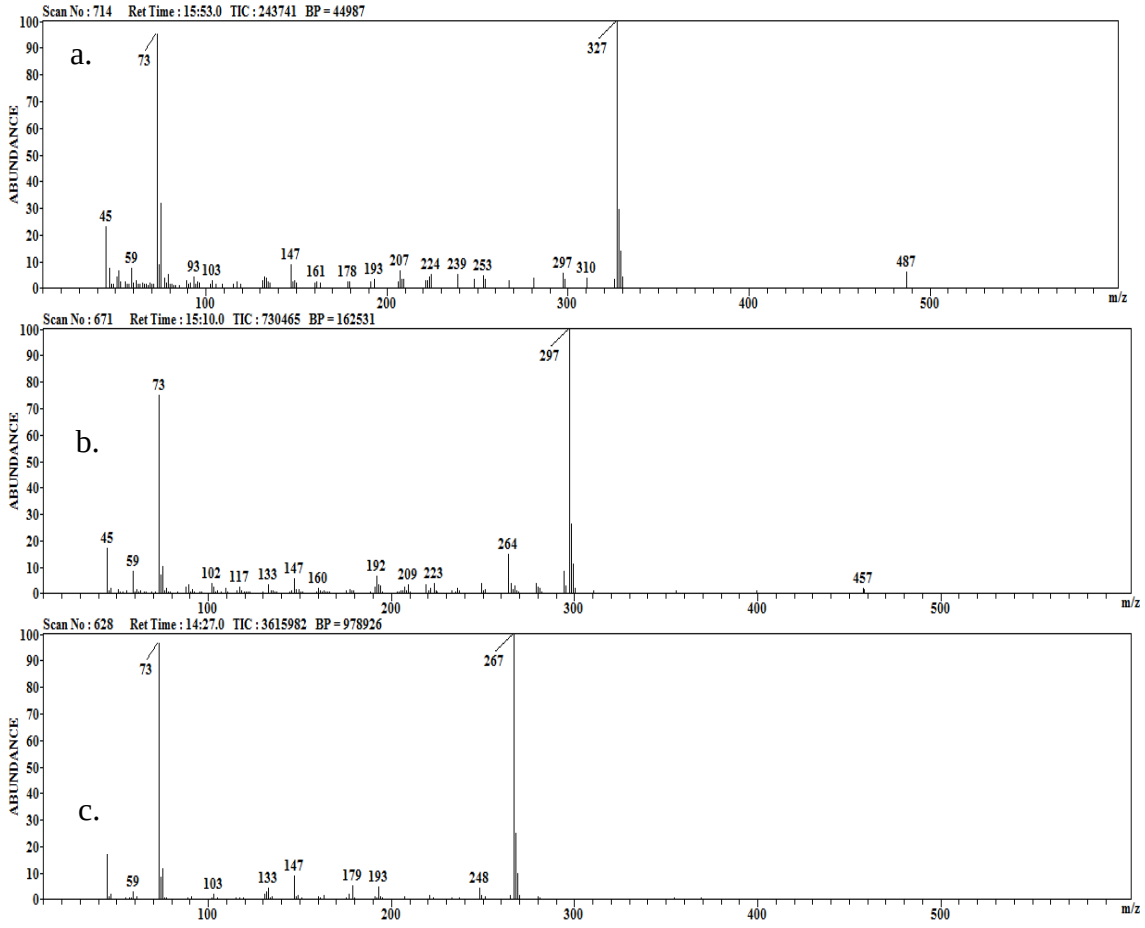

Figure 3.14 TMS derivatives of ethyl ester epoxidation reaction products a) H ethyl ester GC/MS spectrum, b) G ethyl ester GC/MS spectrum, c) S ethyl ester GC/MS spectrum.

ester of G upon epoxidation, showed the major fragmentation peak of *m/z* 297 which is the same fragmentation seen in the epoxidation of the corresponding G alcohol. As hypothesized, the major fragmentation of S ethyl ester, *m/z* 327, was 30 mass units greater than G ethyl ester, *m/z* 297, due to the addition of a methoxy group, and the major fragmentation of H ethyl ester, *m/z* 267, was 30 mass units less than that of G ethyl ester, *m/z* 297. This supports our claim of major fragmentation occurring at the α-β carbon-carbon bond on the alkyl side chain, thus, the characteristic spectrum of the desired arylglycerol product as well as the synthesis of the desired product.

To further support our hypothesis of synthesizing our desired arylglycerol product, we conducted a thioacidolysis of the epoxidation reaction mixture. Although there was a product mixture, we were able to identify the thioacidolysis product (Figure 3.15). Convinced the reaction scheme will proceed as hypothesized and with the ability to qualify reaction parameters by GC/MS and TLC, optimization was required. It was observed that *in situ* peracid generation was limited by the ability to generate the peracid at a rate equal to its consumption. The efficiency/selectivity of the epoxidation reaction is limited by the rate of the *in situ* peracid production being greater than or equal to the rate of peracid consumption. To eliminate this issue, we decided to use a pre-formed peracid.

When utilizing a solvent-free epoxidation of biodiesel, it was reported that not only did higher acid molar ratios increase di-hydroxylation, but increased

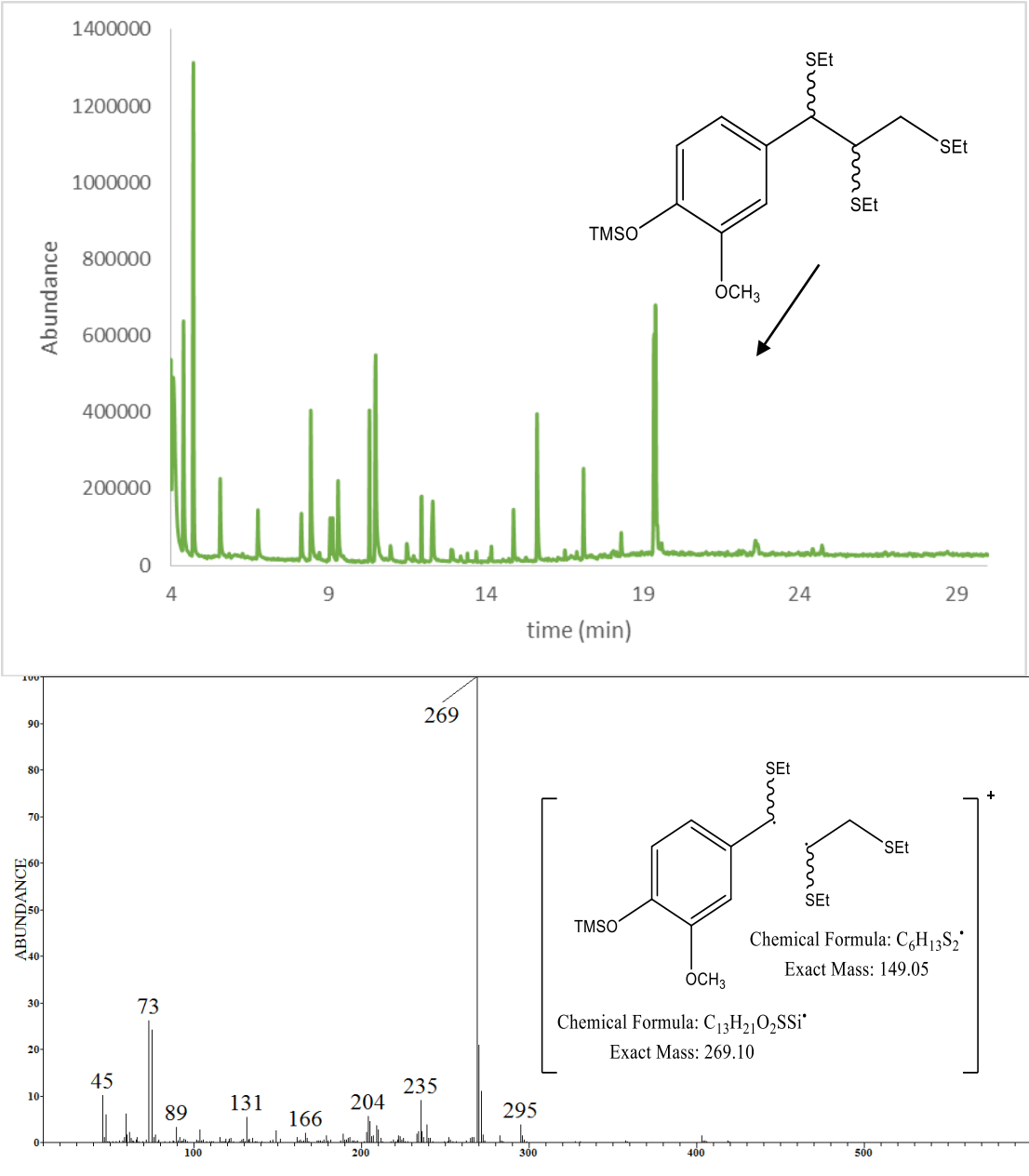

Figure 3.15 TMS derivatives of thioacidolysis reaction mixture of coniferyl alcohol epoxidation top) GC/MS chromatogram (bottom) GC/MS EI spectrum.

temperatures (50 – 60 °C) and increased time of reaction (greater than three hours) increased di-hydroxylation.[44] From our experiments, we found that elevated temperatures, higher than 25 °C, and reaction times longer than 2 hours caused over oxidation of all three monomers with no product detected by GC/MS and TLC. When the reaction was conducted at 25 °C, we were able to detect the arylglycerol product in 65.7% and 68.3% yield for G and S respectively. However, these results were not reproducible and varied from experiment to experiment. At times, over oxidation occurred as indicated by not only the dark brown color of the reaction mixture, but further confirmed by TLC and GC/MS. We determined that decreasing reaction temperatures provided reproducible reaction outcomes which is mostly due to the decreased reaction rate at lower temperatures. At 0 °C, over oxidation was reduced, producing increased yields of 94.2% and 87.4% of our arylglycerol products for G and S respectively. *Para*-coumaryl alcohol, H, was less reactive than G and S. At 0 °C, *p*-coumaryl alcohol (H precursor, starting material) was detected after four hours of reaction time. When *p*-coumaryl alcohol was exposed to peracetic acid at 25 °C, starting material was no longer detected, producing an 86.8 % yield of the arylglycerol after 2 hours of reaction time. It has been observed that while these three monomers are similar in structure, they have very different properties. *Para*-coumaryl alcohol, H, was less reactive than G and S. This is speculated to be due to the difference in methoxy groups on the aromatic ring. With each methoxy group, there is an increase in electron density contributed to the ring, thus making it more easily oxidized.

To the best of our knowledge, this is the first account of characterization of these arylglycerols, trimethylsilyl derivatives, by GC/MS. Figure 3.16a-c, shows the characteristic electron ionization (EI) spectra of the H, G and S arylglycerols, respectively. It was very interesting to find the major fragmentation occurs at the α-β carbon-carbon bond which is analogous to the characteristic EI fragmentation seen in the corresponding thioacidolysis compounds. Syringyl (S) and guaiacyl (G) glycerol spectra provide molecular ion information, but *p*-hydroxyphenyl glycerol (H) did not provide a molecular ion, nevertheless, fragmentation is consistent with the other monomers. Building on the previous discussion of the observed differences between H, G and S, the lack of molecular ion observed by GC/MS (EI), can be contributed to the lack of methoxy group present on the aromatic ring. As the compound is ionized by the 70 eV electron, it ejects an electron generating an excited radical cation, with the methoxy group on the aromatic ring, it donates electron density thus providing more stability.

Upon isolation/purification of the products, proton and ^{13}C NMR were obtained and showed to be consistent with previously published literature. [43b-d, 52] Although GC/MS analysis of crude products showed 86.8, 94.2, and 87.1% yields of H, G and S, respectively, we were only able to isolate 80.5, and 61.7% of analytically pure G and S glycerol, respectively. Purity was greater than 93% as determined by GC/MS and a single spot by TLC. High resolution accurate mass (HRAM) mass spectra produced molecular ions with sodium adducts which were consistent with calculated molecular masses, less than 1 ppm for all these

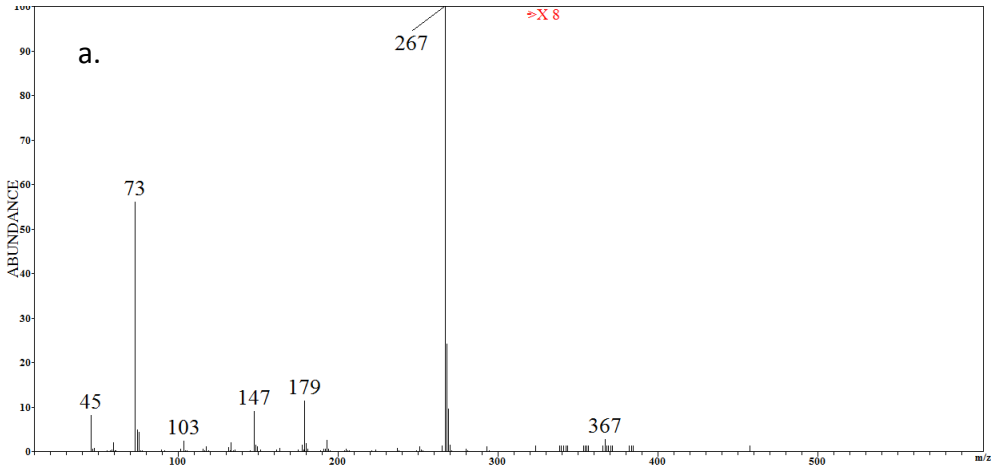
a.
267
X 8
73
45
103
147
179
367
ABUNDANCE
m/z

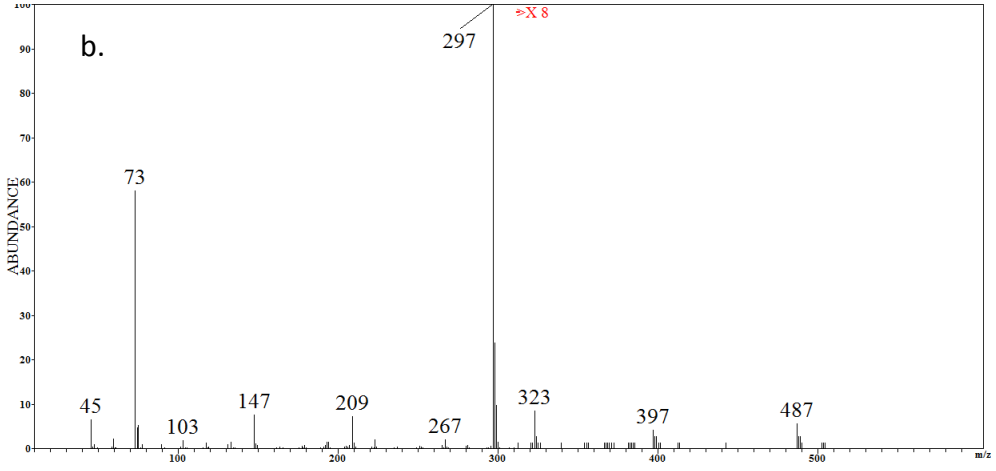
b.
297
X 8
73
45
103
147
209
267
323
397
487
ABUNDANCE
m/z

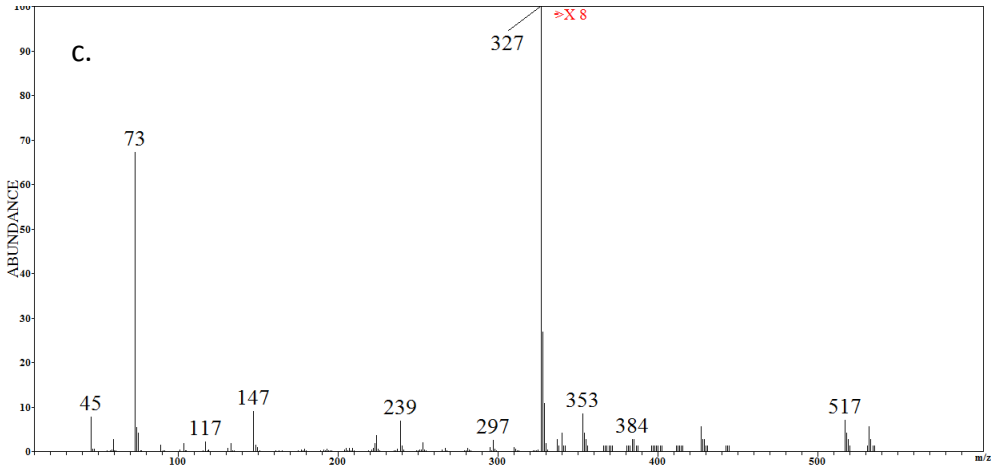

Figure 3.16 TMS derivatives of arylglycerols

a) *p*-coumaryl (H) glycerol GC/MS spectrum, b) guaiacyl (G) glycerol GC/MS spectrum, c) syringyl (S) glycerol GC/MS spectrum

arylglycerols. Syringyl (S) and guaiacyl (G) glycerol products produced crystalline material of sufficient quality to determine their crystal structures (Figure 3.17a, b). *Para*-coumaryl (H) glycerol remained an oil after sitting for several weeks. Thus, we were unable to report an isolated yield.

Once the arylglycerol products were confirmed by GC/MS, NMR, crystallography, and HRAM/MS, we conducted traditional thioacidolysis. Figure 3.18a-c shows the GC/MS spectra of the thioacidolysis products which are consistent with literature spectra.[42] This further supports the previously discussed structural characterizations of the intended arylglycerol products and the proposed one-step synthetic scheme.

3.4. Conclusion

In conclusion, an alternate synthetic route to the arylglycerols was developed utilizing an alkene epoxidation approach with peracetic acid, a one-step reaction scheme. In an aqueous acidic environment, the probability of the epoxide opening to a dihydroxylated product is increased. *Para*-hydroxyphenyl, guaiacyl and syringyl glycerols were successfully synthesized and purified with acceptable yields. It was observed that S and G were quickly oxidized therefore reaction conditions needed to be less aggressive, 0 °C, versus H which proved to be more stable than S and G and required a less sensitive reaction environment, room temperature. Arylglycerols, H, G and S, were characterized by GC/MS, HRAM/MS, proton and ^{13}C NMR. Characteristic EI spectra of H, G and S arylglycerols were elucidated. Arylglycerol monomers proved to have the same

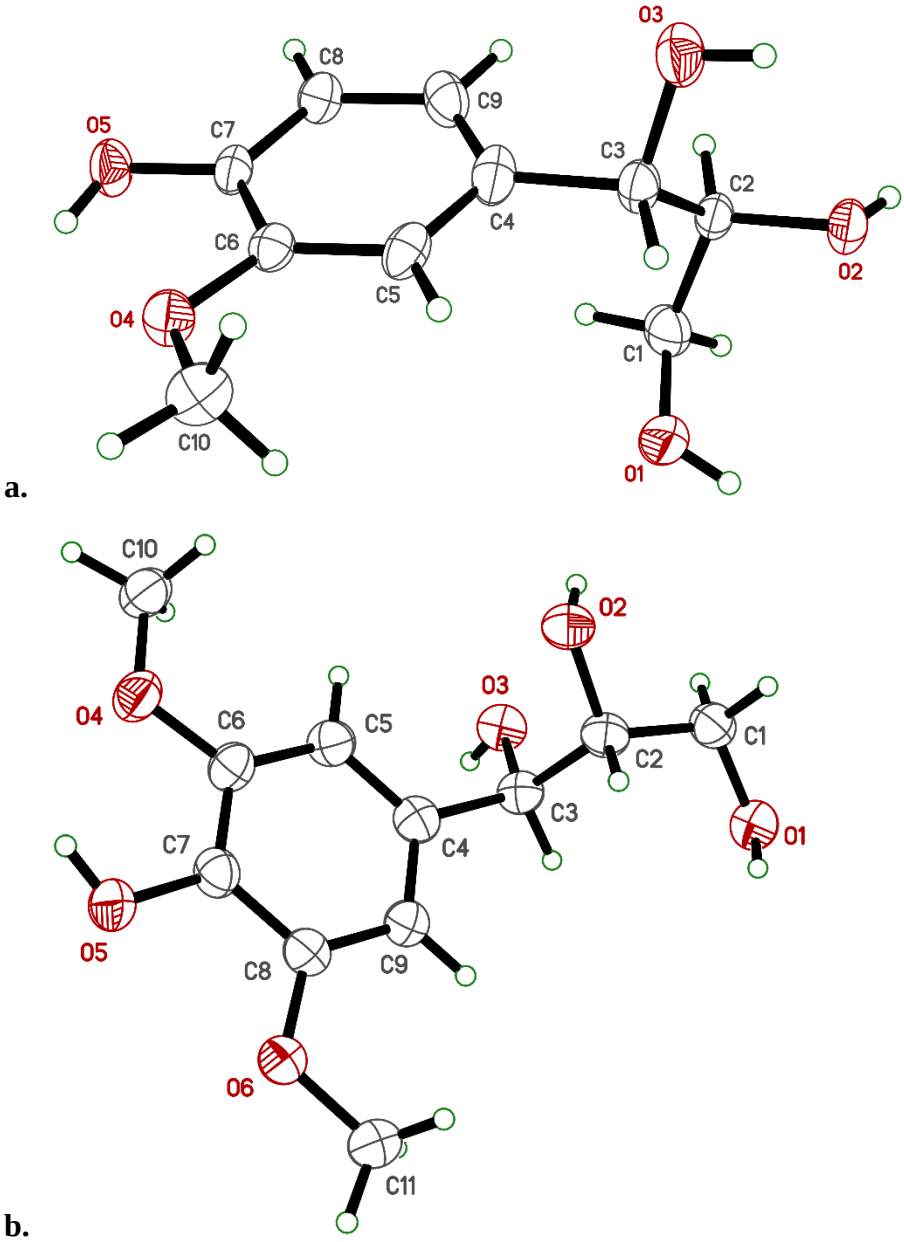

Figure 3.17 X-ray crystal structure of a) guaiacyl glycerol (G), b) syringyl glycerol (S).

Guaiacyl glycerol was partially disordered (minor component not shown) and syringyl glycerol crystallized with a disordered acetone solvent molecule (not shown).

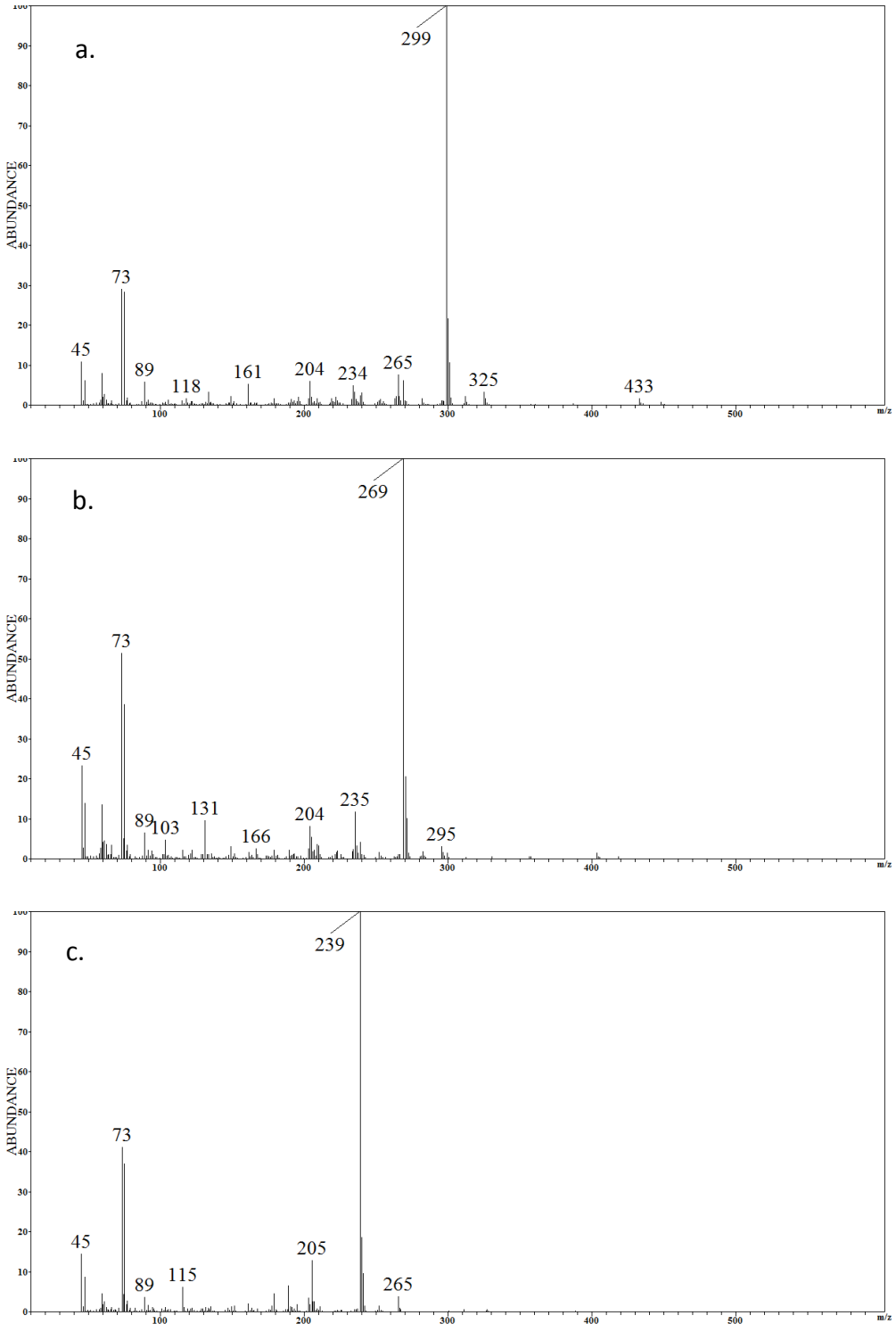

Figure 3.18 TMS derivatives of thioacidolysis monomers.

a) syringyl (S) b) guaiacyl (G), c) *p*-coumaryl (H) thioacidolysis monomers GC/MS spectrum.

characteristic fragmentation at the α-β carbon-carbon bond of the alkyl side chain analogous to that of the corresponding thioacidolysis monomer. Guaiacyl and syringyl glycerols were also characterized by x-ray crystallography. The arylglycerol monomers were then converted to the subsequent lignin-derived thioacidolysis monomers (3a-c) providing consistent GC/MS spectra to those previously reported. To the best of our knowledge, this is the first account of characterization of H, G and S arylglycerols by GC/MS and the first crystal structure of G and S arylglycerols. Lastly, this is the first account showing application of a known synthetic scheme commonly used in organic synthesis, an epoxidation, to synthesize lignin derived compounds, such as arylglycerols.

With the synthesized thioacidolysis compounds, analytical methodologies can be developed in order provide quantitative elucidation of the lignin monomeric composition. This information will contribute to the goal of elucidating the complex lignin ultrastructure.

4. Chapter 4 : Analysis of Lignin-Derived Monomers Using Gas Chromatography/Mass Spectrometry

4.1. Introduction

As previously discussed in Chapters 1 and 2, biomass to biofuel processing has become a topic of interest to many as the need for renewable energy sources increases. Due to the structural rigidity and protective nature of lignin, it has been the focal point in pretreatment strategies. The goal of lignocellulosic biomass pretreatment is to increase the cellulosic conversion efficiency, which has been suggested to directly correlate with the degradation of lignin. Compositional changes in plant cell wall and differences in ultrastructure greatly influence the pretreatment strategy and the conversion efficiencies.[2] As discussed previously in Chapter 2, solution based Fenton pretreatment makes cellulose more bioavailable to both enzymes and microbes, however, it is unknown how this occurs. In order to study Fenton pretreatment on biomass, there is a need for better methods to obtain compositional and structural information of lignin.[35]

Thioacidolysis is a commonly used analytical degradative method which has been used to study an array of lignocellulosic plant materials. Thioacidolysis is a Lewis acid-catalyzed reaction that depolymerizes lignin by cleaving arylglycerols at the aryl ether bonds (β-O-4 linkages). With the analytical thioacidolysis standards synthesized in Chapter 3, quantitative elucidation of the monomeric subunits that compose the β-O-4 linkages can be obtained. Thioacidolysis monomeric ratios are commonly analyzed by GC/MS.

Using the synthesized thioacidolysis monomers, a calibration curve can be made to determine monomeric quantification by GC/MS. This monomeric quantification strategy can be applied to assess solution phase Fenton pretreated lignocellulosic feedstocks, miscanthus, switchgrass, corn stover and wheat straw. It is hypothesized that changes in individual monolignol content upon pretreatment can be observed from quantification.

4.2. Materials and methods

Materials.

All chemicals of reagent grade were obtained and used without further purification. All solvents (methylene chloride, pyridine, BSTFA) were purchased from Thermo Fisher Scientific (Waltham, MA, USA). Miscanthus, switchgrass, corn stover and wheat straw samples (all ~ 2 mm particle size) were obtained from collaborators in the Michael Montross Laboratory, University of Kentucky, Lexington, KY, USA.

Thioacidolysis analysis

Thioacidolysis samples were conducted according to the previously discussed protocol (Chapter 3). Briefly, thioacidolysis solution (4 mL) was added to a glass tune with ground biomass (5 mg) and allowed to stir for 4 hours at 100 °C. The reaction mixture was quenched with 0.4 M $NaHCO_3$ and extracted several times with methylene chloride. Organic phases were combined and evaporated under nitrogen gas. The residue was redissolved in 500 µL of methylene chloride and

split into two samples (GC – 100 µL, CE – 400 µL). The GC sample was redissolved in 20 µL, 1:1 BSTFA/pyridine.

GC/MS samples were derivatized with 1:1 BSTFA/pyridine and 2 µL were injected on a Shimadzu QP5000 GC-MS. Injection temperature was set to 250 °C. Separation occurred on a 30 m, 0.25 µm thick DB-5MS capillary with the following temperature program: 100 °C for 3 min, temperature was ramped at a rate of 12 °C/min to 280 °C (12 min), and finally temperature was held at 280 °C for 5 min.

Linear regression analysis were conducted utilizing Microsoft excel 2014 workbook software. Calibration curves were displayed utilizing Sigmaplot 12.3.

4.3. Results and discussion

With the synthesized thioacidolysis monomers, a calibration curve was created. *Para*-phenylphenol (PPP) was used as the internal standards for all further analyses. PPP was chosen as an internal standard due to its aromatic structural similarity to the thioacidolysis monomers and it does not affect separation efficiencies. Figure 4.1 shows a thioacidolysis standard mixture separation by GC/MS. All three monomers were well resolved proving an appropriate separation method. Figure 4.2 shows the GC/MS calibration curves for all three thioacidolysis monomers (TMS derivatives). The correlation coefficient (R^2) showed sufficient linear fit ($R^2 > 0.95$) for the three thioacidolysis monomer GC/MS calibration curves with a linear range from 0.3-2.5 mg/mL (Table 4.1).

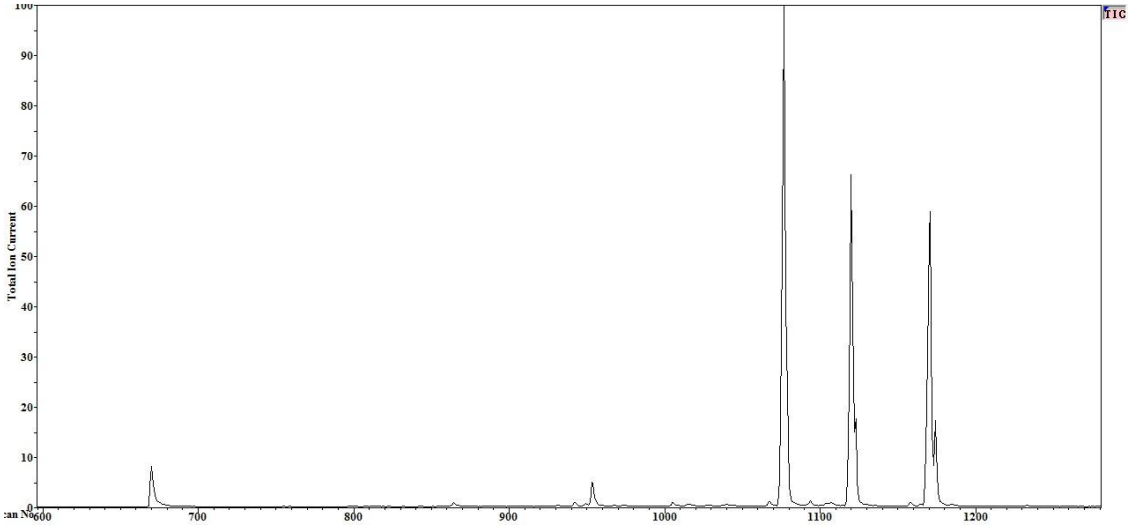

Figure 4.1 GC/MS chromatogram of thioacidolysis standard mixture.

GC/MS H-thioacidolysis Calibration Curve

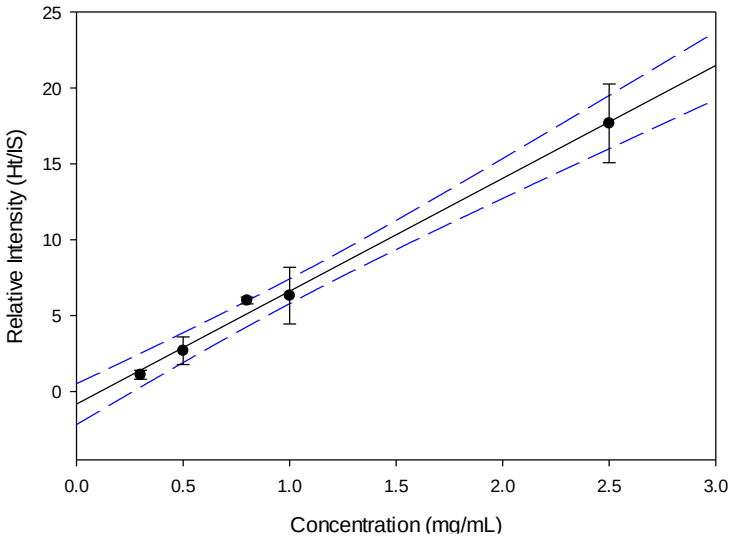

GC/MS G-thioacidolysis Calibration Curve

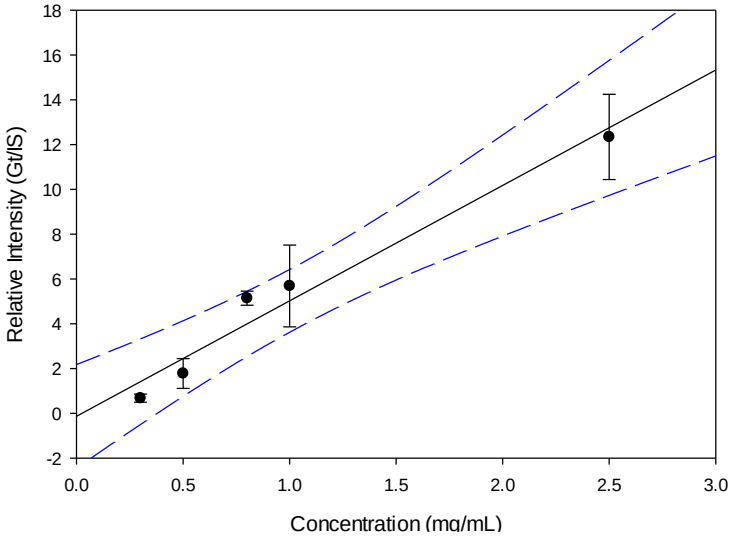

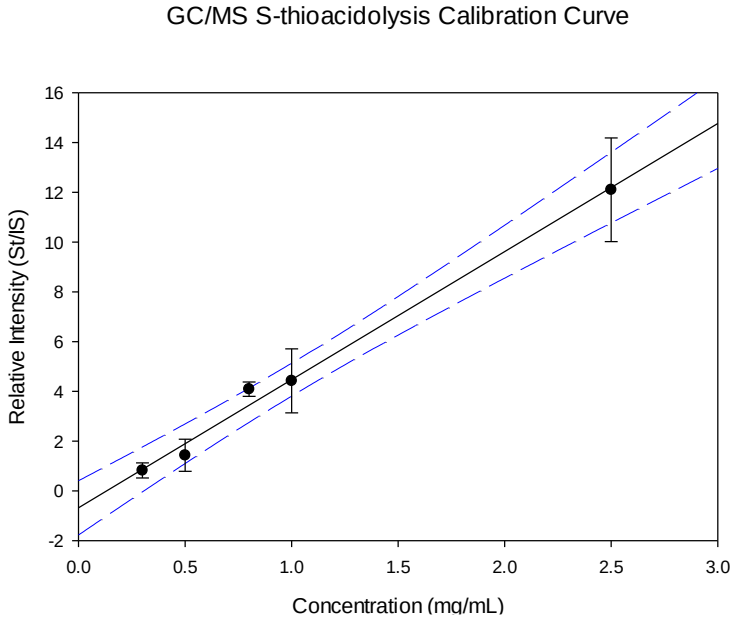

Figure 4.2 GC/MS calibration curves for H, G and S thioacidolysis monomers.

Data is shown with error bars indicating ± one standard deviation.

Table 4.1 GC/MS calibration curve linear regression analysis.

GC/MS CC	Equation of the line	R^2	Linearity
Ht	Y=7.44x-0.831	0.994	0.3 mg/mL – 2.5 mg/mL
Gt	Y=5.16x-0.135	0.965	0.3 mg/mL – 2.5 mg/mL
St	Y=5.15x-0.681	0.992	0.3 mg/mL – 2.5 mg/mL

Thioacidolysis monomeric quantification was conducted on untreated and Fenton treated miscanthus, switchgrass, corn stover and wheat straw using GC/MS. Quantification was calculated utilizing the appropriate line generated by the monomer calibration curves. Figure 4.3 shows a GC/MS chromatogram of a thioacidolysis product mixture from untreated wheat straw. The thioacidolysis product mixture is somewhat complex (Figure 4.3a,b), but with the ability of mass spectrometry to plot extracted ion chromatograms of only the analytes of interest, a simplified chromatogram can be generated (Figure 4.3 b,c). An additional advantage of MS is that analytes can be identified based on EI fragmentation patterns (Figure 4.3d-g). Table 4.2 summarizes the concentrations quantified using GC/MS as well as the relative ratio generated by GC/MS analysis that has been the historical analytical end point of this technique. Considering both the concentrations of Ht, Gt and St and the monomer ratios, Ht/Gt and St/Gt, there was no significant difference between untreated and Fenton treated biomass for any of the feedstocks.

Monomer ratios obtained from untreated and Fenton treated miscanthus samples suggested there was slightly more G than S, but very minimal H. Individual monomeric concentrations obtained was consistent with the suggested lignin content obtained from monomeric ratios. Untreated and Fenton treated miscanthus did not show a significant difference in monomeric ratios (Ht/Gt, St/Gt) or individual lignin content (Figure 4.4).

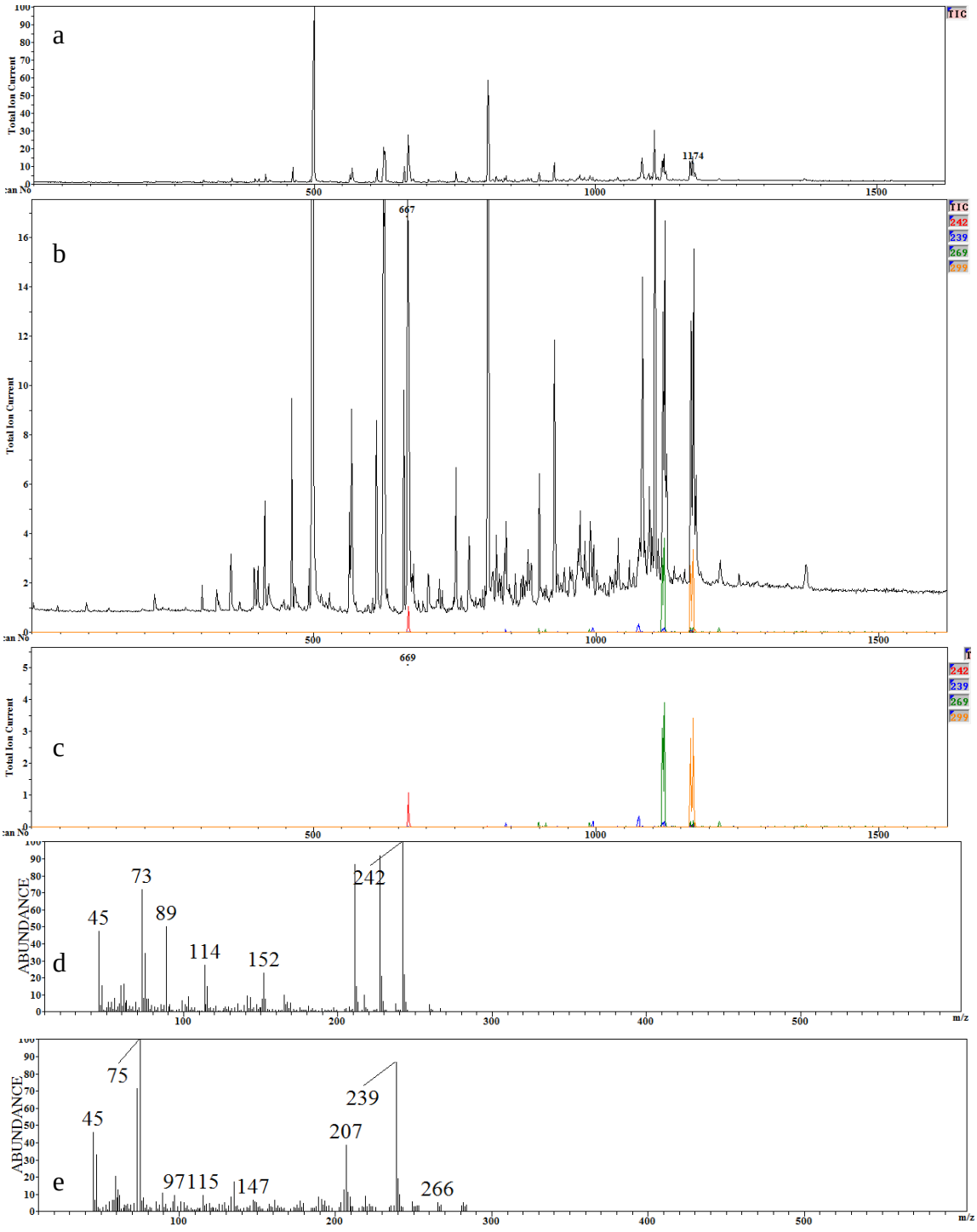
a
Total Ion Current
TIC
1174
b
667
242
239
269
299
c
669
d
ABUNDANCE
73
45
89
114
152
242
m/z
e
75
45
97115
147
239
207
266

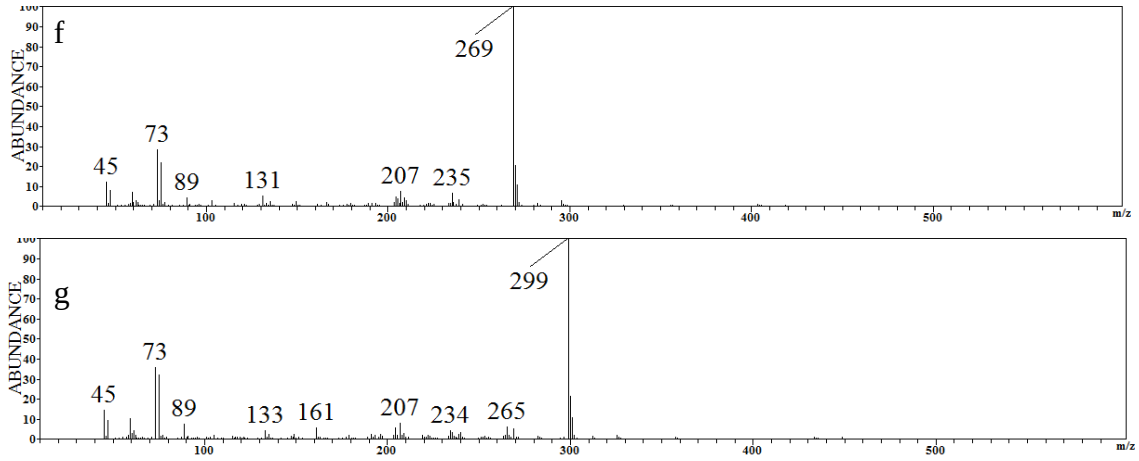

Figure 4.3 Thioacidolysis processed untreated wheat straw a) total ion chromatogram (TIC) b) TIC, magnified, with addition of plotted extracted ion chromatogram (EIC) c) EIC of H, G, S and internal standard (IS, PPP) d) EI mass spectrum of IS e) EI mass spectrum of H f) EI mass spectrum of G g) EI mass spectrum of S.

Table 4.2 GC/MS thioacidolysis monomer concentrations (mg/mL) and monomer ratios.

Untreated miscanthus (Unt Mis), Fenton treated miscanthus (Trt Mis), untreated switchgrass (Unt SG), Fenton treated switchgrass (Trt SG), untreated corn stover (Unt CS), Fenton treated corn stover (Trt CS), alkaline peroxide treated corn stover (B Trt CS), untreated wheat straw (Unt WS) and Fenton treated wheat straw (Trt WS).

Concentration (mg/mL)	**Unt Mis**	**Trt Mis**	**Unt SG**	**Trt SG**	**Unt CS**	**Trt CS**	**B Trt CS**	**Unt WS**	**Trt WS**
Ht	0.437	0.200	0.286	0.159	0.152	0.135	0.119	0.177	0.171
Gt	9.679	2.605	6.739	1.343	1.006	0.577	0.129	1.359	1.345
St	6.151	2.002	4.401	0.983	1.139	0.744	0.267	1.354	1.332
Relative Intensity	**Unt Mis**	**Trt Mis**	**Unt SG**	**Trt SG**	**Unt CS**	**Trt CS**	**B Trt CS**	**Unt WS**	**Trt WS**
Ht/Gt	0.042	0.061	0.042	0.052	0.058	0.062	0.103	0.071	0.065
St/Gt	0.699	0.775	0.6294	0.647	1.016	1.108	1.293	0.913	0.913

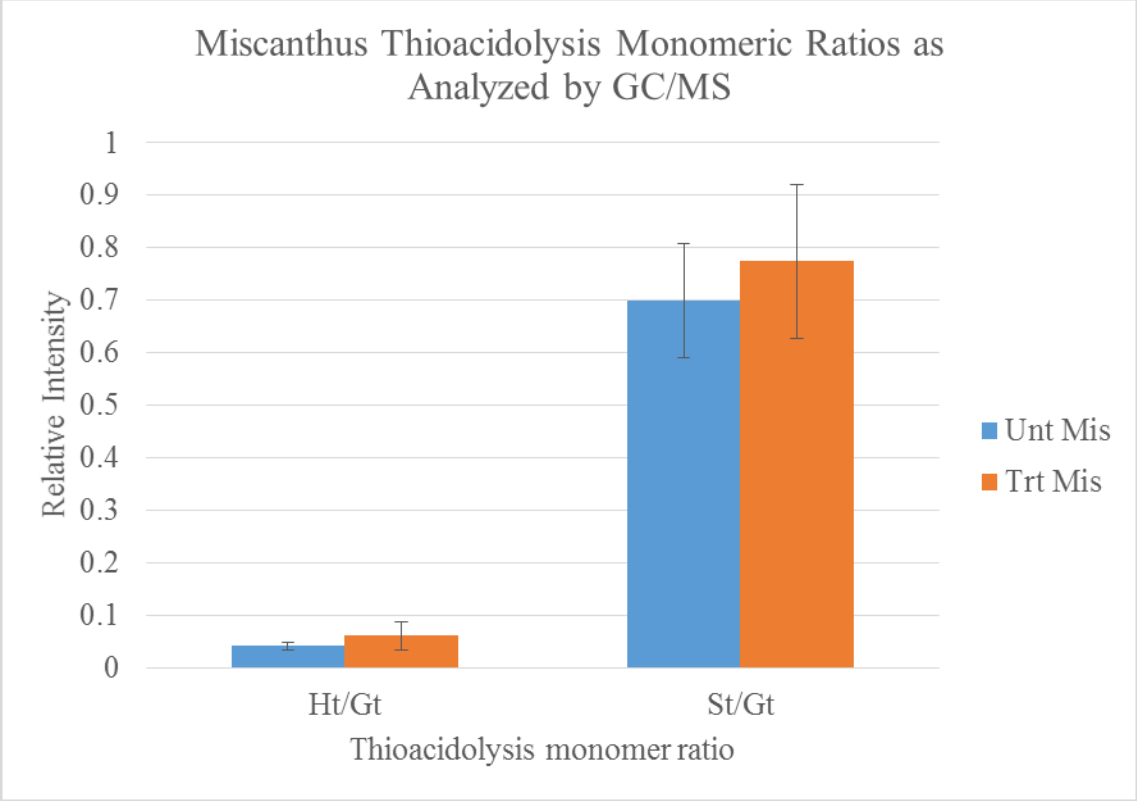

Figure 4.4a GC/MS analysis of untreated and Fenton treated miscanthus monomeric ratios.

Data is shown with error bars indicating ± one standard deviation. [*: statistically significant ($P < 0.05$)].

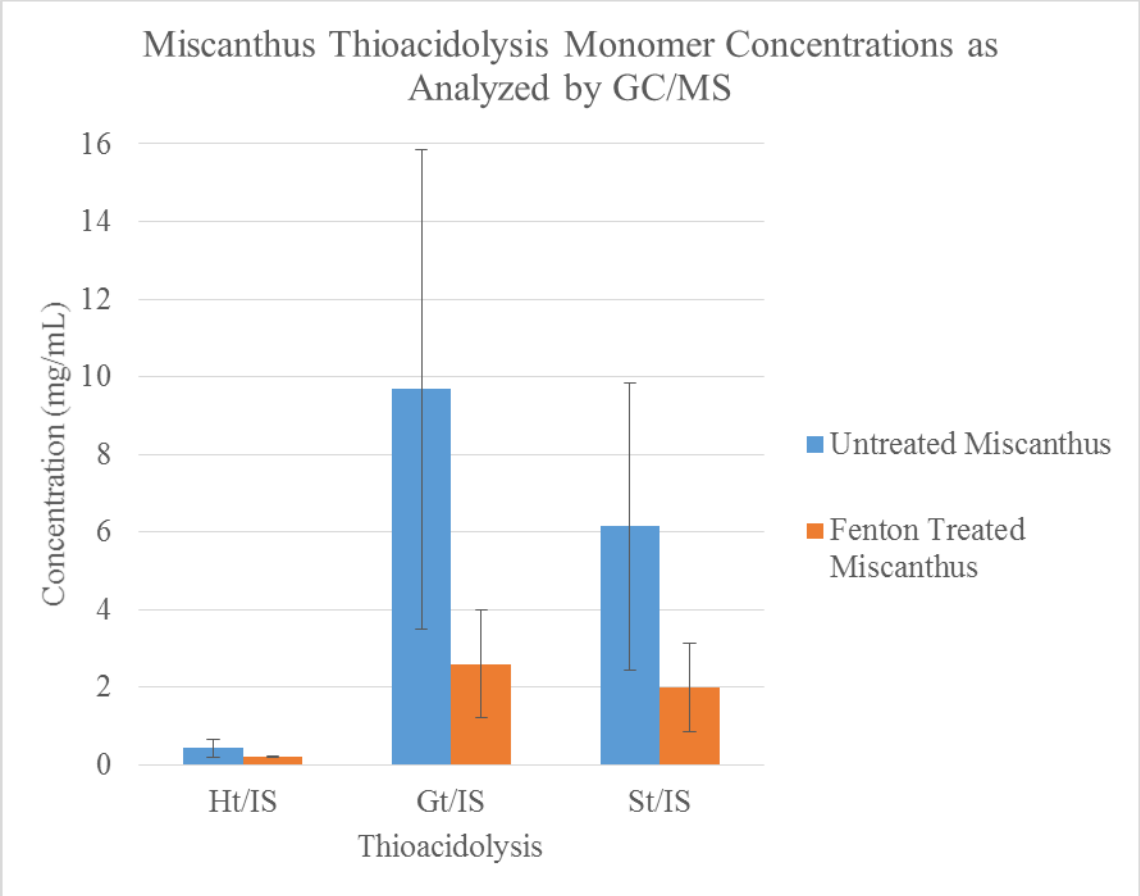

Figure 4.4b GC/MS analysis of untreated and Fenton treated miscanthus individual thioacidolysis monomer concentrations (mg/mL).

Data is shown with error bars indicating ± one standard deviation. [*: statistically significant ($P < 0.05$)].

Switchgrass untreated and Fenton treated did not show a significant difference in monomeric ratios or monomeric concentrations (Figure 4.5). This same trend was seen for corn stover upon Fenton treatment (Figure 4.6). No changes in individual monomer concentrations or monomeric ratios were seen upon Fenton treatment of wheat straw (Figure 4.7). The compilation of the monomeric ratios and individual monomer concentrations were consistent with lignin assays previously discussed (Chapter 2). This further supports the hypothesis that Fenton chemistry does not degrade lignin, but perhaps clips or alters the structure in a way that makes cellulose more bioavailable.

Although significant differences were not seen in individual monomeric concentrations using this quantitative approach, we were able to assess another pretreatment which has been shown to degrade lignin, alkaline peroxide pretreatment (base pretreatment).[6] Alkaline peroxide pretreated corn stover was processed through the thioacidolysis procedure, along with the Fenton pretreated samples, and analyzed by GC/MS (Figure 4.8). Again, the advantageous ability of MS detection to exclusively plot ions of interest greatly decreases chromatographic complexity, as seen in Figure 4.8. Based on the monomeric ratios, there was no significant difference between untreated corn stover and alkaline peroxide treated corn stover. However, individual monomeric concentrations revealed a significant difference between all three monomer concentrations upon alkaline peroxide treatment. Analyzing the monomer quantitative results, H, G and S all produced a significant difference in

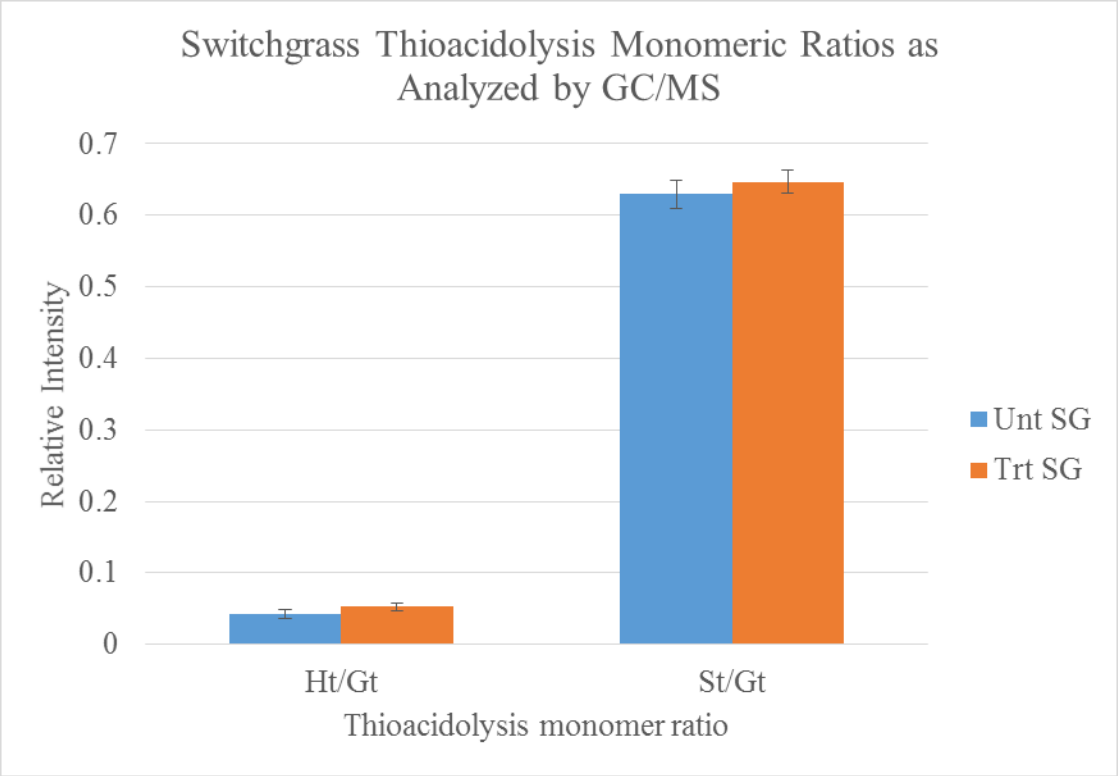

Figure 4.5a GC/MS analysis of untreated and Fenton treated switchgrass monomeric ratios.

Data is shown with error bars indicating ± one standard deviation. [*: statistically significant ($P < 0.05$)].

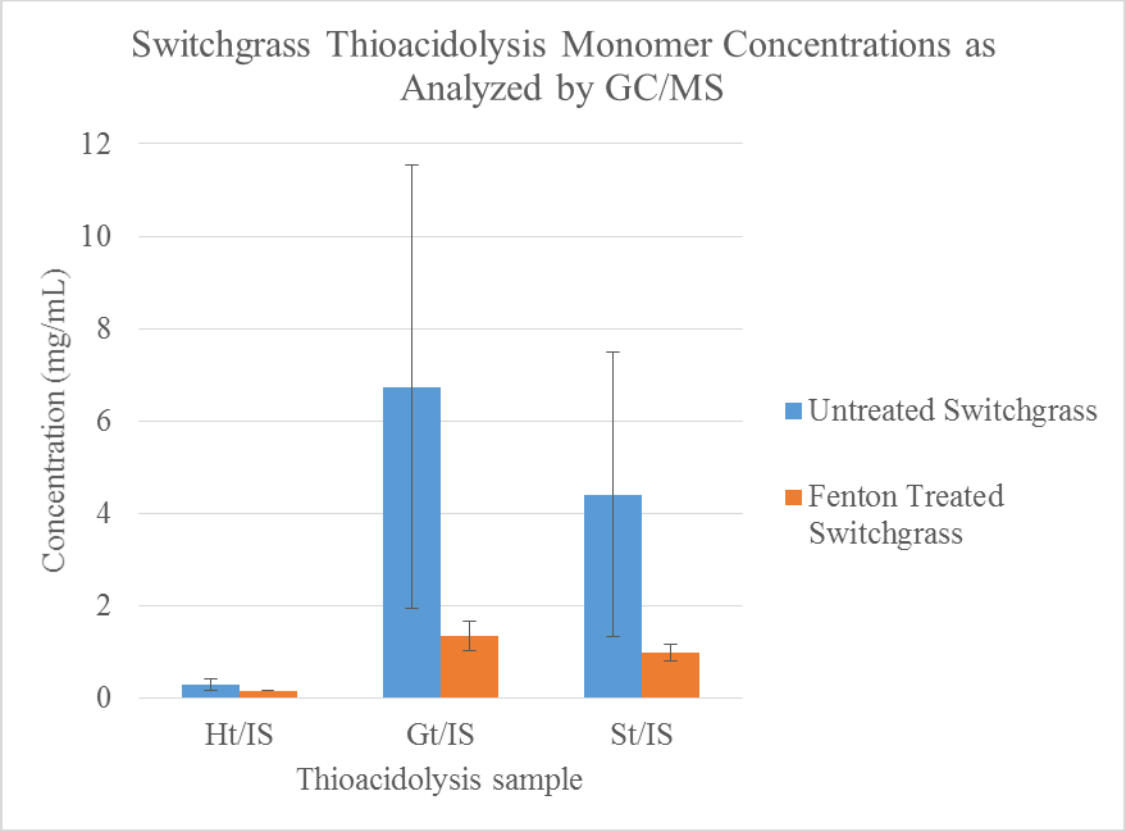

Figure 4.5b GC/MS analysis of untreated and Fenton treated switchgrass individual thioacidolysis monomer concentrations (mg/mL).

Data is shown with error bars indicating ± one standard deviation. [*: statistically significant ($P < 0.05$)].

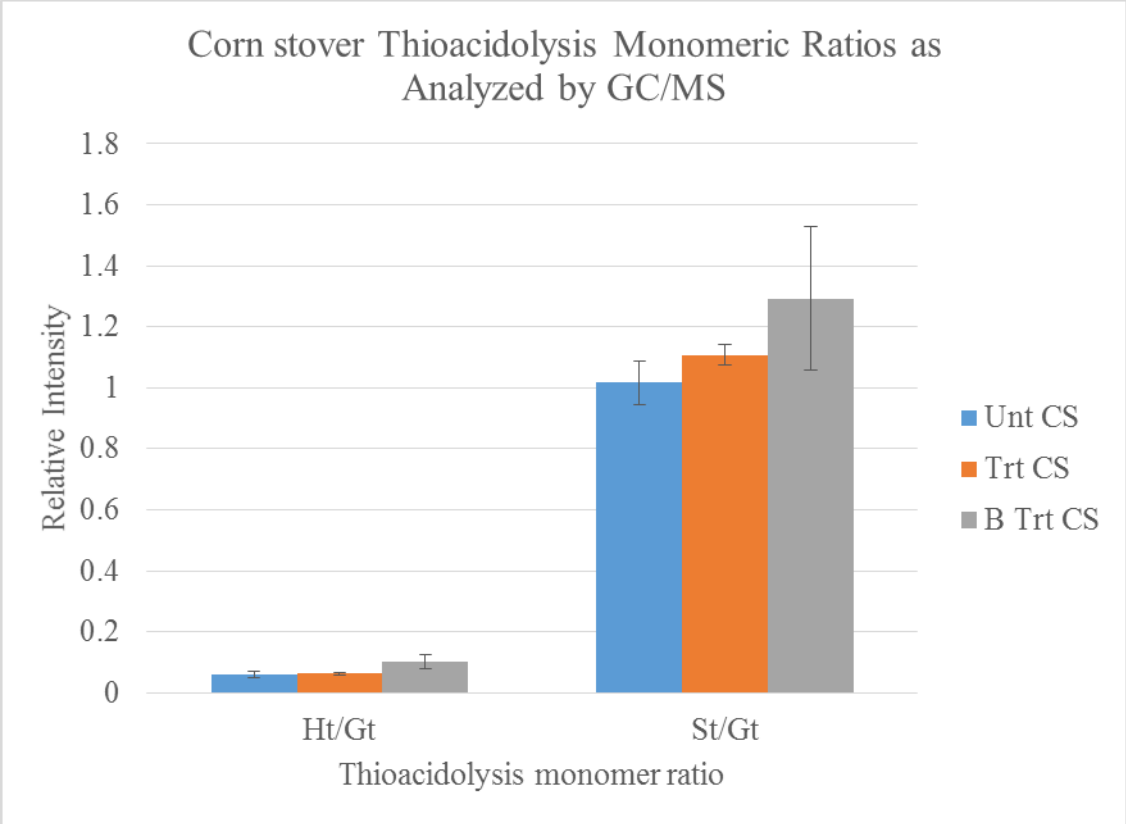

Figure 4.6a GC/MS analysis of untreated and Fenton treated corn stover monomeric ratios.

Data is shown with error bars indicating ± one standard deviation. [*: statistically significant ($P < 0.05$)].

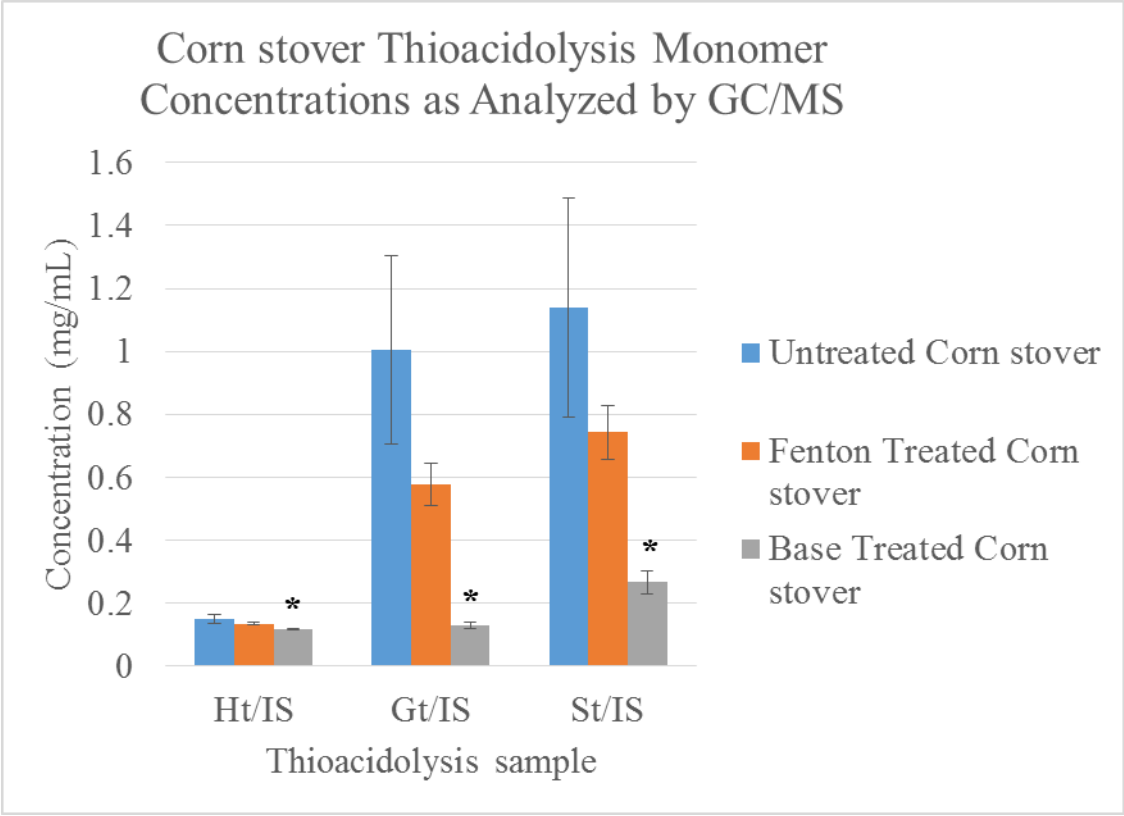

Figure 4.6b GC/MS analysis of untreated and Fenton treated corn stover individual thioacidolysis monomer concentrations (mg/mL).

Data is shown with error bars indicating ± one standard deviation. [*: statistically significant ($P < 0.05$)].

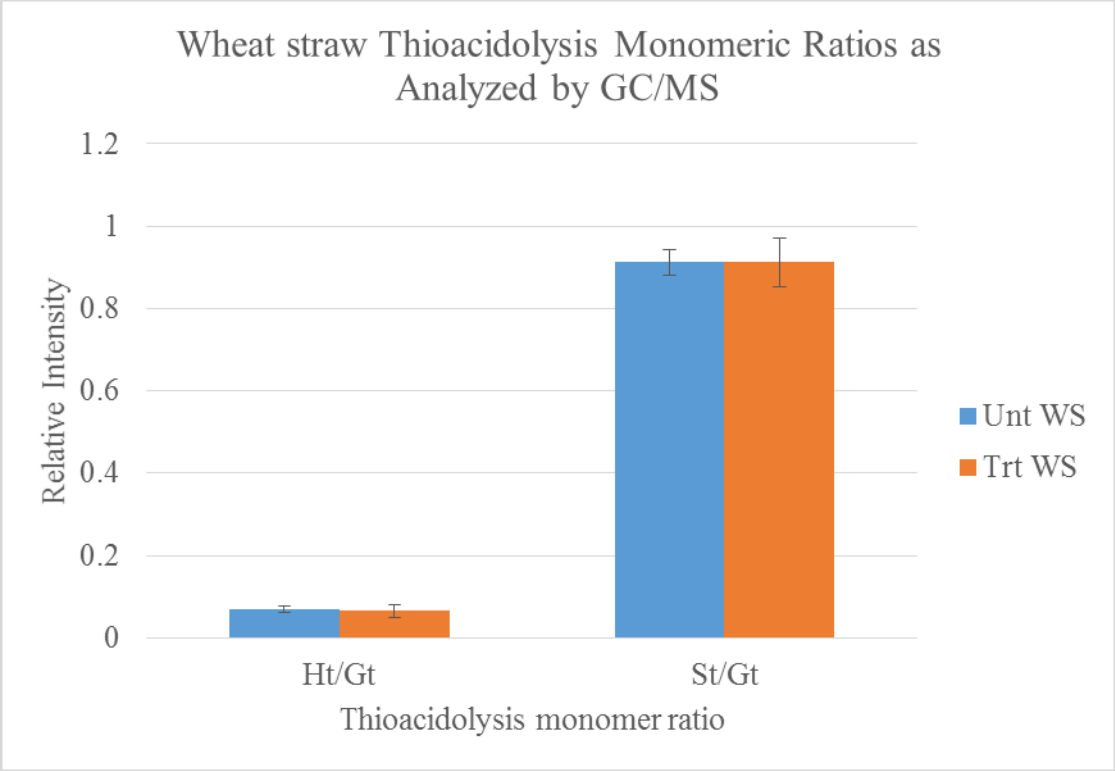

Figure 4.7a GC/MS analysis of untreated and Fenton treated corn stover monomeric ratios.

Data is shown with error bars indicating ± one standard deviation. [*: statistically significant ($P < 0.05$)].

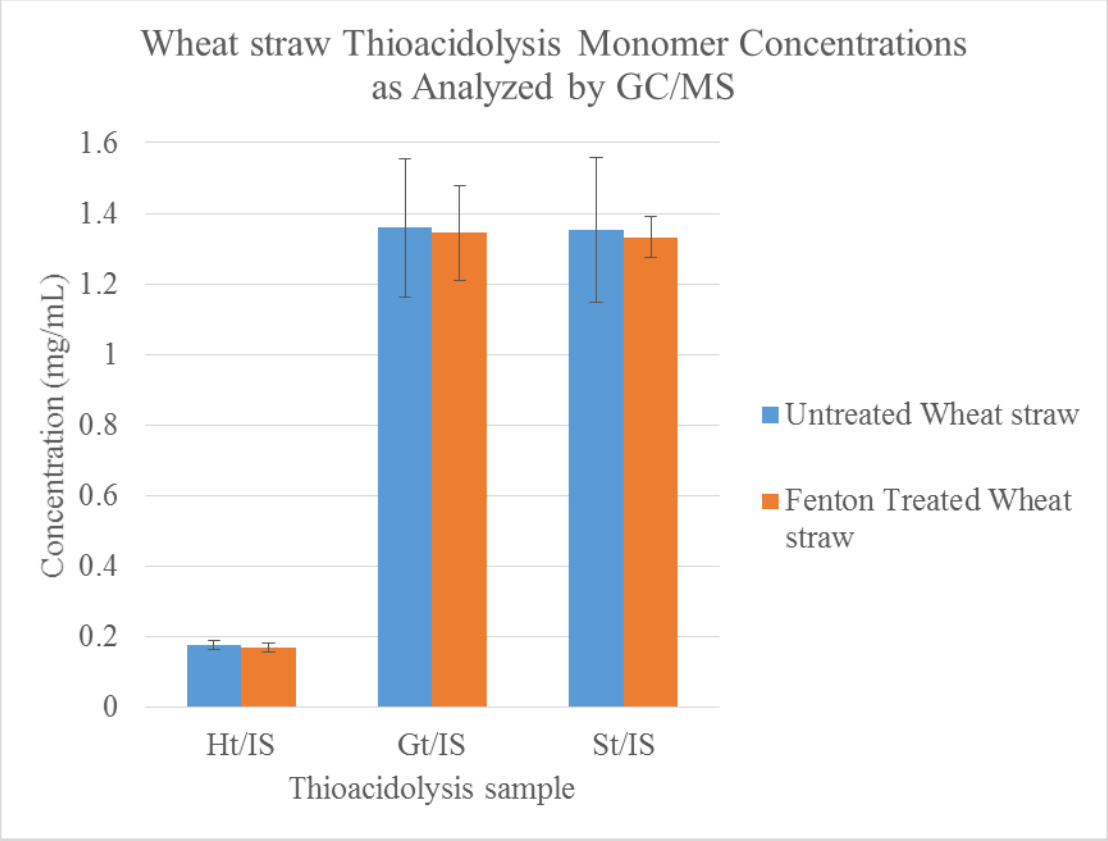

Figure 4.7b GC/MS analysis of untreated and Fenton treated wheat straw individual thioacidolysis monomer concentrations (mg/mL).

Data is shown with error bars indicating ± one standard deviation. [*: statistically significant ($P < 0.05$)].

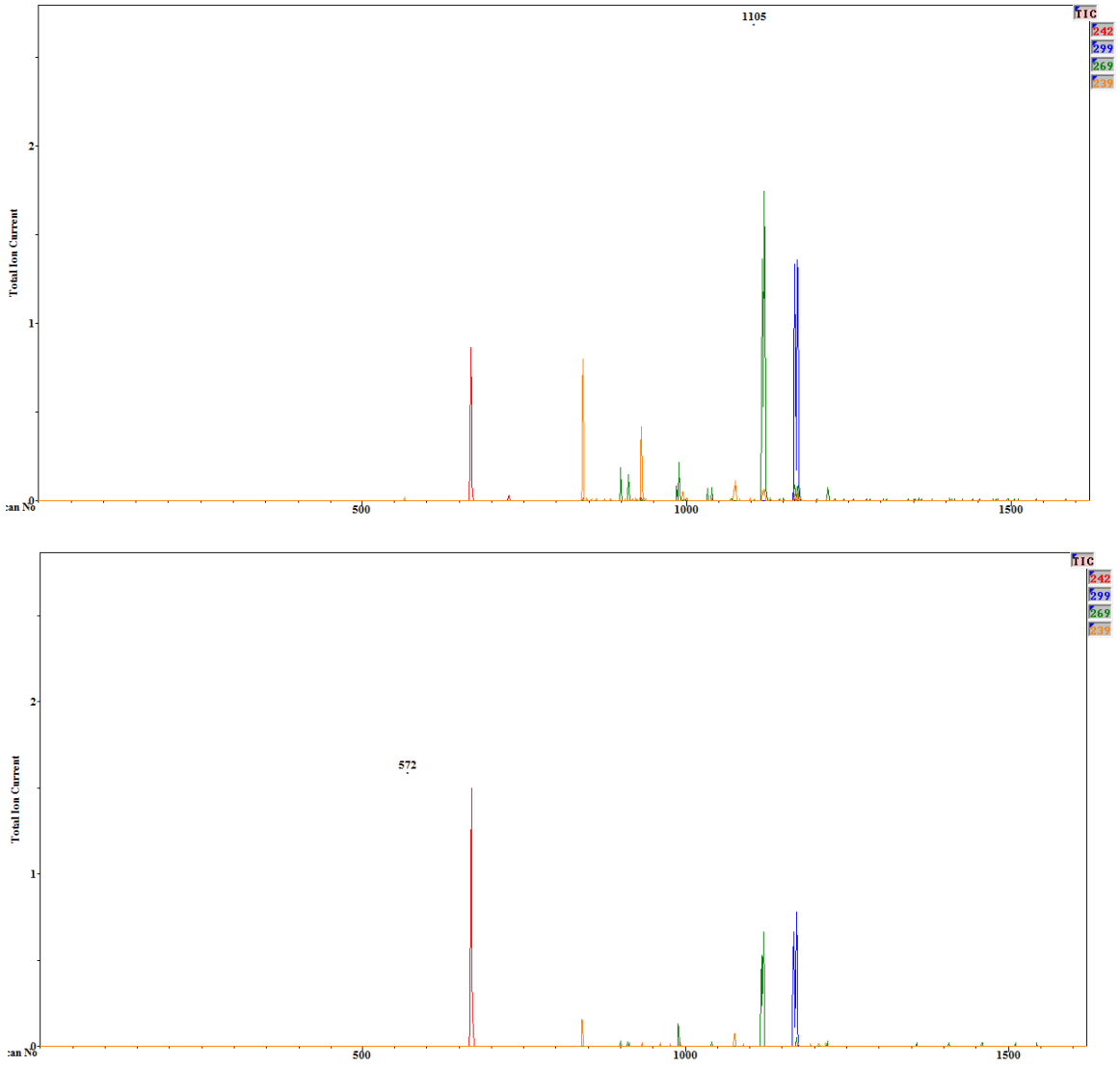

Figure 4.8 EIC of untreated corn stover (top) and alkaline peroxide treated corn stover (bottom).

(red – IS EIC, orange – H EIC, green – G EIC, blue – S EIC).

concentration upon pretreatment. It is not surprising that no statistical difference was seen in the H/G and S/G ratios because monomeric quantification reveals all three monomers decreased, thus, no significant change would be illustrated by a ratio. The significant difference in monomer concentrations were consistent with the significant increase in glucose detected upon enzymatic saccharification of alkaline peroxide pretreated corn stover (Figure 4.9). Alkaline peroxide pretreatment has been known to degrade lignin, thus, we would expect to see a decrease in monomer concentrations. Therefore, the hypothesis that changes in individual monolignol content upon pretreatment can be observed from quantification is supported.

4.4. Conclusion

In conclusion, calibration curves of the three thioacidolysis monomers, Ht, Gt and St were constructed for GC/MS providing sufficient linear correlation. Untreated and Fenton treated miscanthus, switchgrass, corn stover and wheat straw were subjected to analytical thioacidolysis and analyzed by GC/MS. Monomer concentrations were quantified and compared to monomeric ratios traditionally used. Although no significant difference was observed upon Fenton pretreatment, applying the monomeric quantitation to a pretreatment known to degrade lignin, alkaline peroxide treatment, a significant decrease in H, G and S concentrations were observed. Therefore, the project hypothesis is supported.

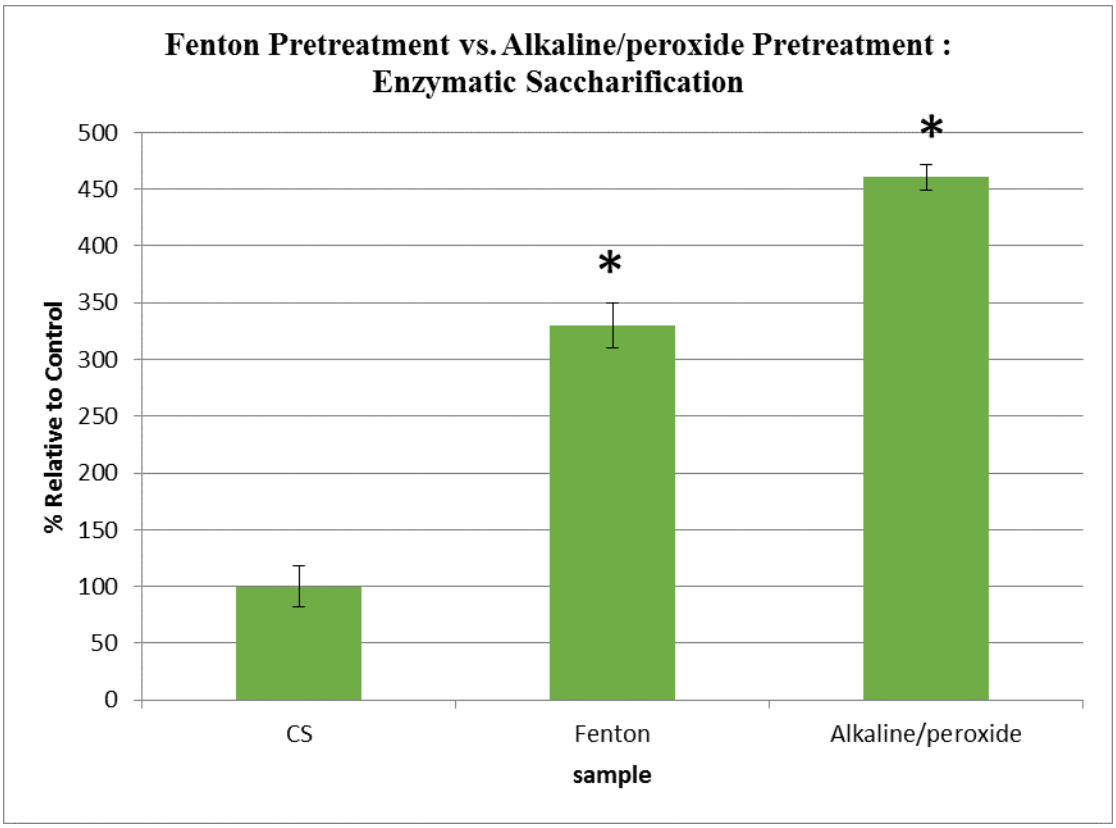

Figure 4.9 Enzymatic saccharification of untreated, Fenton treated and alkaline peroxide treated corn stover.

Data is shown with error bars indicating ± one standard deviation. [*: statistically significant ($P < 0.05$)].

5. Chapter 5 : Analysis of Lignin-Derived Monomers by Capillary Electrophoresis

5.1. Introduction

Capillary electrophoresis is a well-established separation technique utilized in pharmaceutical research and clinical application due to the high resolving power, rapid analysis time and small sample and reagent volume required. As discussed in Chapter 1, when a voltage is applied across the capillary, containing a buffer solution, an electrical double layer develops at the silica/solution interface, this is also known as the Stern layer. At pH values greater than 3, the surface silanol groups are negatively charged. Buffer cations congregate along the negative surface as a double layer, one immobilized and one a diffuse outer layer that is attracted towards the negatively charged cathode, creating an electroosomtic flow (EOF). The EOF is greater than the electrophoretic migration velocities (the velocity of the ion as it moves towards the electrode of interest) of the individual ions, producing bulk flow. When sample analytes are introduced into the CE system, they migrate based on their electrophoretic mobility, essentially size and charge. Cations move towards the cathode (negatively charged) and anions move towards the anode (positively charged). Small ions move faster than larger ones, and multiply charged ions move faster than singly charged ions [15]. Neutral species move with the same velocity as the bulk flow, hence it is a measure of the system EOF [17]. This is the separation mechanism of CE when conducting capillary zone electrophoresis (CZE) experiments.

Capillary electrophoresis has been applied to the analysis of potassium permanganate oxidation of lignin.[53] Potassium permanganate oxidation is an analytical degradation strategy which degrades the aliphatic side chains attached to aromatic rings in lignin. Upon $KMnO_4$ oxidation, a mixture of carboxylic acids are produced. The identification of 4-methoxybenzoic acid, 3,4-dimethoxybenzoic acid and 3,4,5-trimethoxybenzoic acid are the major products produced upon $KMnO_4$ oxidation indicative of uncondensed lignin.[53] The disadvantage of utilizing $KMnO_4$ oxidations to analyze lignin is that it will only degrade structures with free phenolic hydroxyl groups, encompassing only a fraction of the total lignin structure. Nevertheless, in collaboration with the Mark Meier group and the Center for Applied Energy Research (CAER), various lignins were treated with $KMnO_4$ oxidation and analyzed by CE to assess the presence of phenylpropanoid units, H, G and S.

One of the many advantages of CE analysis is the flexibility to conduct a variety of experiments by simply changing the background electrolyte solution (BGE also known as the running buffer). Introducing chiral selector additives into the BGE provides enantiomeric separation capabilities. This is especially important in the pharmaceutical industry where enantiomers can possess different pharmacological and toxicological properties. A commonly used chiral additive is cyclodextrin. Native cyclodextrins are cyclic oligosaccharides consisting of six, α-cyclodextrin (α-CD), seven, β-cyclodextrin (β-CD), and eight, γ-cyclodextrin (γ-CD), glucopyranose units linked by α-(1,4) bonds.[54] These cyclodextrins have the ability to form inclusion complexes with a variety of

compounds. Cyclodextrins have a hydrophilic outside, which provides solubility in water, and a hydrophobic inside or cavity, this produces a truncated cone shape.[54a]

The three commonly used native CDs are α-CD, β-CD and γ-CD. While all three CDs possess the same height or depth of CD cavity, the number of glucose units, solubility, inner diameter and cavity volume differ, as seen in table 5.1.[54b, 55] Alpha-cyclodextrin is the least sterically strained in ring form. Beta-cyclodextrin is the most commonly used CD due to its affordable price, accessibility and highest solubility in water.[54b] Alpha-cyclodextrin is typically used to conduct enantiomeric separation on low molecular weight compounds, β-CD is commonly used for racemic separation of aromatics and γ-CD is commonly used in applications of macrocyclic compounds and steroid due to its larger cavity size.[54b]

Modified cyclodextrins are often used to increase solubility, hydrophobic cavity volume or ability to form inclusion complexes. These factors need to be taken into account when determining the appropriate chiral additive.[54b] We utilized hydroxypropyl-beta-cyclodextrin (HP-β-CD) in this study to provide enantiomeric separation/analysis of synthesized arylglycerol monomers. Four potential diastereomers of the arylglycerols are shown in Figure 5.1. Knowledge of the racemic mixture of arylglycerols, will allow us to assess the stereochemistry of the products produced following epoxidation of monolignols.

Table 5.1 Cyclodextrins (CD) main properties.

CD	# glucopyranose units	Average MW (g/mol)	Solubility in water @ 25 °C (%, w/v)	Outer diameter (Å)	Cavity diameter (Å)	Cavity volume ($Å^3$)	pKa
α-CD	6	972	14.5	14.6	4.7-5.3	174	12.33
β-CD	7	1135	1.85	15.4	6.0-6.5	262	12.20
γ-CD	8	1297	23.2	17.5	7.5-8.3	427	12.08

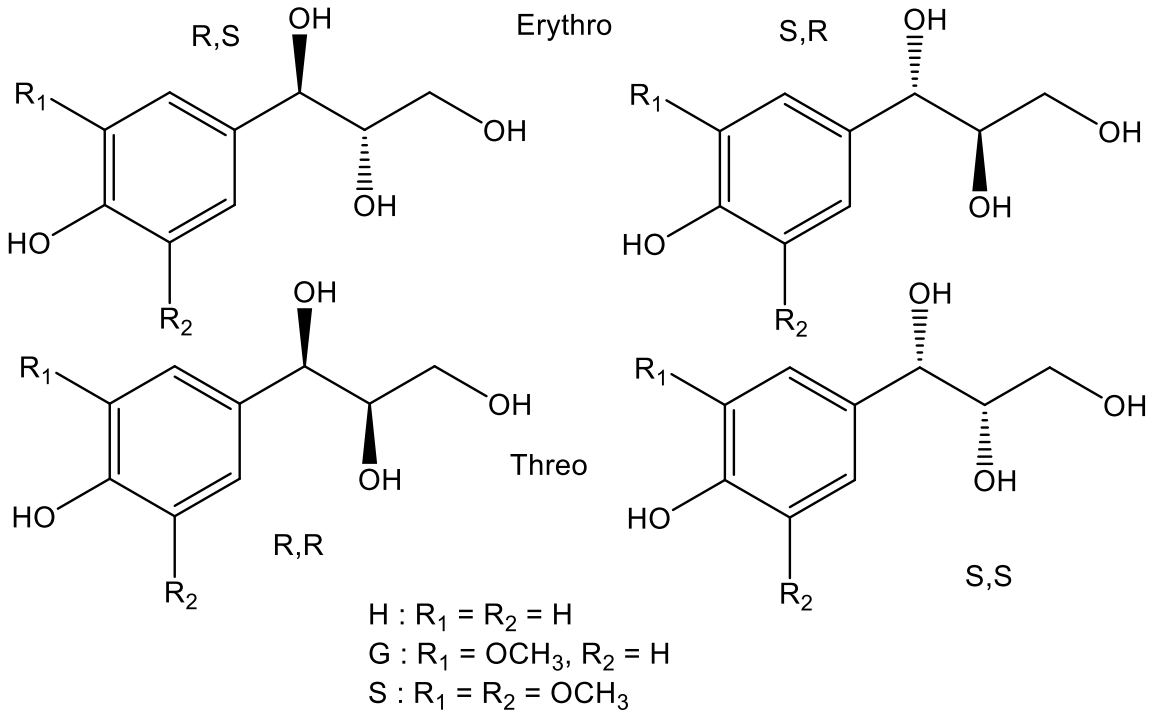

Figure 5.1 Arylglycerol diastereomers structures.

As discussed previously, thioacidolysis is a commonly used analytical degradative technique to assess the phenylpropanoid ratios that compose the β-O-4 linkages. Thioacidolysis is commonly coupled with GC/MS analysis. The EI characteristic spectra of the three thioacidolysis monomers has been well established. In addition to providing monomeric quantification capabilities by GC/MS, the synthesized thioacidolysis standards expands the ability to explore alternate analytical methodologies. Various analytical platforms would provide an additional route to aid in the task of accurate elucidation of the lignin ultrastructure is such a complex problem. Capillary electrophoresis provides a parallel analytical platform for lignin analysis. Unlike GC, CE allows for the analysis of acidic/basic analytes in aqueous systems. Capillary electrophoresis also provides a high resolution technique with an unparalleled theoretical plate count. Thioacidolysis monomers are considered to be slightly acidic with the ability to form phenolate ions in basic conditions, allowing for the separation as an anion in CE.[56] It is hypothesized that CE will provide a more rapid analytical technique, without the need for derivatization, for the analysis of lignin-derived thioacidolysis monomers.

5.2. Materials and methods

Materials.

All chemicals of reagent grade were obtained and used without further purification. Methanol, acetone, and sodium tetraborate decahydrate were purchased from Thermo Fisher Scientific (Waltham, MA, USA).

Methoxybenzoic acid standards (*p*-phenylphenol, 4-methoxybenzoic acid, 3,4-dimethoxybenzoic acid, 3,4,5-trimethoxybenzoic acid) and 2-hydroxypropyl-β-cyclodextrin were purchased from Sigma Aldrich (Milwaukee, WI, USA). Distilled water (18 MΩ) was used to make appropriate solutions/dilutions. Miscanthus, switchgrass, corn stover and wheat straw samples (all ~ 2 mm particle size) were obtained from collaborators in the Michael Montross Laboratory, University of Kentucky, Lexington, KY, USA.

Qualitative CE analysis of supplied lignin samples

Capillary electrophoresis was conducted on the Prince 650/660 CE system equipped with a Bischoff Lambda UV detector. A 50 x 360 µm capillary of 70 cm long, 26 cm effective length was utilized as a separation capillary. The capillary was conditioned daily with deionized water for 5 min at 1000mbar, 1 N NaOH for 5 min at 1000 mbar, 0.1 N NaOH for 5 min at 1000 mbar, deionized water for 3 min at 1000 mbar and finally flushed with BGE solution for 5 min at 1000 mbar. Capillary wall was regenerated by flushing the capillary with BGE for 5 min at 1000 mbar between runs. Analytes were injected hydrodynamically for 5 sec at 50 mbar. Separation was conducted at +15 kV monitoring 260 nm. Background electrolyte solution was 25 mM sodium borate pH 9.0. Methoxybenzoic acid stock standard was a 1.0 mg/mL in 1:1 (v/v) methanol/water. The stock standard mixture was diluted 1:10 with BGE prior to analysis. Potassium permanganate oxidation samples were obtained from collaborators in the Mark Meier Laboratory, University of Kentucky, Lexington, KY, USA. Lignin samples were also diluted with BGE.

Enantiomeric CE separations

Enantiomeric separations experiments were conducted on a Beckman Coulter MDQ capillary electrophoresis system equipped with a photodiode array detector (PDA). A 50 x 360 μm capillary of 60 cm long, 44 cm effective length was utilized as a separation capillary. Capillaries were conditioned daily according to the previously discussed procedure identical to that used to condition the capillaries used with the Prince CE. Capillary wall was regenerated by flushing the capillary with BGE for 5 min at 20 psi between runs. Analytes were injected hydrodynamically for 4 sec at 2.0 psi. Separation was conducted at +30 kV. Background electrolyte solution was 30 mM borax-NaOH pH 10.08 (with the addition of various concentrations of HP-β-CD). Arylglycerol standards were 0.05 mg mL samples in 0.5:10 MeOH/BGE.

Thioacidolysis analysis

Thioacidolysis samples were conducted according to the previously discussed protocol. Upon evaporation of the solvent, the reaction mixture was redissolved in 500 μL of methylene chloride and split into two samples (GC – 100 μL, CE – 400 μL). Both samples were evaporated and redissolved in: GC – 20 μL 1:1 BSTFA/pyridine, CE – 500 μL BGE (75 mM borate-phosphate 50% methanol pH 10.08).

CE/PDA analyses were conducted on a Beckman Coulter P/ACE MDQ capillary electrophoresis system with a PDA detector. Capillaries were conditioned daily, as previously discussed. Background electrolyte solution was flushed through the

capillary for 5 min at 20 psi between runs, BGE - 75 mM borate-phosphate 50% methanol pH 10. Hydrodynamic injection was made for 4 sec at 2 psi. Separation was conducted on a 50 x 360 µm fused silica capillary 60 cm long, 44 cm effective length, at 30 kV. A wavelength of 210 nm was specifically monitored.

Linear regression analysis were conducted utilizing Microsoft excel 2013 workbook software. Calibration curves were displayed utilizing Sigmaplot 12.3.

5.3. Results and discussion

Potassium permanganate oxidation is an analytical degradation method utilized to analyze degraded polymeric lignin in order to assess monomeric ratios, as previously discussed. Three methoxybenzoic acids are the prominent products from $KMnO_4$ oxidations, (Figure 5.2) indicative of the three lignin subunits, H, G and S. We had collaborators whom were interested in obtaining S:G ratios from various lignin sources upon $KMnO_4$ oxidation. Seeing that the products of interest are methoxybenzoic acids, which should deprotonate nicely in basic conditions, we hypothesized that capillary electrophoresis (CE) would be an ideal analytical platform to assess the S:G ratios in various lignin sources.

A CE method to separate the three methoxybenzoic acid standards was developed. Sodium borate is a very common background electrolyte (BGE) used for CE analysis in the basic pH range. Figure 5.3 shows four consecutive runs of a methoxybenzoic acid standard mix analyzed in a 25 mM sodium borate BGE buffer system. Baseline separation was reproducibly achieved with low analysis

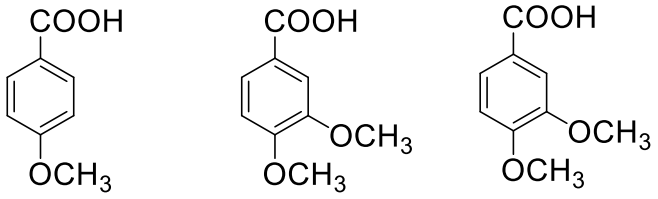

Figure 5.2 Methoxybenzoic acid structures.

(left: 4-methoxybenzoic acid, middle: 3,4-dimethoxybenzoic acid, right: 3,4,5-trimethoxybenzoic acid)

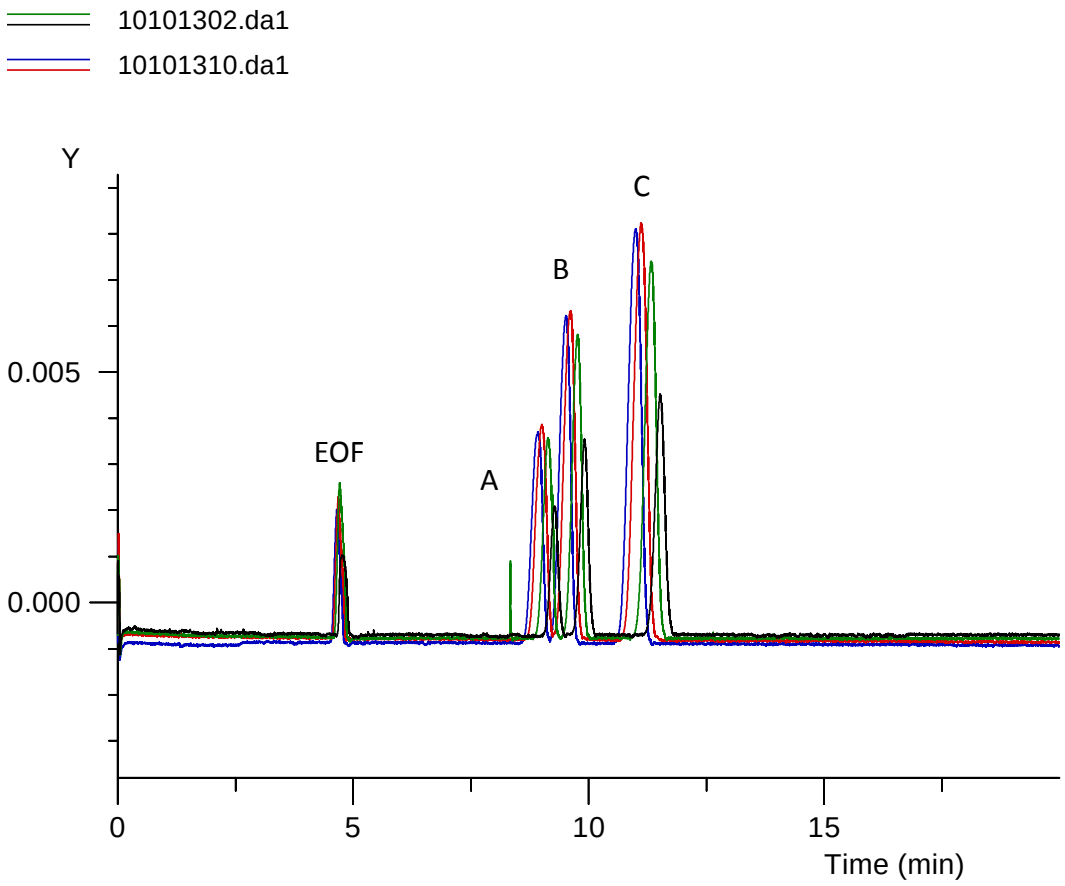

Figure 5.3 Electropherogram of four consecutive CE runs of 0.1 mg/mL methoxybenzoic acid standard mix.

BGE: 25 mM $Na_2B_4O_7$ pH 9.04, 50 mbar 5 sec, +15 kV

A) 3,4,5-trimethoxybenzoic acid, B) 3,4-dimethoxybenzoic acid C) *p*-methoxybenzoic acid

times, less than 15 minutes. A slight change in elution time was seen, however, acetone was added to the sample as a neutral marker or measure of the electroosmostic flow (EOF) to correct for capillary changes. With a wall driven flow, as seen in CE separations, the silanol groups are in constant equilibrium with the system, protonated and deprotonated. In addition, as basic solutions are flushed through the capillary, the protons on the wall get stripped off, thus, with increasing use, the capillary inner diameter expands decreasing EOF and zeta potential, both of which affect resolution. This explains slight variation in elution time.

With an establish CE method, $KMnO_4$ oxidized lignin samples labelled Seth lignin (Figure 5.4), peach pit lignin (Figure 5.5), Canada lignin (Figure 5.6) and H_2O_2 oxidation (Figure 5.7) were analyzed. The three monomers were detected in all four samples, but showed different absorption intensities. Seth lignin (Figure 5.4) electropherogram portrays H>G>S in relative absorption intensity, thus, indicating relative monomeric intensities. These relative intensities suggests Seth lignin could be a grass lignin because grass lignins typically have higher H content. The H_2O_2 (Figure 5.7) oxidation electropherogram detected the three monomers with the same absorption intensities. Suggesting this lignin sample could also be a grass lignin. Peach pit lignin (Figure 5.5) electropherogram while detected the three monomers, G was approximately four times greater than H and S. Gymnosperms typically have greater G content, thus, peach pit lignin could fall into the gymnosperm category. Canada lignin (Figure 5.6) electropherogram has a higher S and G content than H

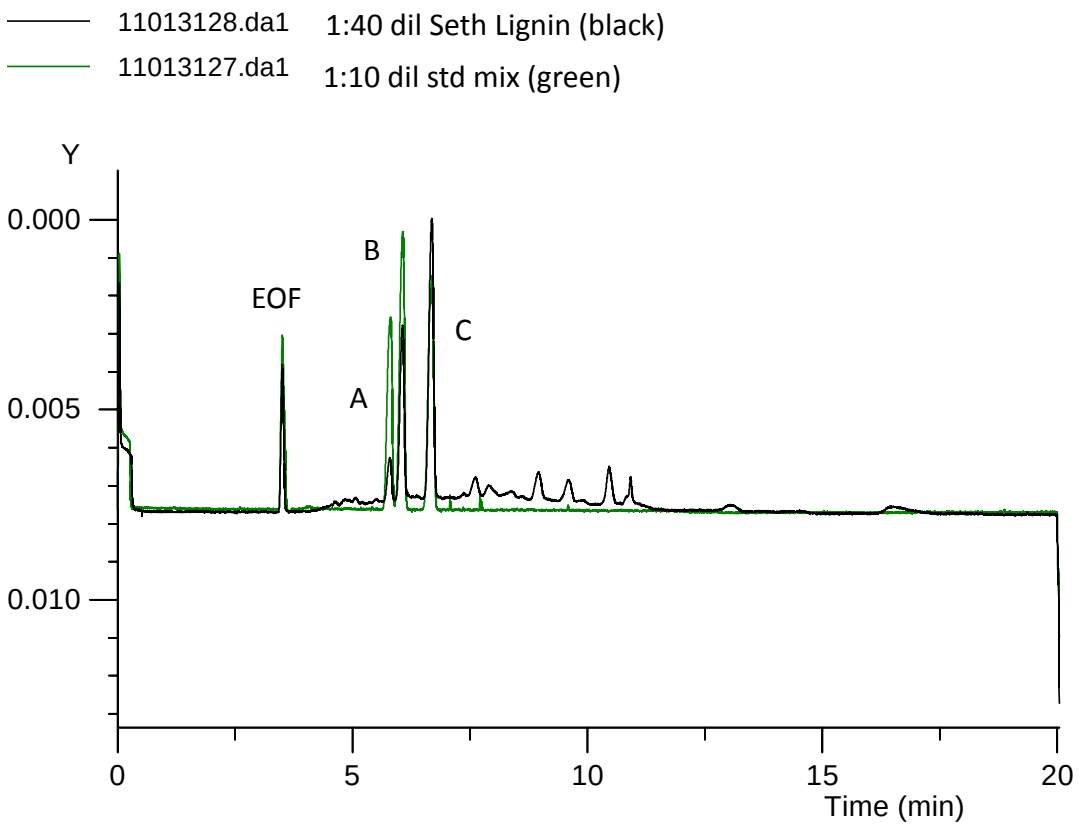

Figure 5.4 Electropherogram of 1:40 dilution, with BGE, of Seth lignin.

BGE: 25 mM $Na_2B_4O_7$ pH 9.04, 50 mbar 5 sec, +15 kV

A) 3,4,5-trimethoxybenzoic acid (S), B) 3,4-dimethoxybenzoic acid (G) C) *p*-methoxybenzoic (H)

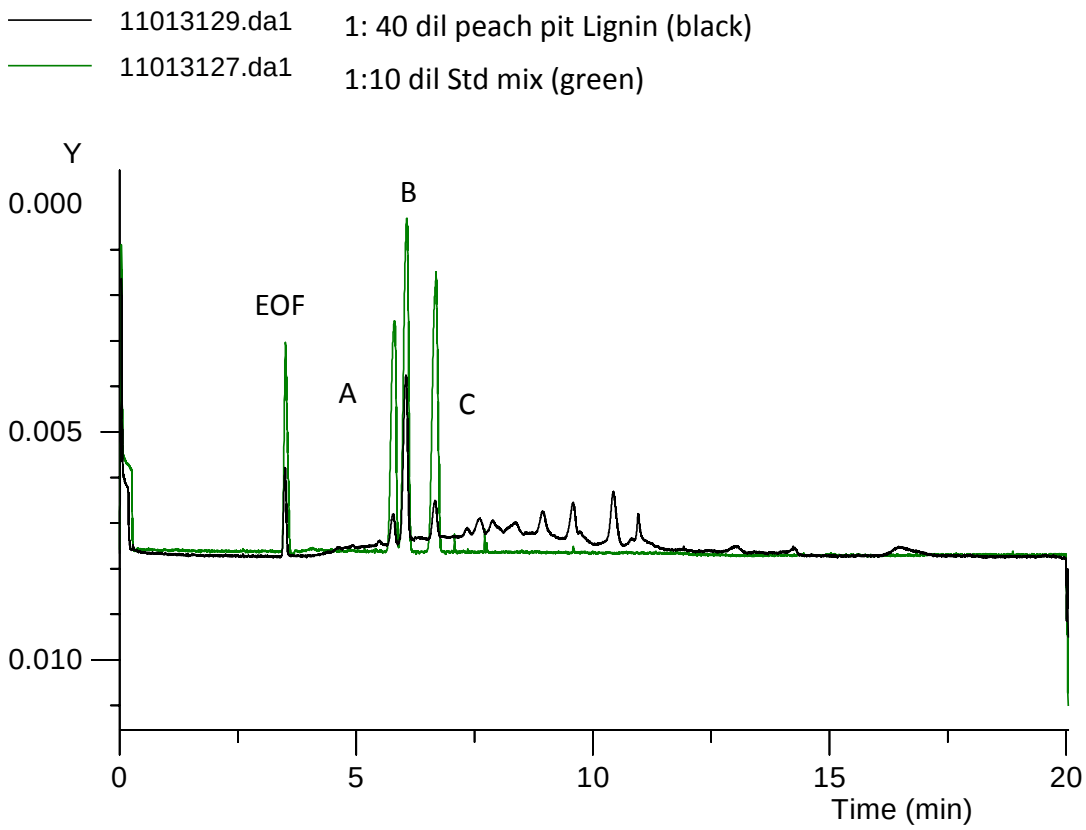

Figure 5.5 Electropherogram of 1:40 dilution, with BGE, of peach pit lignin.

BGE: 25 mM $Na_2B_4O_7$ pH 9.04, 50 mbar 5 sec, +15 kV

A) 3,4,5-trimethoxybenzoic acid (S), B) 3,4-dimethoxybenzoic acid (G) C) *p*-methoxybenzoic (H)

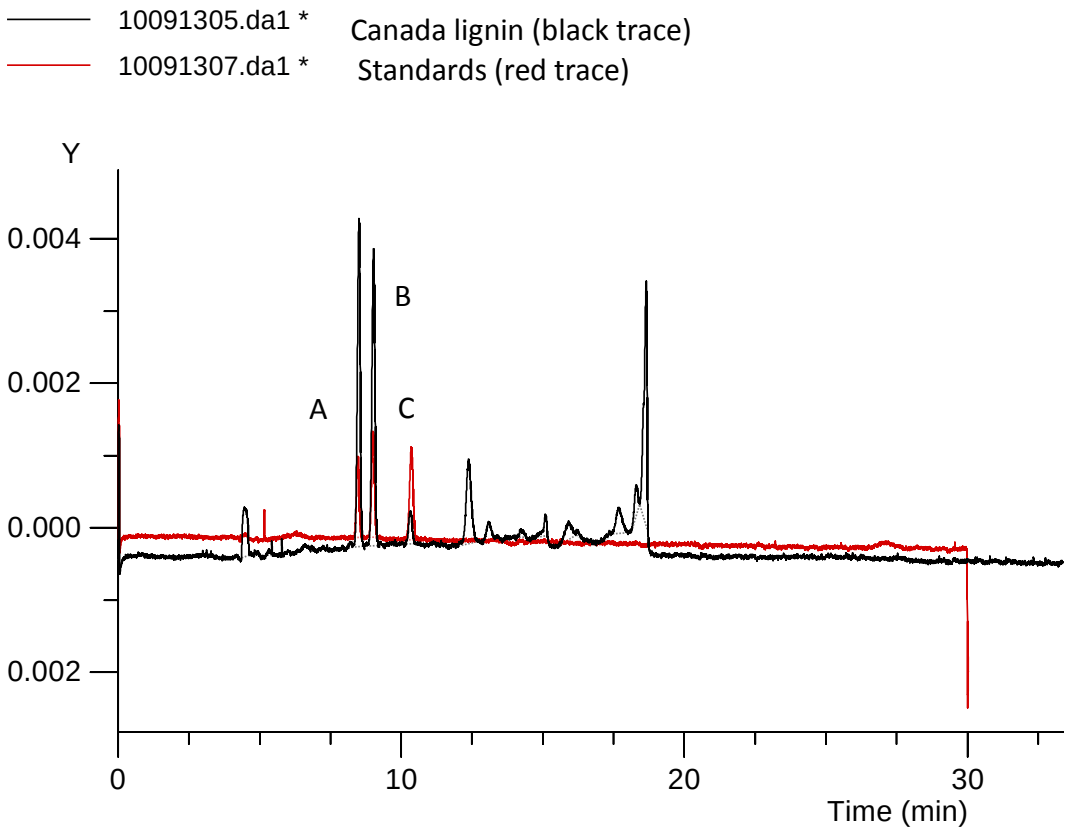

Figure 5.6 Electropherogram of 1:10 dilution, with BGE, of Canada lignin.

BGE: 25 mM $Na_2B_4O_7$ pH 9.04, 50 mbar 5 sec, +15 kV

A) 3,4,5-trimethoxybenzoic acid (S), B) 3,4-dimethoxybenzoic acid (G), C) *p*-methoxybenzoic (H)

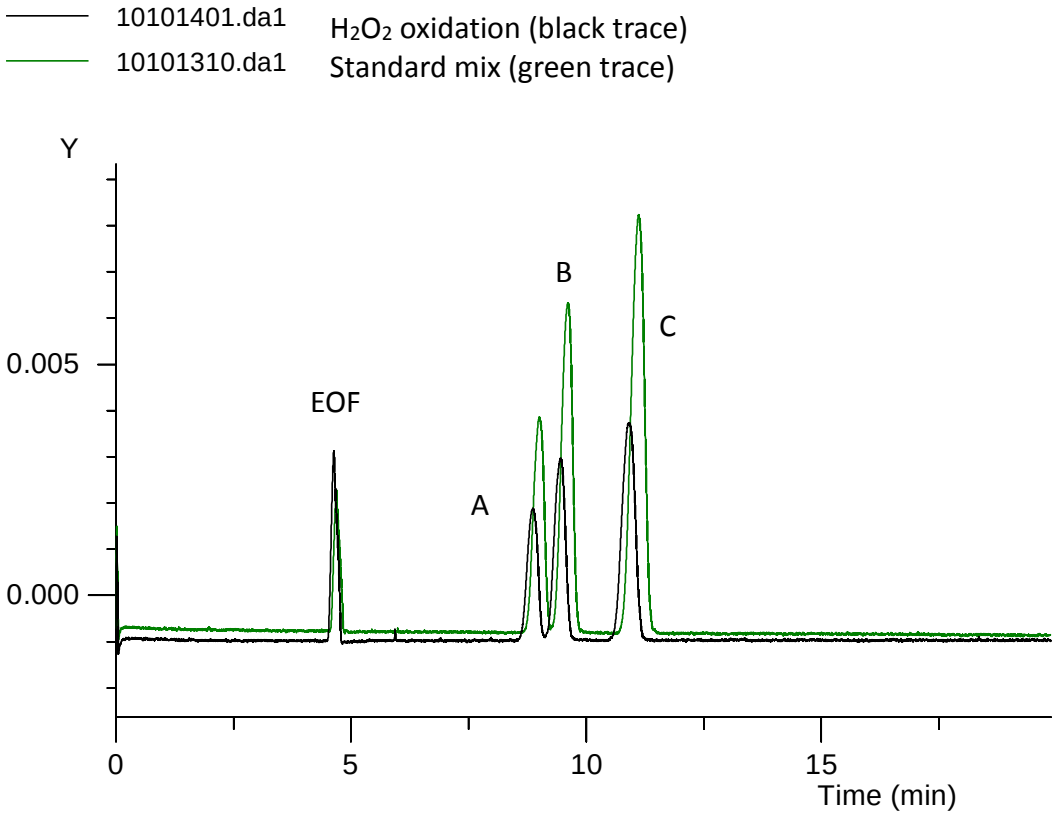

Figure 5.7 Electropherogram of H_2O_2.

BGE: 25 mM $Na_2B_4O_7$ pH 9.04, 50 mbar 5 sec, +15 kV

A) 3,4,5-trimethoxybenzoic acid (S), B) 3,4-dimethoxybenzoic acid (G), C) *p*-methoxybenzoic (H)

suggesting Canada lignin to be an angiosperm due to angiosperm lignins being primarily composed of G and S subunits. Monomeric ratios obtained from CE analysis were consistent with monomeric ratios from pyrolysis GC/MS as conducted by our collaborators.[57]

Utilizing our CE method to successfully identify lignin-derived $KMnO_4$ oxidized monomer products lead us to hypothesize the use of CE to detect lignin degradation products due to pretreatment. A preliminary CE experiment was conducted on "BCL lignin", which was a preliminary Fenton pretreated material. The electropherogram of BCL lignin (Figure 5.8) suggests the detection of the three methoxybenzoic acids, however, S and G peaks from the standard trace lined up under a peak with an unresolved shoulder. This suggests the potential for additional/alternate compounds under the shouldered peak. Although this question remained unresolved, this preliminary experiment lead us to believe we could utilize CE to assess the affects pretreatment, more specifically, solution phase Fenton pretreatments, has on lignin.

It was at this point a new capillary electrophoresis instrument, the Beckman Coulter MDQ equipped with a photodiode array detector (PDA) was obtained. A feature of the MDQ that differs from the Prince CE is the use of a capillary cartridge. The Prince CE allows more flexibility in operation, for example, the capillary length is limited by the minimum length from inlet to outlet. However, the MDQ has a cartridge the capillary is required to be threaded through which has a set length and set effective length. This feature of the MDQ

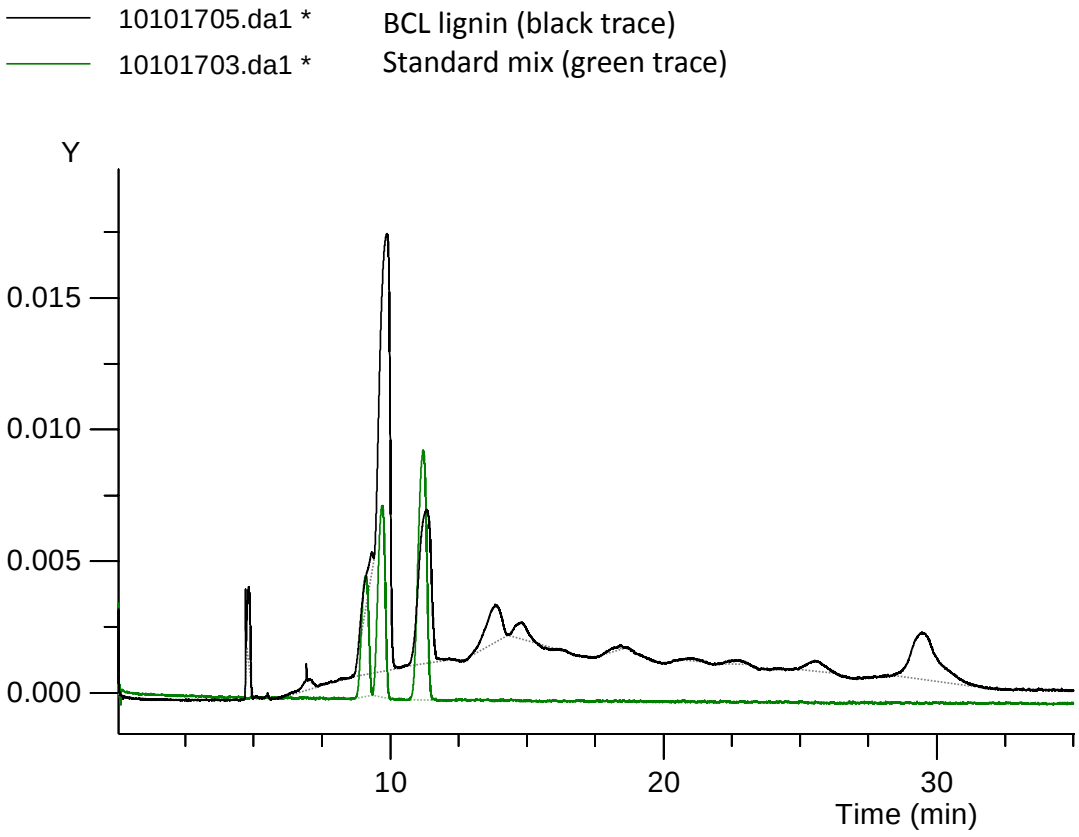

Figure 5.8 Electropherogram of BCL lignin sample.

1:50 dilution with BGE (BGE: 25 mM $Na_2B_4O_7$ pH 9.04, 50 mbar 5 sec, +15 kV)

required a longer effective length than that previously used with the Prince. This effective length provided more real estate for separation, thus higher resolution/separation between peaks, but longer analysis time. Figure 5.9 shows the elution of the three methoxybenzoic acid standards. Although there is an increase in analysis time, the gain of increased resolution will be highly beneficial for complex samples with a large number of potential compounds. Table 5.2 shows the elution times and peak areas of four replicate analyses of a standard mix shown in Figure 5.9. Elution times showed high reproducibility with less than 3% relative standard deviations (RSD). Peak area reproducibility was also acceptable with less than 16% RSDs.

Upon demonstrating the ability to identify lignin-derived $KMnO_4$ oxidation products by CE and the reproducibility of CE, we aimed to develop an alternate CE methodology that paralleled the analytical $KMnO_4$ oxidation approach. We know that lignin is a complex problem due to its highly variable composition. Currently, an array of analytical degradation methods are utilized to assess lignin in its monomeric form. It is also known that majority of the linkages that exist in lignin is the β-O-4 linkage and thioacidolysis has been shown to be the most selective analytical degradation method of the β-O-4 linkage.[39, 41] Thus, we chose to utilize thioacidolysis as our analytical degradative method for the elucidation of lignin monomeric composition.

As previously discussed in Chapter 3, we needed to synthesize the thioacidolysis monomers in order to provide quantitative monomeric information.

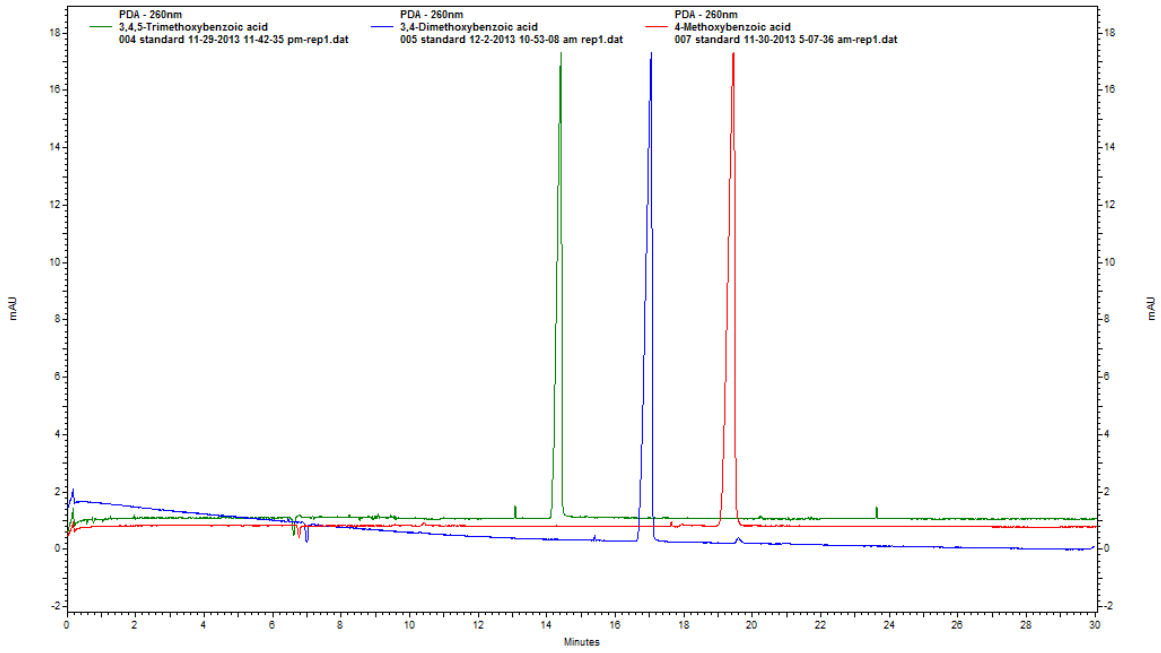

Figure 5.9 Electropherogram of 3,4,5-trimethoxybenzoic acid (S, green), 3,4-dimethoxybenzoic acid (G, blue) and p-methoxybenzoic acid (H, red).

BGE: 25 mM $Na_2B_4O_7$ pH 9.04, 50 mbar 5 sec, +15 kV

Table 5.2 Capillary electrophoresis elution times and peak areas for methoxybenzoic acid standards.

(0.1 mg/mL in BGE; BGE: 25 mM $Na_2B_4O_7$ pH 9.04, 50 mbar 5 sec, +15 kV).

Elution time	**3,4,5-trimethoxybenzoic acid**	**3,4-dimethoxybenzoic acid**	**4-methoxybenzoic acid**
1	14.417	17.050	19.450
2	14.542	16.729	19.217
3	14.704	16.475	19.204
4	14.538	16.142	19.017
Average	14.550	16.599	19.222
Stdev	0.118	0.385	0.177
RSD	0.809	2.319	0.923
Peak area	**3,4,5-trimethoxybenzoic acid**	**3,4-dimethoxybenzoic acid**	**4-methoxybenzoic acid**
1	216915	355433	470015
2	239478	273745	531588
3	222059	388523	555000
4	189973	384505	561139
Average	217106.25	350551.50	529435.50
Stdev	20504.27	53284.59	41609.63
RSD	9.44	15.20	7.86

The thioacidolysis monomers could be synthesized by a traditional thioacidolysis reaction once the arylglycerol version was made. According to the proposed synthetic scheme seen in Chapter 3, the arylglycerol can be synthesized through the use of an epoxidation. Based on this synthetic strategy, theoretically, only one form of the possible diastereomers can be synthesized. The arylglycerol monomers have two chiral centers, thus, the potential for a racemic mixture (Figure 5.1).[52a] The potential diastereomers are referred to as the erythro or threo form. The erythro form can have S/R or R/S stereochemistry and the threo can have S/S or R/R stereochemistry at the chiral carbons. However, because we generate an oxirane ring that will open/dihydroxylate, the hydroxyl group will add on the opposite side, not the same side the ring is on. This is thought to occur due to the steric hindrance of the oxirane ring. We hypothesize the synthesized arylglycerol product to exist as the erythro form.

Liu *et al*., showed the application of CE using a chiral additive to conduct enantiomeric separations of guaiacyl glycerol.[52a] Applying the experimental set up discussed by Liu *et al.*, we aimed to conduct analyses of the three synthesized arylglycerols, Hg, Gg and Sg, using 2-hydroxypropyl-beta-cyclodextrin (HP-β-CD) as the chiral additive. Analysis was conducted first on guaiacyl glycerol, Gg, to repeat what was reported. If we have a diastereomeric mixture of our product, we should get two peaks without chiral additive, HP-β-CD. With the addition of HP-β-CD, we should be able to separate the enantiomers of each diastereomer, if the two diastereomer forms are present, four peak should be detected. Figure 5.10 shows the electropherogram of Gg without a chiral additive. Expecting a single

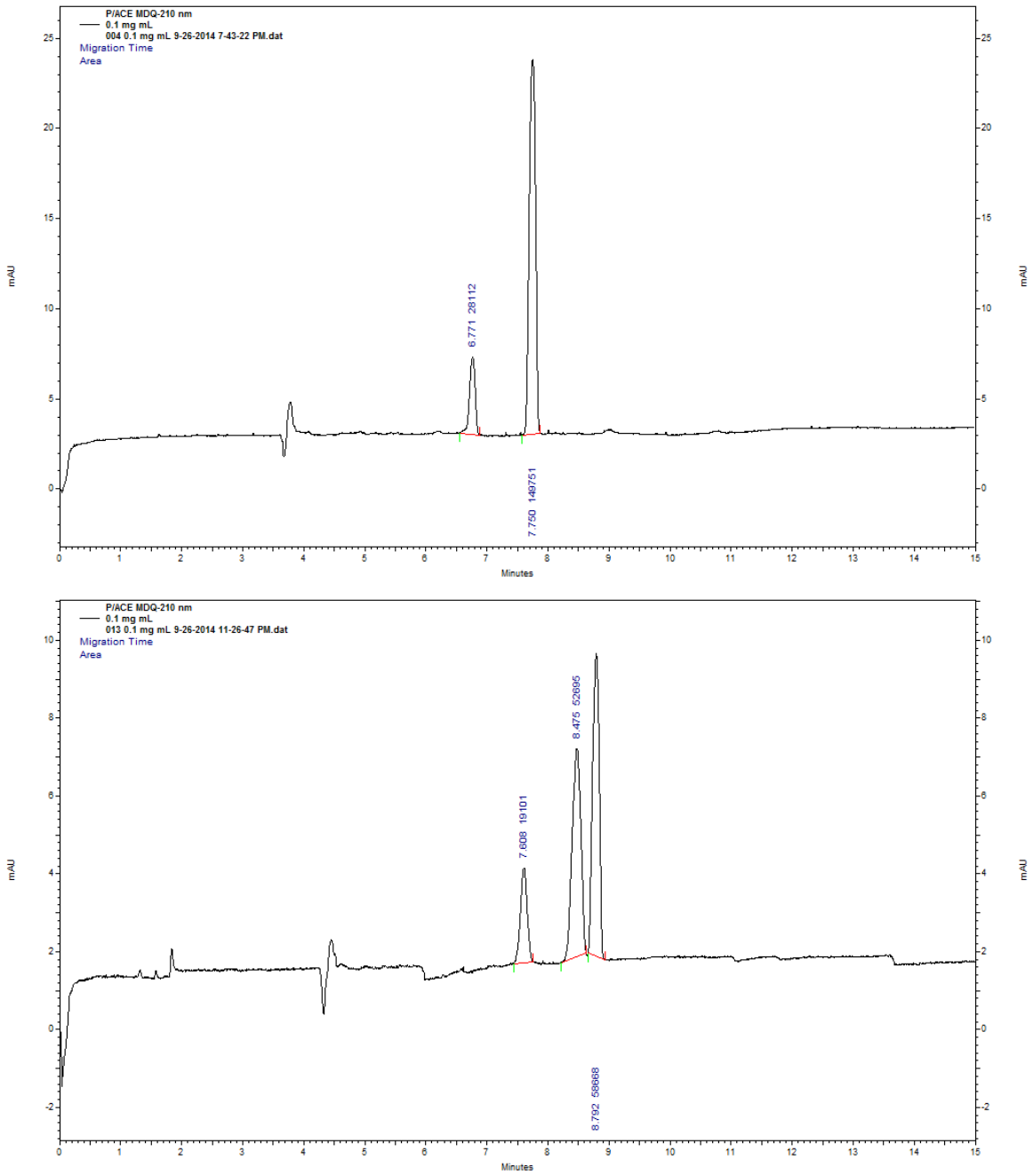

Figure 5.10 Electropherogram of guaiacyl glycerol (Gg, 0.1 mg/mL) without HP-β-CD (top) and with 40 mM HP-β-CD (bottom).

peak based on the reaction scheme, an additional peak was observed which generated doubt of the hypothesized single diastereomer product. However, with our original hypothesis in mind, we set to figure out if the additional peak was the other diastereomer of our product or due to some other reason. If there was in fact a racemic mixture of the two diastereomers present and the two peaks are the diastereomers, we should see four peaks with the addition of the chiral additive, HP-β-CD. Figure 5.10 shows the electropherogram of the synthesized guaiacyl glycerol (Gg) standard with the addition of 40 mM HP-β-CD. Three peaks are detected with the addition of the chiral additive. This suggests the extra peak seen without the cyclodextrin was not a result of a diastereomeric mixture. This is also supported by the enantiomeric separation of the larger product peak which supports enantiomeric resolution with the chiral additive. Figure 5.11 shows the electropherogram of Sg without chiral additive, CD. Again, two peaks are detected. When 40 mM HP-β-CD was added, three peaks were detected (Figure 5.11), which was consistent with the results seen for Gg. The same experiments were repeated for Hg (Figure 5.12). The electropherogram without CD (Figure 5.12) shows two peaks as seen for Sg and Gg. The addition of HP-β-CD provided enantiomeric separation of the arylglycerol product peak.

Using HP-β-CD as a chiral additive provided enantiomeric resolution for the arylglycerol products synthesized which support the reaction scheme and the hypothesis that only one diastereomeric form was synthesized, although it is an enantiomeric mixture. What is this additional peak? Experimental results reject

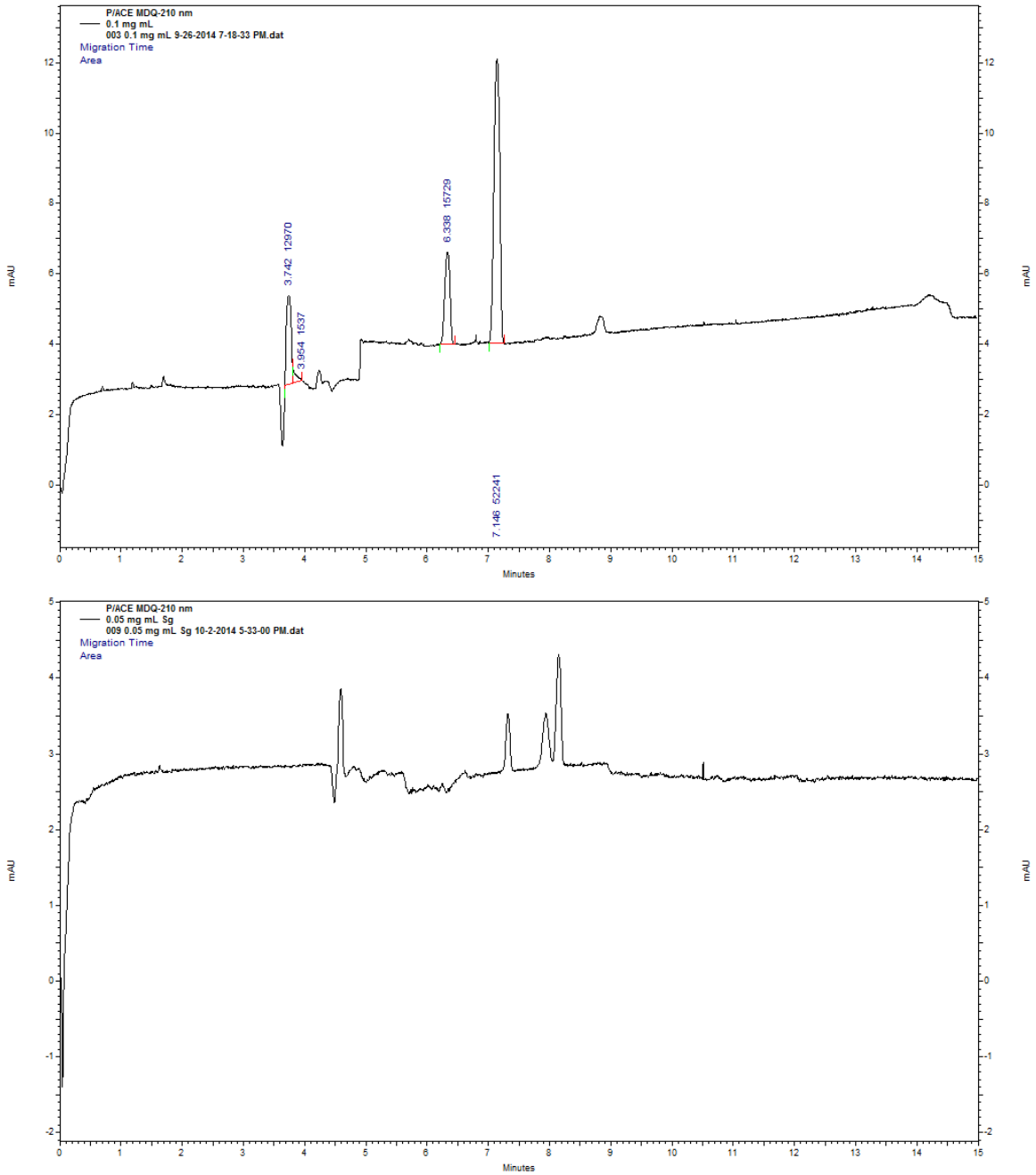

Figure 5.11 Electropherogram of syringyl glycerol (Sg, 0.1 mg/mL) without HP-β-CD (top) and with 40 mM HP-β-CD (bottom).

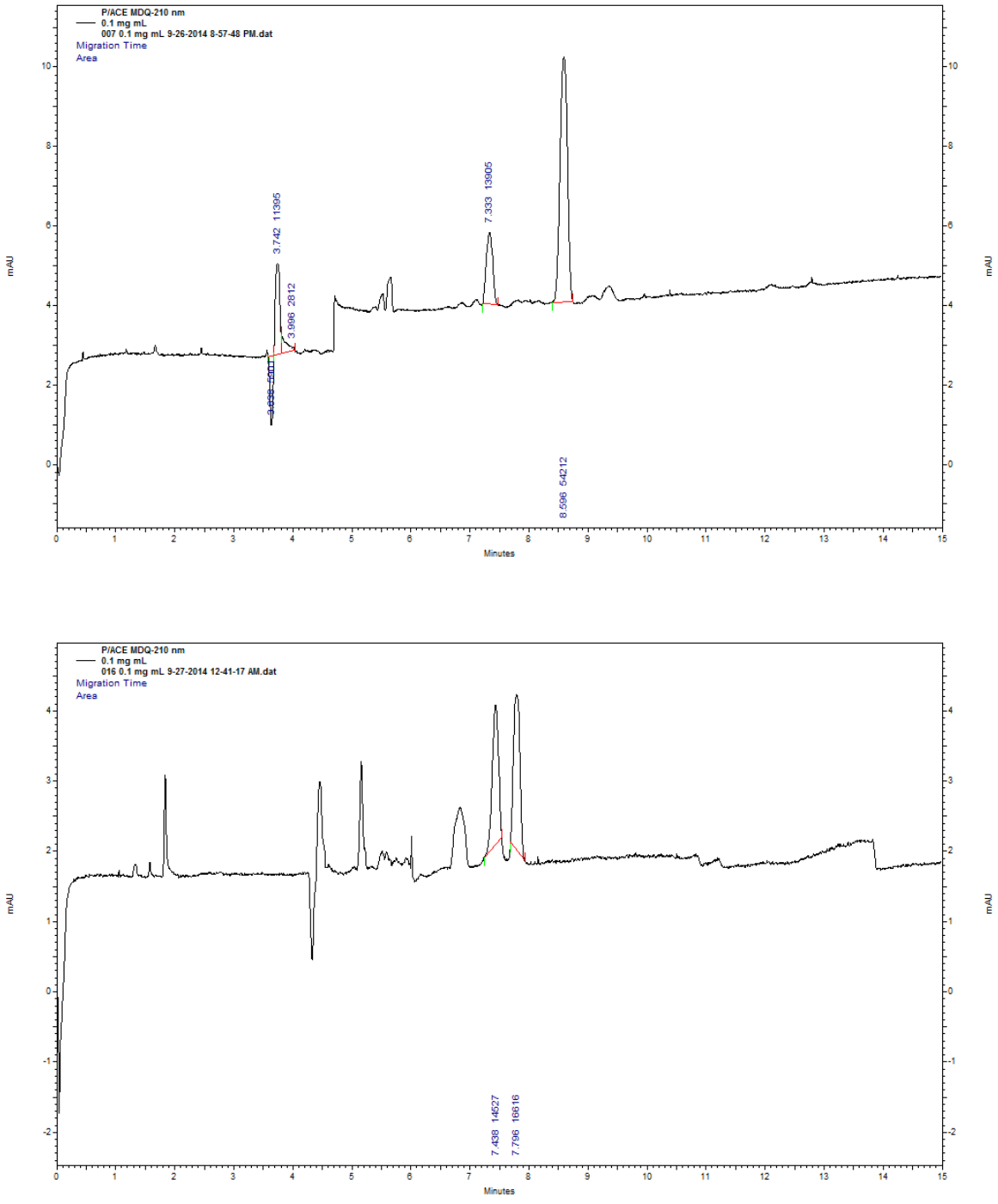

Figure 5.12 Electropherogram of *p*-hydroxyphenyl glycerol (Hg, 0.1 mg/mL) without HP-β-CD (top) and with 40 mM HP-β-CD (bottom).

the hypothesis that it is the other diastereomer product, and it is unlikely that it is an impurity in the standard because the standard solutions for Gg and Sg were made from weighed out crystallized product confirmed by x-ray crystallography, NMR, TLC and GC/MS with analytical purity greater than 93%. An alternate hypothesis is needed. Literature teaches that borate has the ability to form complexes and the BGE used was a borate buffer.[58] Thus, it can be speculated that the additional peak seen in Sg, Gg and Hg electropherogram could be a borate complex with the product. When the same Gg standard solution was analyzed in an ammonium acetate BGE buffer, only a single peak was detected, further supporting the speculation of a borate complex.

We have generated data supporting the ability of CE to provide enantiomeric resolution of the synthesized arylglycerol products with the addition of a chiral additive. It is widely accepted that the amount of chiral additive directly correlates with the enantiomeric resolution capabilities of the analytical method. While studying chiral CE, we wanted to see the effects of HP-β-CD concentration on enantiomeric separation of arylglycerol products. Figure 5.13 shows the electropherograms of Gg with increasing concentrations of HP-β-CD. With addition of 25 mM HP-β-CD, we start to see separation of the enantiomers but they are not baseline resolved. Increasing the CD concentration to 40 mM provides baseline resolution, but as the CD concentration increases to 60 mM, peak broadening is observed as well as a baseline drift. Baseline drift, in CE, is often a sign of Joule heating. At 80 mM concentration of HP-β-CD, spikes are seen throughout the electropherogram further suggesting Joule heating generated

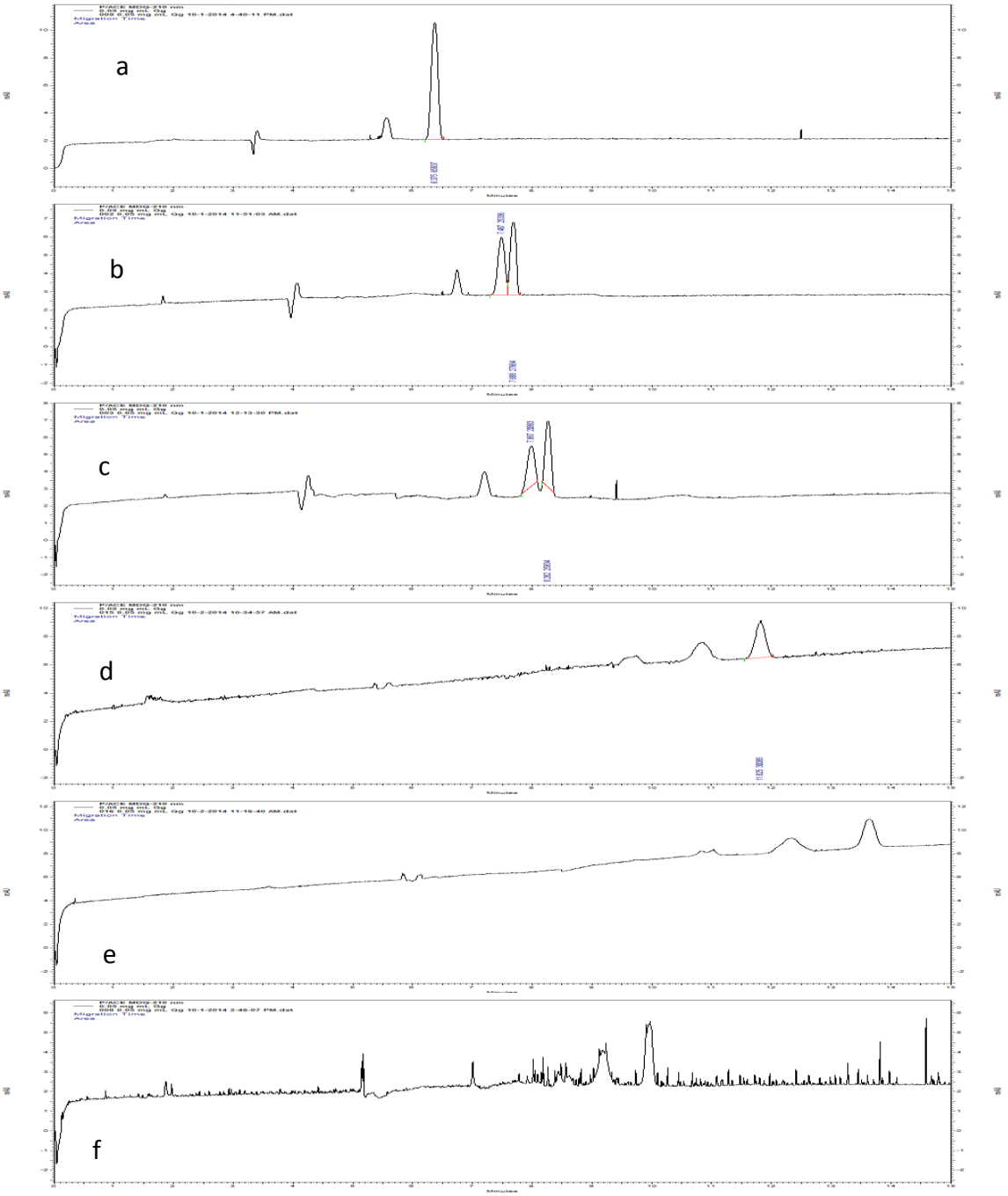

Figure 5.13 Guaiacyl glycerol (Gg, 0.1 mg/mL) electropherogram of a) no HP-β-CD b) 25 mM HP-β-CD c) 40 mM HP-β-CD d) 60 mM HP-β-CD e) 70 mM HP-β-CD f) 80 mM HP-β-CD.

by the large number of ions in solution. Figures 5.14 and 5.15 show analogous experiments for Sg and Hg. The results for Sg and Hg were consistent with the observed trend of Gg.

The conclusion of our chiral CE experiments are that with the addition of 40 mM HP-β-CD, we are able to achieve enantiomeric separation for all three synthesized arylglycerols. Chiral CE and GC/MS experiments support the hypothesis that one form of the potential diastereomers were synthesized, thus, supporting the suggested reaction scheme. Lastly, at 60 mM HP-β-CD, sufficient peak broadening was observed as well as Joule heating which is detrimental to the separation efficiency of CE. We can now confidently state that the arylglycerol product synthesized exists as one diastereomeric form.

A CE/PDA method for the separation of the thioacidolysis monomers was developed. *Para*-phenylphenol (PPP) was used as the internal standards for all further analyses. PPP was chosen as an internal standard due to its aromatic structural similarity to the thioacidolysis monomers and it does not affect separation efficiencies. In addition, PPP has a unique UV spectrum from that of the thioacidolysis monomers providing peak identity confirmation by CE/PDA. In developing a CE method, several parameters are to be considered such as organic modifier, voltage applied, pH and buffer composition. Previous studies have shown the phenolic pKa is greater than 10, therefore, the buffer pH was required to be highly basic (pH >10).[56] In searching through highly basic buffer systems, a glycine-NaOH buffer was chosen. Thioacidolysis monomers

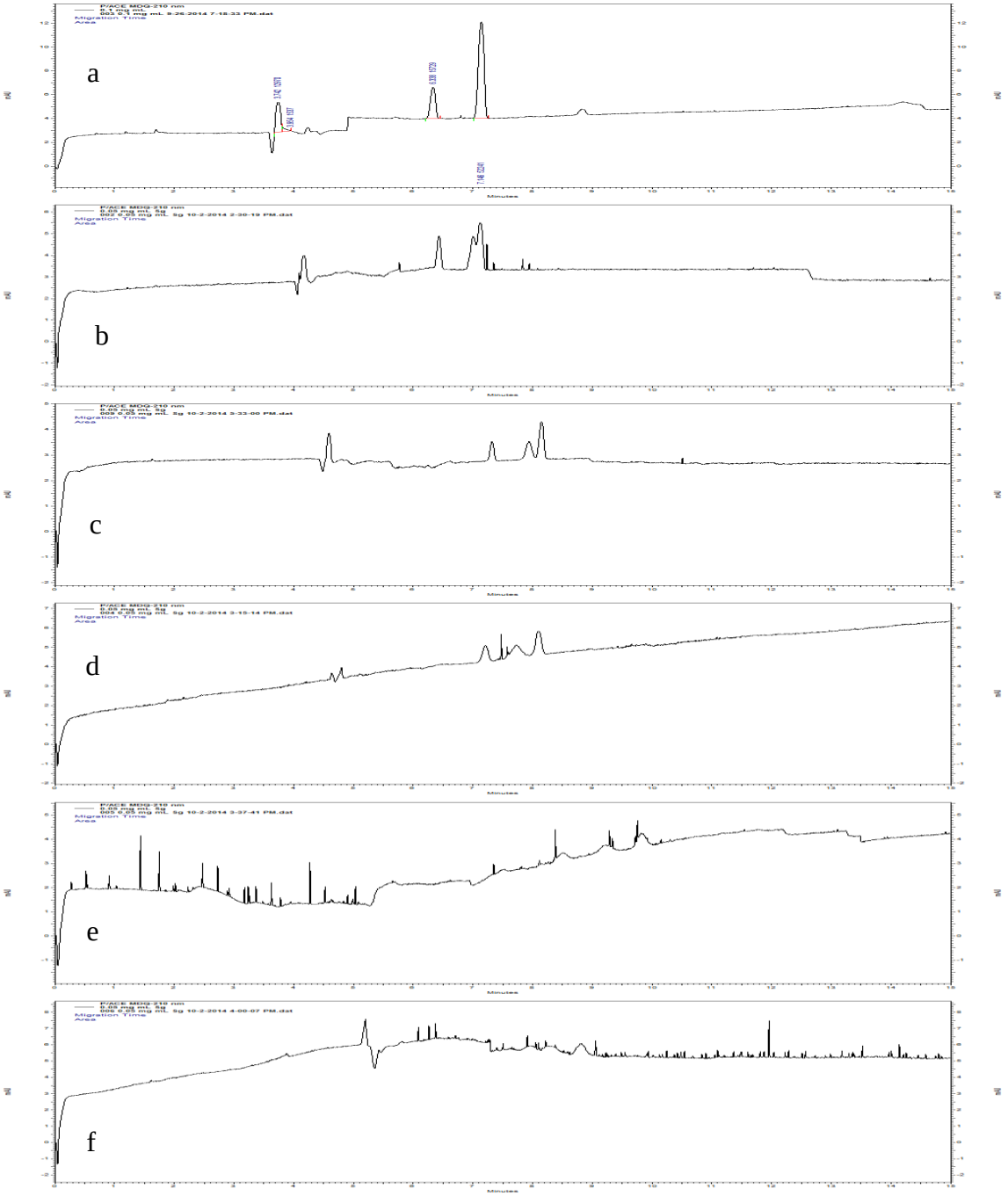

Figure 5.14 Syringyl glycerol (Sg, 0.1 mg/mL) electropherogram of a) no HP-β-CD b) 25 mM HP-β-CD c) 40 mM HP-β-CD d) 60 mM HP-β-CD e) 70 mM HP-β-CD f) 80 mM HP-β-CD.

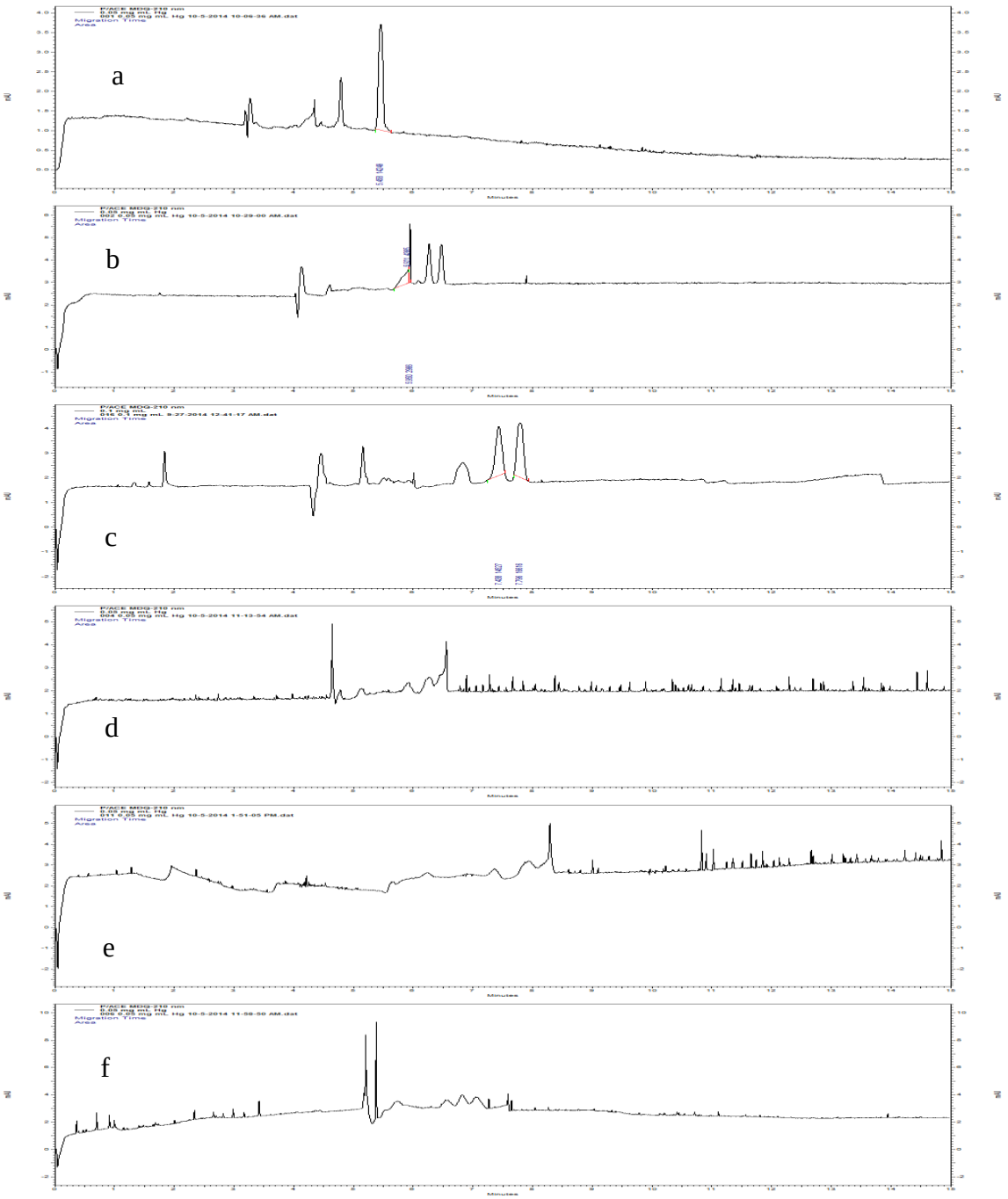

Figure 5.15 *p*-hydroxyphenyl glycerol (Hg, 0.1 mg/mL) electropherogram of a) no HP-β-CD b) 25 mM HP-β-CD c) 40 mM HP-β-CD d) 60 mM HP-β-CD e) 70 mM HP-β-CD f) 80 mM HP-β-CD.

have sufficient hydrophobic nature, therefore, it was important to consider solubility issues. Utilizing an organic modifier in our BGE solution would not only increase solubility of the thioacidolysis monomers, but it would provide increased separation by retarding the EOF. Adding an organic modifier retards the EOF by decreasing the zeta potential of the Stern layer. Figure 5.16 demonstrates the effects of adding an organic modifier. It was observed during CE method development that the hydrophobic alkyl side chain of the thioacidolysis monomers has a large enough collisional cross section ultimately limiting electrophoretic mobility. Without the addition of methanol, the organic modifier, baseline resolution was not obtained for the three thioacidolysis monomer standards. As the methanol concentration increased, baseline resolution also increased; 30% methanol provided the baseline resolution with short analysis time. At 50% methanol, baseline resolution is achieved, but peak broadening is also observed. The peak broadening observed is most likely due to the lengthened residence time in the capillary, increasing the potential for longitudinal diffusion. Separation voltage is another separation parameter worth exploration/optimization. Figure 5.17 shows the effects of applied separation voltage. Increasing voltage applied, decreases analysis time, but also decreases resolution. It is a balancing act. At 15 kV, analysis time is longest, but resolution is also increased, however, peak broadening is observed, again, due to longer residence time in the capillary, thus increased longitudinal diffusion. At 30 kV, analysis time is shortest while still achieving baseline resolution and nice, sharp

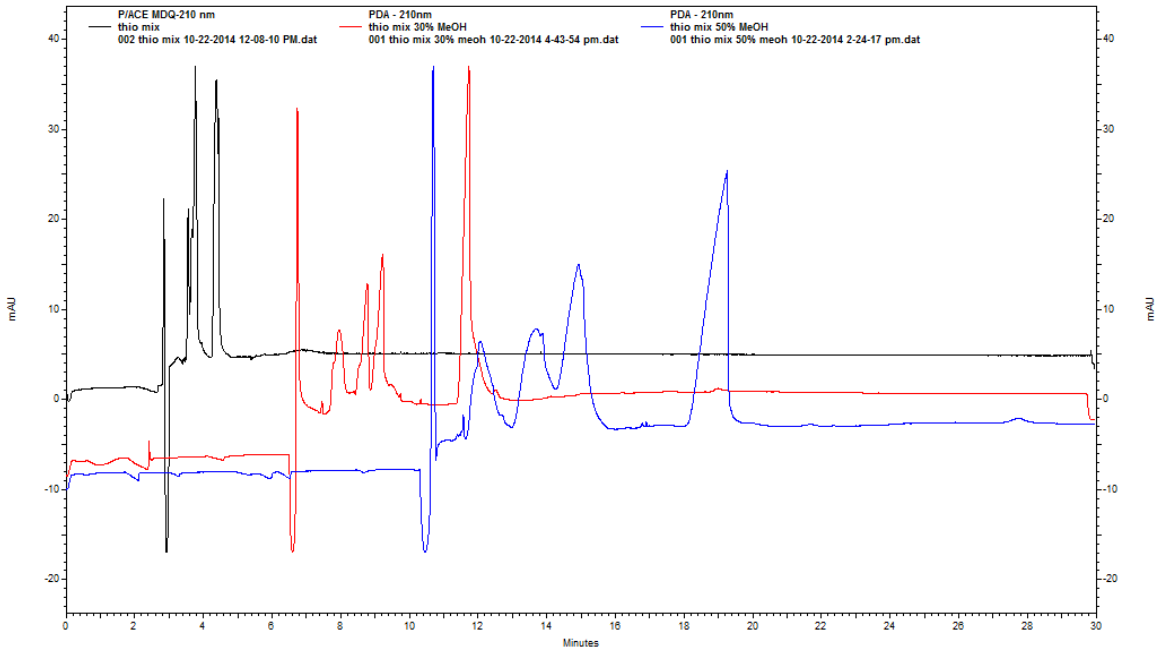

Figure 5.16 Electropherogram of 0.1 mg/mL thioacidolysis mix with various methanol concentrations.

(black – 0% methanol, red – 30% methanol, blue – 50% methanol); BGE: 50 mM Gly-NaOH pH 10.5; +30 kV

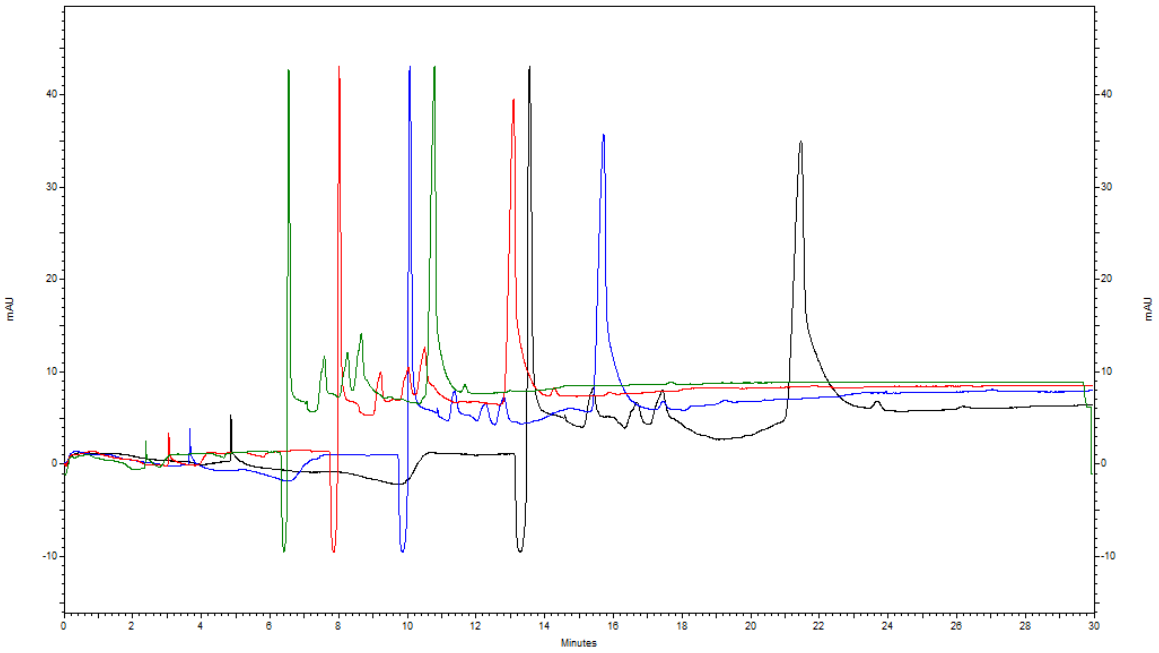

Figure 5.17 Electropherogram of 0.1 mg/mL thioacidolysis mix with various separation voltages applied.

(black – 15 kV, blue – 20 kV, red – 25 kV, green – 30 kV); BGE: 50 mM Gly-NaOH pH 10.5; 30% methanol

peaks are achieved. It was decided that 30 kV would be the separation voltage used.

Preliminary CE/MS experiments revealed glycine from the glycine-NaOH buffer dominated the mass spectrum, therefore, analytes were not detected above the background from the BGE. Close in proximity to this discovery, another issue arose. Originally, the goal was to conduct CE/MS analysis, thus, the choice for using a glycine-NaOH buffer, however, during method development stages, the CE instrument failed and is in need of extensive maintenance inhibiting our ability to conduct further CE/MS analyses. However, we were able to generate some preliminary CE/MS data for the separation of the thioacidolysis standards shown in Figure 5.18. Although, baseline resolution was not yet achieved, detection of the thioacidolysis through a CE/MS platform was achieved which is promising for future experimentation.

Without the ability to conduct further CE/MS studies, we decided to utilize a different buffer for CE/PDA analysis. Fournand *et al*., utilized CE to separate syringyl (S) and guaiacyl (G) thioacidolysis monomers using a borate-phosphate buffer.[56] Using a 50% methanol borate-phosphate BGE solution, baseline resolution was achieved for all three thioacidolysis monomers (Figure 5.19). With an established CE/PDA method for thioacidolysis analysis, a calibration curve was generated (Figure 5.20). Linear regression analysis showed a good linear fit with correlation coefficients of greater than 0.99 for all three thioacidolysis monomer calibration curves (Table 5.3). The linear range for

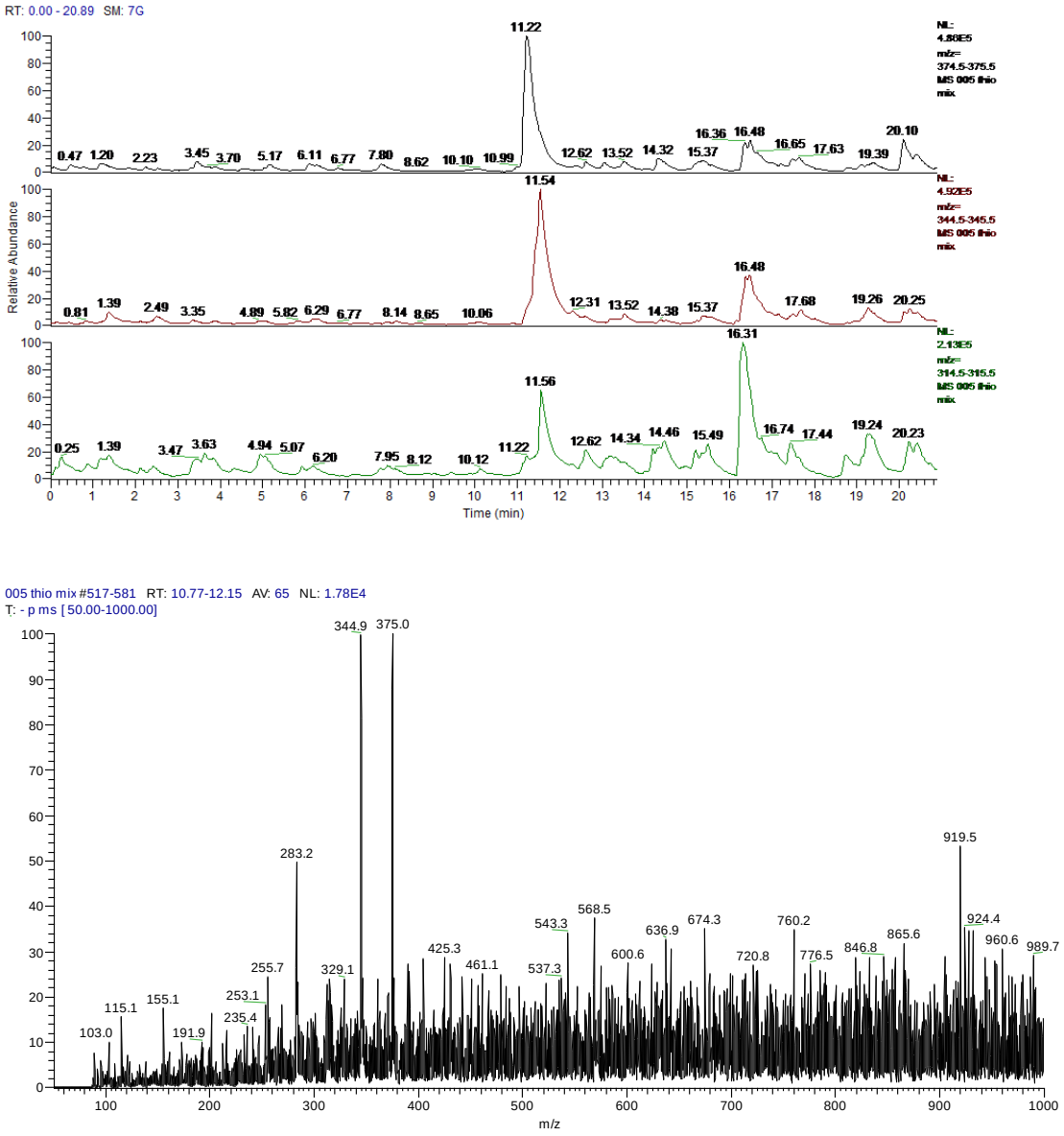

Figure 5.18 Capillary electrophoresis/mass spectrometry extracted electropherogram (top) and mass spectrum (bottom) of thioacidolysis monomer standards.

Ht (green trace), Gt (red trace) and St (black trace).

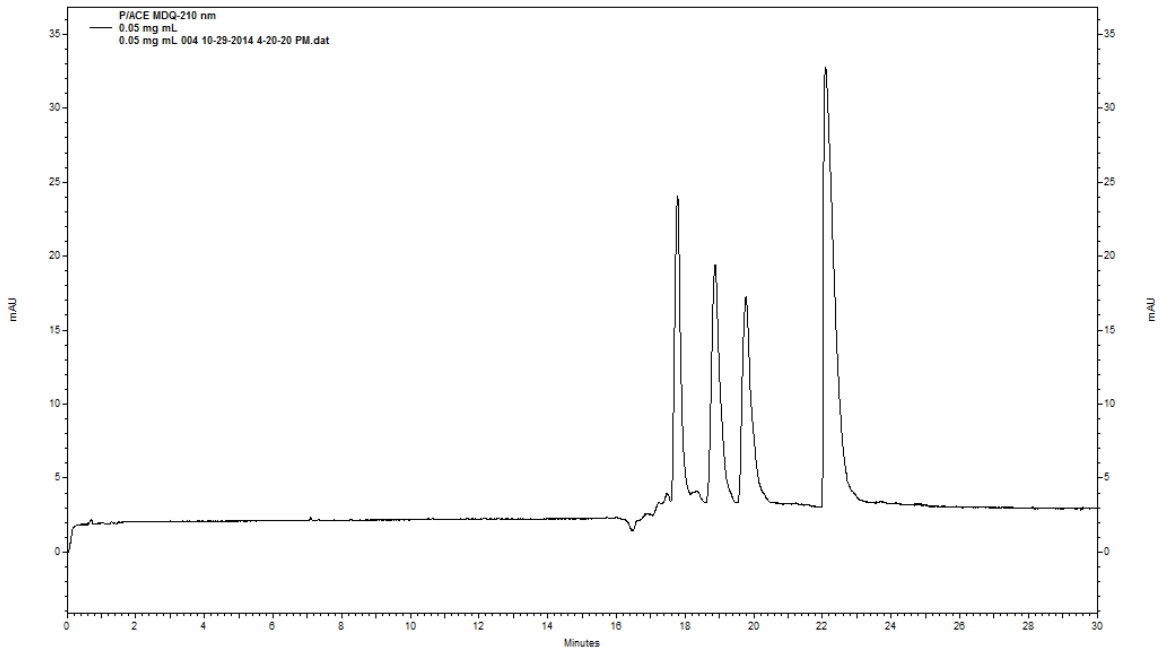

Figure 5.19 Electropherogram of 0.05 mg/mL thioacidolysis mixture (0.05 mg/mL PPP, IS).

BGE: 75 mM borate-phosphate 50% methanol pH 10.5, 30 kV.

CE/PDA H-thioacidolysis Calibration Curve

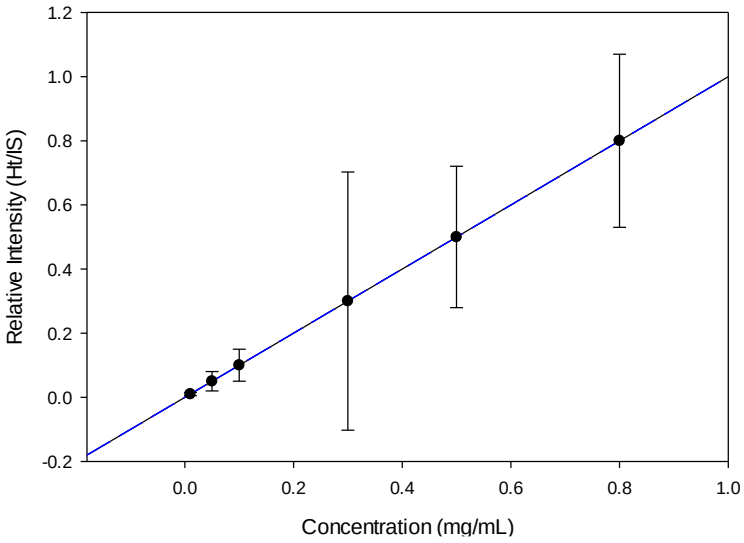

CE/PDA G-thioacidolysis Calibration Curve

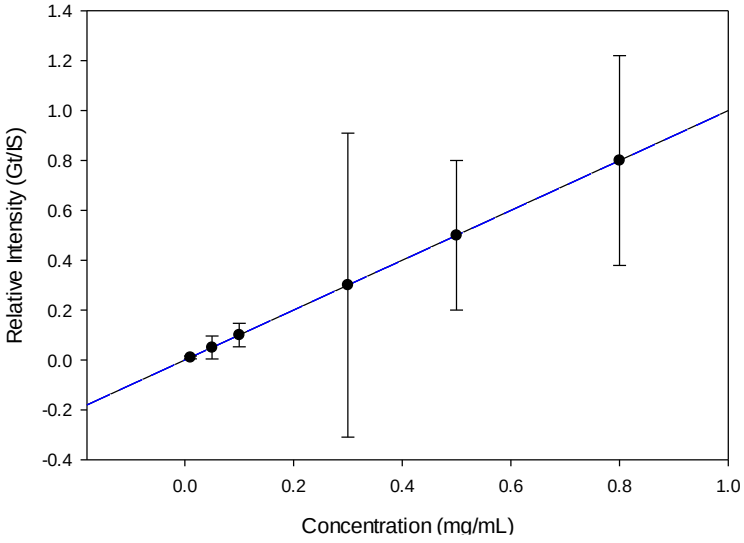

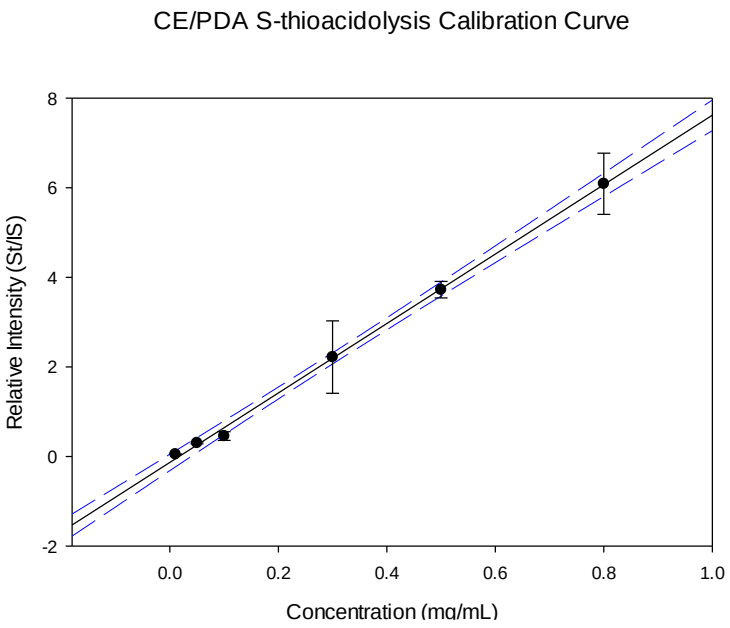

Figure 5.20 CE/PDA calibration curves for H, G and S thioacidolysis monomers.

Data is shown with error bars indicating ± one standard deviation.

Table 5.3 CE/PDA calibration curve linear regression analysis.

CE/PDA CC	Equation of the Line	R^2	Linear Range
Ht	Y=4.9961x-0.0258	0.997	0.01 mg/mL – 0.8 mg/mL
Gt	Y=6.0815x-0.0464	0.997	0.01 mg/mL – 0.8 mg/mL
St	Y=7.7552x-0.1344	0.998	0.01 mg/mL – 0.8 mg/mL

CE/PDA analysis was 0.01-0.8 mg/mL (Table 5.3). Capillary electrophoresis provides a highly efficient and rapid separation technique, however, with the small inner diameter of the separation capillary, concentrations of 1.0 mg/mL and above produce broad, unresolved peaks due to column overload. Large sample band injections lead to decreased separation efficiency, as expected in other commonly utilized chromatographic separation systems.

With established calibration curves, the thioacidolysis processed untreated and treated biomass samples previously analyzed by GC/MS were analyzed by CE/PDA. Capillary electrophoresis peak identity was done by matching the elution times of the standards with detected peaks from thioacidolysis samples (Figure 5.21). A bar graph of all the thioacidolysis samples analyzed/quantified by both GC/MS and CE/PDA is shown in Figure 5.22. Automatically, attention is drawn by the large difference in G and S concentrations as quantified by GC/MS relative to the quantified values by CE/PDA. Although, it is an acceptable practice to utilize standard retention times for peak identification, without mass spectral information to confirm the peak identity, we cannot be absolutely confident in the quantitative determination using CE/PDA. In addition, while analyzing the biomass thioacidolysis samples, the separation capillary had to be switched regularly due to current leakage. Current leakage in CE is typically attributed to a couple issues (assuming it is not an electronic issue): 1) a crack or break in the separation capillary or 2) air bubbles or analyte precipitating out in the capillary. Each time the analysis failed due to a "current leakage", the separation capillary was checked for cracks, various solvents were

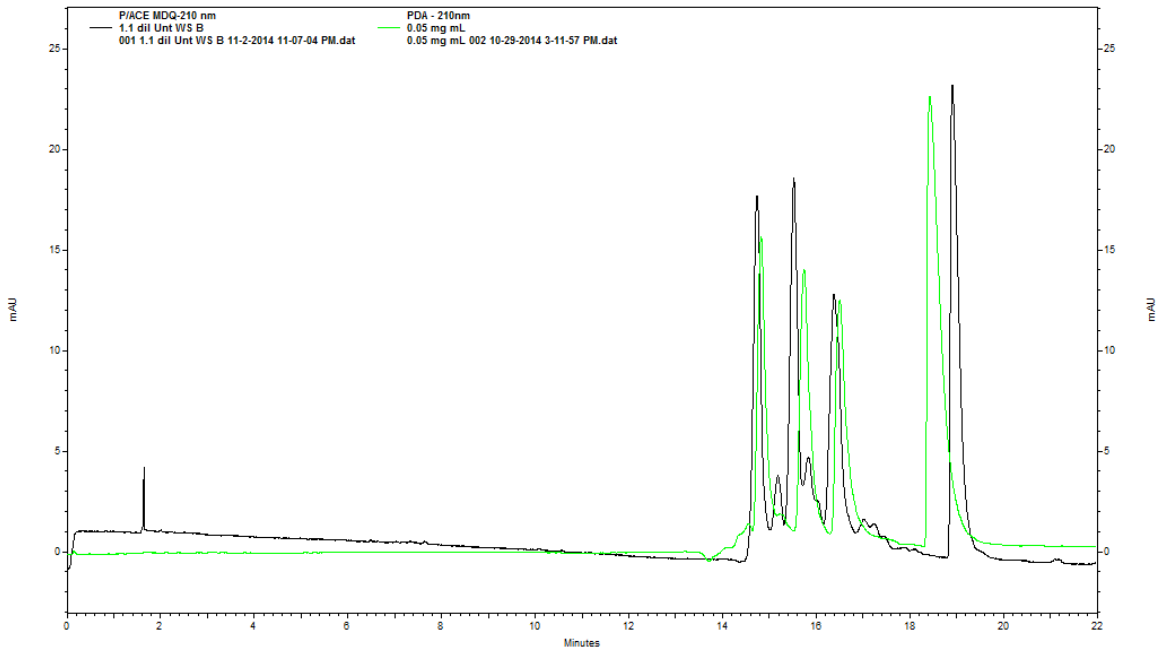

Figure 5.21 Electropherogram of 1:1 diluted thioacidolysis untreated wheat straw (black) with standard mixture electropherogram overlaid (neon green).

BGE: 75 mM borate-phosphate 50% methanol pH 10.5, 30 kV.

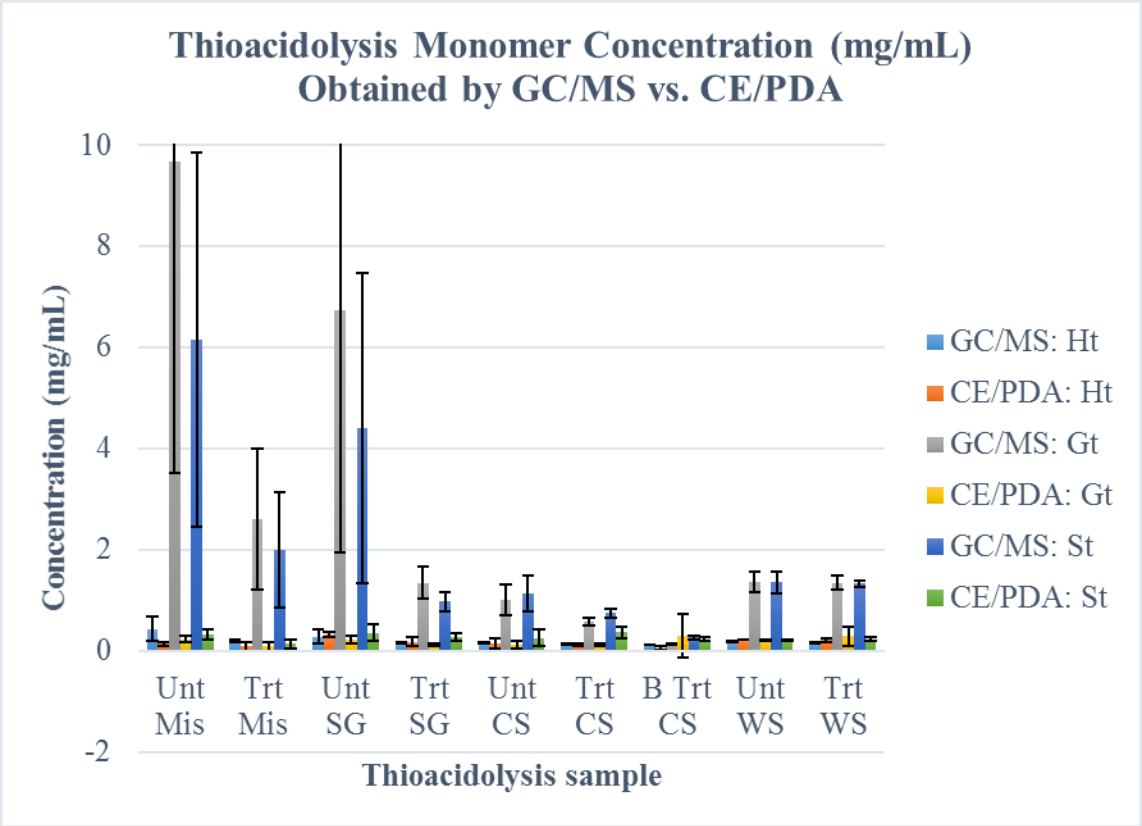

Figure 5.22 Bar graph depicting quantified concentrations of thioacidolysis monomers using GC/MS and CE/PDA.

Data is shown with error bars indicating ± one standard deviation.

hydrodynamically injected at low and high pressures (0.5 psi up to 20 psi) to confirm a capillary leak/crack did not exist. Ultimately, it was speculated that the complexity and harshness of the sample contributed to either analyte precipitation or a buildup of insoluble compounds within the capillary. This speculation is supported by the GC/MS injector liner, as seen in Figure 5.23. As seen in the picture, following several injections of the thioacidolysis processed biomass, a black film of particulate nature formed inside the injector liner of the GC/MS. This could also decrease our ability to quantify the thioacidolysis monomers in biomass samples.

Although CE/PDA was not successful in producing monolignol quantification, CE still provides attractive advantages. Application of CE/MS to conduct monolignol quantification will combine the advantages of sensitivity and ability for peak identification based on mass spectral data of MS with the high separation efficiency, low analysis times of CE.

5.4. Conclusion

In conclusion, CE analyses on various $KMnO_4$ oxidized lignin samples provided qualitative identification of the three methoxybenzoic acid products. The identification of the $KMnO_4$ monomeric products lead to the hypothesis that CE could be utilized to analyze product streams from other lignin analytical degradative methods such as thioacidolysis. With the successful synthesis of arylglycerol monomers, chiral CE was utilized to support the hypothesis of a single diastereomer being synthesized and thus support the proposed synthetic

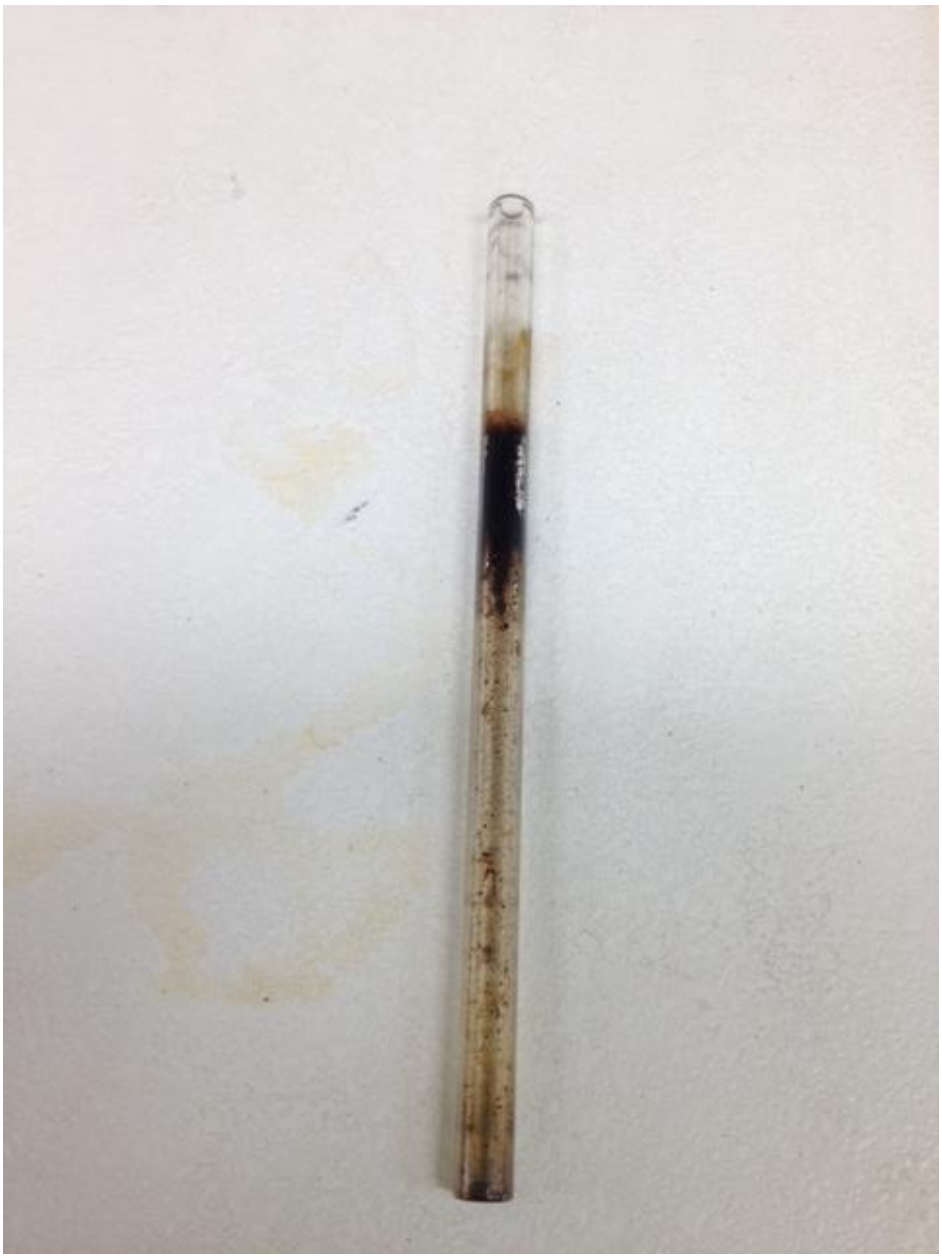

Figure 5.23 GC injector liner after several thioacidolysis samples were analyzed.

scheme. The addition of 40 mM HP-β-CD to the BGE provided enantiomeric resolution for the three synthesized arylglycerol monomers, Sg, Gg and Hg. Calibration curves of the three thioacidolysis monomers, Ht, Gt and St were constructed using CE/PDA, each providing sufficient linear correlation. Untreated and Fenton treated miscanthus, switchgrass, corn stover and wheat straw were subjected to analytical thioacidolysis and analyzed by CE/PDA. Although CE/PDA did not provide monomeric quantitative data we could be confident in, we were able to match elution time of the standards to detected peaks of the real samples. The potential to conduct CE analyses on the thioacidolysis products can be readdressed once a working CE/MS system is available.

6. Chapter : Conclusion

Biomass pretreatment was the unifying theme throughout this dissertation. Second generation biofuel production focuses on nonfood based feedstocks, such as lignocellulosic biomass. Cellulose is the major component of industry for fuel production because it can be microbially converted to biofuel such as acetone, butanol and ethanol. Lignin reduces the ability for chemicals and microbes to utilize cellulose, providing a protective layer and rigidity to plant materials. Various pretreatment strategies have been studied to reduce/alter lignin with the ultimate goal of increasing cellulosic conversion efficiencies.

The first hypothesis of this dissertation was that solution based Fenton chemistry could be utilized as a pretreatment strategy to degrade lignin. The rationale for this hypothesis is based on the ability of lignocellulolytic *Basidiomycetes* to degrade lignin by *in vivo* Fenton chemistry. This hypothesis was tested utilizing an array of analytical assays. Enzymatic saccharifications provided a comparison of cellulosic conversion to glucose. Acid soluble and acid insoluble lignin assays were conducted to assess changes in lignin content before and after pretreatment. The results from this project showed a significant increase in glucose detected upon enzymatic saccharification for Fenton pretreated biomass across all four feedstocks. However, lignin assays did not show a significant difference in lignin content upon Fenton pretreatment. The significant increase in glucose production upon Fenton pretreatment, but lack of change in lignin content, lead to the conclusion that solution based Fenton chemistry was not degrading lignin. Therefore, the projects initial hypothesis was rejected.

However, cellulose was shown to be more bioavailable, thus, a new hypothesis was generated. The new hypothesis was that solution based Fenton chemistry was not degrading lignin, but it was altering it in a way that makes cellulose more bioavailable to both enzymes and microbes. Lignin assays suggested lignin was not being degraded, as originally hypothesized, thus, an interest in the affects Fenton chemistry had on lignin evolved.

It is well known that lignin is a complex polymer with high variability which makes it a difficult problem to assess. Lignin analysis has been assessed utilizing a suite of analytical degradative methods in order to analyze lignin in monomeric form. The β-O-4 linkage makes up majority of linkages present in lignin, therefore, we chose to utilize an analytical degradative approach which cleaved lignin at this linkage, thioacidolysis. In studying lignin, thioacidolysis provides monomeric ratios of S/G or H/G. These ratios provide some insight to the compositional make up of various lignin sources, however, they do not provide insight on the affects pretreatment has on lignin. If a pretreatment degrades lignin, perhaps there is a decrease in S and G subunits, however, the monomeric ratio will not portray this if both S and G decrease. If the S/G ratio decreases, it is unknown if S is decreasing or G is increasing. Very little information can be obtained by monomeric ratios in relation to the effects of pretreatment on lignin. However, we hypothesize that with the ability to provide monomeric quantification, we will be able to see changes in individual monolignol content.

To test this hypothesis, we needed to synthesize the thioacidolysis monomers because they are not commercially available. Thioacidolysis monomers can be synthesized utilizing a traditional thioacidolysis reaction of the corresponding arylglycerols. Synthesis of the arylglycerols has been conducted utilizing a five step procedure, traditionally. A five step synthesis not only requires lots of reagents but can be quite costly, in addition to labor and time intensive. This motivated a need for an alternate synthetic approach. The next project hypothesis was that the arylglycerols could be synthesized utilizing a one-step approach through an epoxidation. Utilizing this reaction scheme it was also hypothesized that the arylglycerol product would exist in one form of the possible diastereomers. Reaction scheme and parameters were addressed utilizing GC/MS and TLC. The arylglycerol products were successfully synthesized in moderate yields and confirmed by GC/MS, x-ray crystallography, HRMS, carbon and proton NMR. This project not only provided an alternate route to synthesize arylglycerols, but it also elucidated the GC/MS EI characteristic spectra for the three arylglycerols. Syringyl, guaiacyl and *p*-hydroxyphenyl glycerols were not previously characterized by GC/MS. With the elucidation of GC/MS spectra, the three arylglycerols can now be identified utilizing a library match without further characterization. In addition, the first crystal structures were obtained for guaiacyl and syringyl glycerols. Both of these results contribute to furthering our knowledge in the world of lignin and will be beneficial for those wanting to study lignin. We established analytical end points for the arylglycerol products, thus, those who follow will be able to reference them. Our second hypothesis was

tested utilizing the enantiomeric resolution capability of CE with the addition of a chiral additive.

Capillary electrophoresis provides a highly efficient separation technique with low analysis times and little sample/reagent consumption. An additional advantage of CE is the ability to analyze a variety of analytes by simply changing the composition of the background electrolyte (BGE) solution. A chiral additive, 2-hydroxypropyl-beta-cyclodextrin (HP-β-CD) was utilized to conduct enantiomeric separation experiments of the arylglycerol synthesized products. Chiral CE separation illustrated the presence of a racemic mixture from one diastereomer. NMR data were consistent with literature values and suggested the erythro form to be the synthesized product. Results supported the hypothesis that one form for the potential diastereomers was synthesized.

With the synthesized thioacidolysis monomers, we could test the next project hypothesis, changes in individual monolignol content upon pretreatment can be observed from quantification. To test this hypothesis, methods were developed on two analytical platforms, GC/MS and CE/MS with an additional hypothesis that CE/MS would provide a more sensitive and robust analytical method to quantify thioacidolysis monomers due to its increased separation efficiency and wide range of analyte application relative to GC/MS.

A CE method was developed concomitantly with the CE/MS interface development. However, during CE/MS development the CE instrument failed and we were not able to address the previously stated hypothesis.

Nevertheless, a calibration curve was obtained by GC/MS. All three calibration curves for the three standards provided sufficient linear fit upon linear regression analysis. Lignocellulosic biomass, untreated and Fenton treated, was processed through analytical thioacidolysis and analyzed by GC/MS. Individual monomeric concentrations were obtained and compared to the monomeric ratios, S/G and H/G. Results from this project did not show a significant change in monomeric ratios or individual monomeric concentration upon Fenton pretreatment. These results were consistent with lignin assay conducted previously further supporting that Fenton pretreatment is not degrading lignin.

To further test the hypothesis changes in individual monolignol content upon pretreatment can be observed from quantification, we processed alkaline peroxide pretreated corn stover through analytical thioacidolysis and quantified the monomeric composition. A significant difference was seen for all three monomers upon alkaline peroxide pretreatment. In comparison to the monomeric ratios, no significant change was seen in the S/G and H/G ratio. However, with the ability to quantify individual monomer concentrations, we observed that all three monolignols significantly decreased upon treatment, but S and G had a larger decrease than H. The method proposal of monomeric quantification for elucidation of the changes in monolignol concentration upon pretreatment was verified with the analysis of both Fenton pretreated biomass and alkaline peroxide pretreated biomass. The pretreatment method that was shown to not degrade lignin, Fenton pretreatment, according to tradition lignin content assays, did not show a significant decrease in monolignol concentrations, but the pretreatment

known to degrade lignin, alkaline peroxide, did exhibit a significant change in monolignol concentration. The monomer quantification showed this, but the monomer ratios did not. This highlights the importance of this method which will be beneficial for future lignin pretreatment analyses.

Future work of this project pertains to the application and expansion of this project. Alkaline peroxide pretreated corn stover showed a significant change in H, G and S subunits upon analytical thioacidolysis. Expansion of this quantitative approach to other feedstocks and other known lignin degradation pretreatments will further verify this method. This will allow us to assess pretreatment strategies and assess if degradation of one monolignol over another plays a larger role in increasing cellulose conversion efficiency. Increasing the variety and quantity of samples processed/analyzed utilizing this quantitative approach has the potential to provide substantial information regarding effects of pretreatment on the monolignol content of lignin. With the knowledge of how pretreatment affect the monomeric compositions, pretreatment can be optimized to be selective. Furthermore, quantitative thioacidolysis can contribute to the evolving world of lignomics. This approach could provide a lignomic analytical tool analogous to bottom up proteomics.

Future work should include an exploration into the large variation observed in the quantification of monolignols from untreated miscanthus and untreated switchgrass (Figure 4.4b, 4.5b). It has been speculated that this variation could be due to the differential heating during the thioacidolysis process. Alternatively, the large variation might arise from the inability of the

thioacidolysis reagents to penetrate into the lignin to reproducibly break the β-O-4 linkages in untreated material. The Fenton treated material, which has been shown to be more bioavailable to enzymes and microbes, showed less variability. Perhaps, the smaller variability observed in the treated material reflects the availability of the linkages in lignin to the chemicals which provides a more uniform process.

Throughout the project, it was seen that solution based Fenton pretreatment was not degrading lignin. Therefore, the alternate hypothesis, that solution based Fenton chemistry was clipping or altering the lignin which made cellulose more bioavailable to enzymes and microbes, was made. An alternative hypothesis is that solution based Fenton pretreatment is not affecting lignin at all, but perhaps it is degrading another polymeric component of the biomass, such as hemicellulose. Solution based Fenton pretreatment could be degrading hemicellulose or decreasing the crystallinity of cellulose, both of which would increase cellulosic conversion efficiencies. It would be interesting to assess the effects of solution based Fenton pretreatment on cellulose and hemicellulose.

With synthesized standards, other analytical methodologies can be developed which could contribute to solving the puzzle of lignin. Although CE/PDA monomeric quantification was not successful in this project, applying CE/MS to the quantification of thioacidolysis monomers is hypothesized to provide an alternate analytical method to GC/MS. Capillary electrophoresis is a more widely applicable separation technique, allowing for the analysis of more compounds in a single analytical analysis. Capillary electrophoresis is a field

with great potential to further the scientific world, however, it has not yet found its "problem". As the knowledge and use of CE and CE/MS matures, highly sensitive analytical techniques are produced. I believe CE is ideally suited to conduct CE-ion mobility-MS. Ion mobility will provide an added dimension of separation for complex problems, such as lignin. The rationale for this hypothesis is that ion mobility is an analogous technique to CE, just in the gas phase as opposed to aqueous solution as in CE, and it is an ideal segway to MS analysis. In addition, CE/MS provides the capability to analyze lignin as larger oligomers, a limiting factor of GC/MS. Dimer, trimmers, etc. could be analyzed with CE, as long as a charge exists. Add ion mobility to the possibilities, and a wide array of analytical experiments become possible. This can be applied to a vast number of compounds, such as lignin oligomers using a single analytical technique. Oligomers analysis can be beneficial for the analysis of pretreatment because lignin most likely doesn't degrade completely into monomeric form. It's likely that an amount of monomers are oxidized, but it is also likely that larger pieces of lignin can be cleaved such as dimers, trimers, tetramers, etc. The possibility of analyzing larger pieces or oligomers of lignin will provide information on the native lignin structure which can help answer the raised question of chemical changes on the native lignin structure upon analytical degradative chemistry.

In a recent review by Balan[2], the "current challenges in commercially producing biofuels from lignocellulosic biomass" was discussed. The large challenges of lignocellulosic biofuel processing lies in cost and realistic implementation. Utilizing lignocellulosic biomass for biofuels present cost and

energy barriers at many of the required steps. Bioenergy feedstock availability and transport cost contributes significantly to the overall cost of lignocellulosic biomass processing. Pretreatment is another bottleneck which significantly contributes to the cost and energy requirements necessary for biofuel production from lignocellulosic biomass.[59]

My research can aid in addressing the challenges of lignin and pretreatment costs. The quantification of monolignol composition before and after pretreatment will contribute to understanding the impacts various pretreatments have on different sources of lignin. It is well known that all lignins vary and all pretreatments have its various impacts on lignin. To gain an understanding of how specifically each pretreatment affects the various lignins, will allow us to design better pretreatment methods that can target certain monomers or target certain types of lignin. Designing targeted and specific methods of pretreatment for lignin can be thought of as an analogous method to personalized medicine for humans. If we can design pretreatments specific for certain lignins, this would greatly increase pretreatment efficiencies and could decrease the overall costs of pretreatment. More efficient pretreatment strategies producing higher cellulose conversion efficiencies, decrease the cost of lignocellulosic biofuel processing which can facilitate the implementation of lignocellulosic biofuels and thus decrease the cost of energy/fuel. In addition, it is perceivable that knowledge of specific impacts of pretreatments on the monolignol concentrations could also provide key information that would allow

us to design pretreatment methods on farm which would greatly decrease the biomass transport costs.

REFERENCES

1. Laboratory, N. R. E. http://www.nrel.gov/learning/re_biofuels.html?print.
2. Balan, V., Current Challenges in Commercially Producing Biofuels from Lignocellulosic Biomass. *ISRN Biotechnology* **2014**, 1-31.
3. Biofuels, B., Producing Biofuels in Brazail. BP, Ed.
4. S. N. Naik, V. V. G., Prasant K. Rout, Ajay K. Dalai, Production of first and second generation biofuels: A comprehensive review. *Renewable and Sustainable Energy Reviews* **2010,** *14*, 578-297.
5. Agency, E. P. http://www.epa.gov/ncea/biofuels/basicinfo.htm#whatis.
6. Parveen Kumar, D. M. B., Michael J. Delwiche, Pieter Stroeve, Methods for Pretreatment of Lignocellulosic Biomass for Efficicent Hydrolysis and Biofuel Production. *Industrial & Engineering Chemistry Research* **2009,** *48*, 3713-3729.
7. A.T.W.M. Hendricks, G. Z., Pretreatments to enhance the digestibility of lignocellulosic biomass. *Bioresource Technology* **2009,** *100*, 10-18.
8. (a) Ruben Vanholme, B. D., Kris Morreel, John Ralph, Wout Boerjan, Lignin Biosynthesis and Structure. *Plant Physiology* **2010,** *153* (3), 895-905; (b) Nathan Mosier, C. W., Bruce Dale, Richard Elander, Y.Y. Lee, Mark Holtzapple, Michael Ladisch, Features of promising technologies for pretreatment of lignocellulosic biomass. *Bioresource Technology* **2005,** *96*, 673-686.
9. Joseph Zakzeski, P. C. A. B., Anna L. Jongerius, Bert M. Weckhuysen, The Catalytic Valorization of Lignin for the Production of Renewable Chemicals. *Chemical Reviews* **2010,** *110* (6), 3552-3599.
10. Kris Morreel, H. K., Fachuang Lu, Oana Dima, Takuya Akiyama, Ruben Vanholme, Claudiu Niculaes, Geert Goeminne, Dirk Inze, Eric Messens, John Ralph, and Wout Boerjan, Mass Spectrometry-Based Fragmentation as an Identification Tool in Lignomics. *Analytical Chemistry* **2010,** *82* (19), 8095-8105.
11. Valdeir Arantes, J. J., Barry Goodell, Peculiarities of brown-rot fungi and biochemical Fenton reaction with regard to their potential as a model for bioprocessing biomass. *Applied Microbiology Biotechnology* **2012,** *94*, 323-338.
12. Douglas A. Skoog, F. J. H., Stanley R. Crouch, *Principles of Instrumental Analysis*. 6th ed.; Thomson Brooks/Cole: Belmont, CA, 2007; p 1039.
13. Philip E. Miller, M. B. D., The Quadrupole Mass Filter: Basic Operating Concepts. *Journal of Chemical Education* **1986,** *63*, 617-623.
14. Li, J.; Chan, W.; Cai, Z., On-line capillary electrophoresis-electrospray ionization mass spectrometry analysis of urinary porphyrins. *Electrophoresis* **2009,** *30* (10), 1790-7.
15. Skoog, D. A.; West, D. M.; Holler, F. J.; Crouch, S. R., Capillary Electrophoresis. In *Fundamentals of Analytical Chemistry*, 8 ed.; Kiselica, S., Ed. David Harris: Belmont, 2004; pp 1003-110.
16. Xu, Y., Tutorial: Capillary Electrophoresis. In *The Chemical Educator*, Schimpif, M., Ed. Springer-Verlag New York Inc.: New York, 1996; Vol. 1, pp 1-14.
17. Chromatography D, 10p. In *Capillary Electrophoresis (CE) - Lab Manual* [Online]. http://www.anachem.umu.se/ChromD/Labs/CE.pdf (accessed 8/17/10).

18. Biomass Resources. http://energy.gov/eere/energybasics/articles/biomass-resources (accessed 10/23/13).
19. Michael E. Himmel, S.-Y. D., David K. Johnson, William S. Adney, Mark R. Nimlos, John W. Brady, Thomas D. Foust, Biomass Recalcitrance: Engineering Plants and Enzymes for Biofuels Production. *Science* **2007,** *315*, 804-807.
20. (a) Valdeir Arantes, A. M. F. M., Timothy R. Filley, Barry Goodell, Lignocellulsic polysaccharides and lignin degradation by wood decay fungi: the relevance of nonenzymatic Fenton-based reactions. *J. Ind. Microbiol. Biotechnol.* **2011,** *38*, 541-555; (b) Evans, J. M. P. a. C. S., The enzymatic degradation of lignin by white-rot fungi. *Phil. Trans. R. Soc. Lond. B* **1983,** *300*, 293-303; (c) Takashi Watanabe, M. S., Rudianto Amirta, Noor Rahmawati, Syafwina, Bambang Prasetya, Toshiaki Tanabe, Yasunori Ohashi, Takahito Watanabe, Yoichi Honda, Masaaki Kuwahara, Kanji Okano, Lignin-degrading fungi as a biotechnological tool for biomass conversion. *Journal of applied and industrial biotechnology in tropical region* **2009,** *2* (2), 1-5.
21. Ricardo D. Villa, A. G. T., Raquel F. Pupo Nogueira, Environmental implications of soil remediation using the Fenton process. *Chemosphere* **2008,** *71*, 43-50.
22. Fritz Haber, J. W. In *The catalytic decomposition of hydrogen peroxide by iron salts*, Proceedings of the royal society of London. Series A, Mathematical and Physical Sciences, 1934; pp 332-351.
23. (a) Petr Baldrian, V. V., Degradation of cellulose by basidiomycetous fungi. *FEMS Microbial Reviews* **2008,** *32*, 501-521; (b) Flournoy, D. S., Chemical changes in wood components and cotton cellulose as a result of brown rot: Is Fenton chemistry involved? *Biodeterioration research 4; myocotoxins, wood decay, plant stress, biocorrosion, and general biodeterioration* **1994**, 257-293; (c) T. Kent Kirk, R. I., Michael D. Mozuch, Anthony H. Conner, L. Highley, Characteristics of cotton cellulose depolymerized by brown-rot fungus, by acid, or by chemical oxidants. *Holzforschung* **2009,** *45* (4), 239-244.
24. Karina Michalska, K. M., Liliana Krzystek, Stanislaw Ledakowicz, Influence of pretreatment with Fenton's reagent on biogas production and methane yield from lignocellulosic biomass. *Bioresource Technology* **2012,** *119*, 72-78.
25. (a) Prateek Jain, N. V., Effect of Fenton's pretreatment on cotton cellulosic substrates to enhance its enzymatic hydrolysis response. *Bioresource Technology* **2012,** *103*, 219-226; (b) Namgoo Kang, D. S., Lee Jeyong Yoon, Kinetic modeling of Fenton oxidation of phenol and monochlorophenols. *Chemosphere* **2002,** *47*, 915-924.
26. Peroxide, U. Iodometric Titration. http://www.h2o2.com/technical-library/analytical-methods/default.aspx?pid=70&name=Iodometric-Titration.
27. M. Selig, N. W., Y. Ji *Enzymatic Saccharification of Lignocellulosic Biomass*; NREL/TP-510-42629; NREL: 3/21/2008, 2008.
28. (a) A. Sluiter, B. H., D. Hyman, C. Payne, R. Ruiz, C. Scarlata, J. Sluiter, D. Templeton, J. Wolfe *Standard Method for Determination of Total Solids in Biomass*; NREL: 2008; (b) A. Sluiter, B. H., D. Hyman, C. Payne, R. Ruiz, C. Scarlata, J. Sluiter, D. Templeton, D. Crocker *Determination of Structural Carbohydrates and Lignin in Biomass*; NREL: 2012.
29. Goutami Banerjee, S. C., Tongjun Liu, Daniel L. Williams, Sarynnna Lopez Meza, Jonathan D. Walton, David B. Hodge, Scale-Up and Integration of Alkaline Hydrogen

Peroxide Pretreatment, Enzymatic Hydrolysis, and Ethanolic Fermentation. *Biotechnology and Bioengineering* **2012,** *109* (4), 922-931.
30. (a) Petr Balddrian, V. V., Degradation of cellulose by basidiomycetous fungi. *FEMS Microbial Reviews* **2008,** *32*, 501-521; (b) Kenneth E. Hammel, A. N. K., Kenneth A. Jensen Jr., Zachary C. Ryan, Review: Reactive oxygen species as agents of wood decay by fungi. *Enzyme and Microbial Technology* **2002,** *30*, 445-453.
31. Mehdi Dashtban, H. S., Tarannum A. Syed, Wensheng Qin, Review Article: Fungal biodegradation and enzymatic modification of lignin. *International Journal of Molecular Biology* **2010,** *1* (1), 36-50.
32. J.A. Zazo, J. A. C., A.F. Mohedano, M.A. Gilarranz, J.J. Rodriguez, Chemical pathway and kinetics of phenol oxidation by Fenton's reagent. *Environ. Sci. Technol.* **2005,** *39*, 9295-9302.
33. Umezawa, T., The cinnamate/monolignol pathway. *Phytochemistry Reviews* **2010,** *9*, 1-17.
34. Malcolm M. Campbell, R. R. S., Variation in Lignin Content and Composition. *Plant Physiol.* **1996,** *110*, 3-13.
35. Arthur J. Ragauskas, G. T. B., Mary J. Biddy, Richard Chandra, Fang Chen, Mark F. Davis, Brian H. Davison, Richard A. Dixon, Paul Gilna, Martin Keller, Paul Langan, Amit K. Naskar, Jack N. Saddler, Timothy J. Tschaplinski, Gerald A. Tuskan, Charles E. Wyman, Lignin Valorization: Improvinng Lignin Processing in the Biorefinery. *Science* **2014,** *344*, 709-721.
36. Y.-Z. Lai, H. X., and R. Yang, An Overview of Chemical Degradation Methods for Determining Lignin Condensed Units. In *Lignin: Historical, Biological, and Materials Perspectives*, Wolfgang G. Glasser, R. A. N., and Tor P. Schultz, Ed. American Chemical Society: Washington D. C., 2000; pp 239-249.
37. Catherine Lapierre, B. M., Thioacidolysis of Poplar Lignins: Identification of Monomeric Syringyl Products and Characterization of Guaiacyl-Syringyl Lignin Fractions. *Holzforschung* **1986,** *40*, 113-118.
38. Brunow, G., Methods to Reveal the Structure of Lignin. pp 89-99.
39. Catherine Lapierre, B. M., Christian Rolando, Thioacidolysis of Lignin: Comparison with Acidolysis. *Journal of Wood Chemsitry and Technology* **1985,** *5* (2), 277-292.
40. C. Rolando, B. M., and C. LaPierre, Thioacidolysis. In *Springer Series in Wood Science*, Springer: Verlag Berlin Heidelberg, 1992; pp 334-349.
41. Kevin M. Holtman, H.-M. C., Hasan Jameel, John F. Kadla, Elucidation of Lignin Structure through Degradative Methods: Comparison of Modified DFRC and Thioacidolysis. *Journal of Agricultural and Food Chemistry* **2003,** *51*, 3535-3540.
42. Fengxia Yue, F. L., Run-Cang Sun, and John Ralph, Syntheses of Lignin-Derived Thioacidolysis Monomers and Their Uses as Quantitation Standards. *Journal of Agricultural and Food Chemistry* **2012,** *60*, 922-928.
43. (a) Marina DellaGreca, A. F., Pietro Monaco, Lucio Previtera, Enantioselective Synthesis of Phenylpropanetriols. *Synthetic Communications* **1998,** *28* (19), 3693-3700; (b) Toru Ishikawa, E. F., Junichi Kitajima, Water-Soluble Constituents of Anise: New Glucosides of Anethole Glycol and Its Related Compounds. *Chemical and Pharmaceutical Bulletin* **2002,** *50* (11), 1460-1466; (c) Lennart N. Lundgren, T. P., Olof Theander,

Arylglycerol Glucosides from *Pinus sylvestris*. *Acta Chemica Scandinavica B* **1982,** *36*, 695-699; (d) Hideyuki Matsuura, H. M., Chikako Asakawa, Midori Amano, Teruhiko Y. Yoshihara, Junya Mizutani, Isolation of α-glusosidase inhibitors from hyssop (*Hyssopus officinalis*). *Phytochemistry* **2004,** *65*, 91-97; (e) Theander, O., The Constituents of Conifer Needles: III. Isolation of β-D-Glucosides of Guaiacyl Glycerol from *Pinus silvestris* L. *Acta Chemica Scandinavica B* **1965,** *19* (7), 1792-93.
44. Debora R. Lehnen, R. G., Diego Defferrari, Louidi L. Albornoz, Dimitrios Samios, Solvent-free biodiesel epoxidation. *Environmental Chemistry Letters* **2013**.
45. (a) Swern, D., *Organic Peroxides*. John Wiley & Sons, Inc.: Canada, 1971; Vol. 2; (b) L. G. Wade, J., *Organic Chemistry*. 2 ed.; Prentice-Hall, Inc.: Englewood Cliffs, New Jersey, 1991.
46. Otwinowski, Z. M., W., *Methods in Enzymology*. Academic press: New York, 1997; Vol. 276, p 307-326.
47. Bruker, APEX2. Inc., B. A., Ed. Madison, Wisconsin, USA, 2006.
48. Sheldrick, G. M., *Acta Crys* **2008,** *A64*, 112-122.
49. Spek, A. L., *Acta Crys* **2009,** *D65*, 148-155.
50. Parkin, S., *Acta Crys* **2000,** *A56*, 157-162.
51. Stephane Quideau, J. R., Facile Large-Scale Synthesis of Coniferyl, Sinapyl, and *p*-coumaryl Alcohol. *Journal of Agricultural and Food Chemistry* **1992,** *40*, 1108-1110.
52. (a) Yi Liu, H. S., Zhe Sun, Xiaomei Ling, Pengfei Tu, Enantiomer Separation of the Four Diastereomers of Guaiacyl Glycerol from *Hydnocarpus annamensis* by Capillary Electrophoresis with HP-β-CD as a Chiral Selector. *Journal of Chromatographic Science* **2007,** *45*, 605-609; (b) E. Adler, S. Y., Synthesis and Reactions of α-(3-Methoxy-4-hydroxyphenyl)glycerol ("Guaiacylglycerol"). II Synthesis. *Acta Chemica Scandinavica B* **1953,** *7*, 570-581; (c) Erich Adler, E. E., Guaiacylglycerol and its β-Guaiacyl Ether. *Acta Chemica Scandinavica B* **1955,** *9*, 341-342.
53. Tatjana Javor, W. B., Oskar Faix, Capillary electrophoretic determination of lignin degradation products obtained by permanganate oxidation. *Analytica Chimica Acta* **2003,** *484*, 181-187.
54. (a) M. Cristina Vescina, A. M. F., Yong Guo, Comparing cyclodextrin derivatives as chiral selectors for enantiomeric separation in capillary electrophoresis. *Journal of Chromatography A* **2002,** *973*, 187-196; (b) Valle, E. M. M. D., Cyclodextrins and their uses: a review. *Process Biochemistry* **2004,** *39*, 1033-1046.
55. Fanali, S., Enantioselective determination by capillary electrophoresis with cyclodextrins as chiral selectors. *Journal of Chromatography A* **2000,** *875* (89-122).
56. David Fournand, I. M., Catherine Lapierre, Capillary Zone Electrophoresis of Syringyl and Guaiacyl Monomers Resulting from Lignin Thioacidolysis. *Phytochemical Analysis* **2002,** *13*, 338-342.
57. Anne E. Harman-Ware, M. C., Aman Preet Kaur, Mark S. Meier, Dawn Kato, Bert Lynn, Pyrolysis-GC/MS of sinapyl and coniferyl alcohol. *Journal of Analytical and Applied Pyrolysis* **2013,** *99*, 161-169.
58. Sabrina Hoffstetter-Kuhn, A. P., Ernst Gassmann, H. Michael Widmer, Influence of Borate Complexation on the Electrophorestic Behavior of Carbohydrates in Capillary Electrophoresis. *Analytical Chemistry* **1991,** *63*, 1541-1547.

59. Lane, J. Top 10 Scariest Challenges for the Biofuels Industry *Biofuels Digest* [Online], 2013.

VITA

The author was born in Honolulu, Hawai'i. She attended Hawai'i Baptist Academy and graduated with her prestigious high school diploma in 2004. She then enrolled at Creighton University in Omaha, Nebraska where she obtained her B.S. in Chemistry in 2008 under Dr. David Dobberphul. Following her undergraduate studies, she started graduate school at the University of Kentucky in the Department of Chemistry under the advising of Dr. Bert C. Lynn. She is a member of the American Chemical Society (ACS) and the American Society for Mass Spectrometry (ASMS).

Presentations:

1. A Potential Alternate Synthetic Route to Lignin Thioacidolysis Standards and Their Characterization by GC-MS. **Dawn Kato**; Bert C. Lynn, 62nd Annual ASMS Conference on Mass Spectrometry and Allied Topics, Baltimore, MD, June 15-19, 2014, Section- Energy: Biofuels and Algae.
2. Development of Capillary Electrophoresis-Mass Spectrometry for Analysis of Fenton Chemistry Biomass Pretreatment for Biofuels Production. **Dawn Kato**; Bert C. Lynn, 61st Annual ASMS Conference on Mass Spectrometry and Allied Topics, Minneapolis, MN, June 9-13, 2013, Section- Energy: Biofuels and Algae.
3. Inlet Ionization with Voltage: A Hybrid between Electrospray and Thermospray. **Dawn Kato**; Bert C. Lynn, 60th Annual ASMS Conference on Mass Spectrometry and Allied Topics, Vancouver, BC, May 20-24, 2012, Section- Instrumentation: New Developments in Ionization and Sampling II.

Publications:

1. **Dawn M. Kato**, Sean R. Parkin, Bert C. Lynn. "One-step Synthesis of Arylglycerols." Submitted to 09/2014.
2. **Dawn M. Kato**, Noelia Elía, Michael Flythe, Bert C. Lynn. "Pretreatment of Lignocellulosic Biomass Using Fenton Chemistry." *Bioresource Technology*. 162 (2014) 273-278.
3. Anne E. Harman-Ware, Mark Crocker, Aman Preet Kaur, Mark S. Meier, **Dawn Kato**, Bert Lynn. "Pyrolysis-GC/MS of Sinapyl and Coniferyl Alcohol." *Journal of Analytical and Applied Pyrolysis*. 99 (2013) 161-169.